Electronic Theses and Dissertations

Theses, Dissertations, and Major Papers

11-1-1970

Pressure-time relationship in laterally stressed frozen granular soils.

Khandker Abdul Aziz
University of Windsor

Follow this and additional works at: https://scholar.uwindsor.ca/etd

INFORMATION TO USERS

This manuscript has been reproduced from the microfilm master. UMI films the text directly from the original or copy submitted. Thus, some thesis and dissertation copies are in typewriter face, while others may be from any type of computer printer.

The quality of this reproduction is dependent upon the quality of the copy submitted. Broken or indistinct print, colored or poor quality illustrations and photographs, print bleedthrough, substandard margins, and improper alignment can adversely affect reproduction.

In the unlikely event that the author did not send UMI a complete manuscript and there are missing pages, these will be noted. Also, if unauthorized copyright material had to be removed, a note will indicate the deletion.

Oversize materials (e.g., maps, drawings, charts) are reproduced by sectioning the original, beginning at the upper left-hand corner and continuing from left to right in equal sections with small overlaps.

UMI®

PRESSURE-TIME RELATIONSHIP IN LATERALLY

STRESSED FROZEN GRANULAR SOILS

A THESIS

Submitted to the Faculty of Graduate Studies Through the

Department of Civil Engineering In Partial Fulfilment

of the Requirements for the Degree of

Master of Applied Science at the

University of Windsor

by

KHANDKER ABDUL AZIZ

Windsor, Ontario, Canada

November 1970

UMI Number:EC52786

UMI®

APPROVED BY:

Z. Reif

Jan T. Orda

G. Abdel Sayed

332666

ABSTRACT

The main object of the investigation presented in this
thesis was, to study the general tendency in which the reduc-
tion of lateral stress with time takes place in a frozen sand
layer subjected to radial pressure.

Two different types of sand were used to prepare 62 speci-
mens. The specimens were composed of either sand and a variety
of initial porosity and degree of ice saturation. They were
tested at various constant temperatures under selected initial
pressure. The magnitude of pressure retained by the frozen
sand sample at any time was measured by means of a pressure
gauge attached to the pressure unit. The strain in the frozen
soil was measured by using bonded resistance strain gauges em-
bedded in the sand-ice system.

The reduction in lateral stress, R_t, in frozen sand was
found to be a function of five variables; the initial porosity
of the sand (n), the degree of ice saturation (S_i), sample
temperature (T_F), initial pressure (σ_i) and the time (t) elaps-
ed after the application of initial pressure.

Experimental results were plotted in the form of " pressure
time " curves which showed the same tendency of rapid decrease
in pressure for the first few hours and then a very slow rate
of reduction in pressure with time. Reduction in stress, R_t,
expressed as a percentage of Initial Pressure, was also plotted

against time for each test to study the influence of the above
mentioned variables.

Summarizing the experimentally obtained results a general
equation, to predict the value of lateral pressure retained by
the sand ice layer at any time after the application of a known
initial pressure, was derived empirically in terms of the var-
iables, i.e. n, S_i, T, σ_i and t.

ACKNOWLEDGMENTS

The author expresses his gratitude to Dr. J. T. Laba, Associate Professor of Civil Engineering, the author's advisor, for his wholehearted encouragement and advice and for reading and improving the draft manuscript of the thesis.

The author's thanks go to the Canadian Commonwealth Scholarship and Fellowship Administration for the financial support of this work and to all whose timely help and advice accelerated the completion of this project.

v

TABLE OF CONTENTS

TABLE OF CONTENTS (continued)

LIST OF FIGURES

LIST OF FIGURES (continued)

x

xi

LIST OF TABLES

NOMENCLATURE

A	Coefficient (Reduction Factor)
B	Time Factor
B'	Corrected Value of Time Factor for higher Temperatures
C	Coefficient
C_1, C_2, C_3	Coefficients
C_4, C_5, C_6	Coefficients
C_7	Coefficient
c	Constant, used in equation (2-9)
E	Modulus of Elasticity
E_{init}	Initial Modulus of Elasticity
E_{end}	Final Modulus of Elasticity
e	Base of Natural System of Logarithms
K	Factor used in equation (2-10)
k	Exponent in equation (4-5)
L	Exponent in equation (2-10)
M	A Function of Temperature, Term in equation (4-5)

xvii

m	A function of Ice Saturation, Term in equation (2-9)
n	Initial Porosity of Sand
p	Exponent used in equation (2-10)
$\bar{R}$	Range
R_t	Reduction in Lateral Stress after Time t, expressed as a percentage of Initial Pressure
R_{24}	Reduction in Lateral Stress after 24 hours
r	Relaxation Time
S_i	Degree of Ice Saturation
S	Standard Deviation
T	Temperature below Freezing Point in Fahrenheit scale
T_F	Temperature in Fahrenheit scale
T_o	Initial Sample Temperature
t	Time
t_m	Time required to reach Maximum Pressure
t_r	Time of Relaxation
V	Coefficient of Variation

z	Term used in equation (2-4)
ϵ	Total Strain
ϵ_{el}	Elastic Strain
ϵ_{pl}	Plastic (creep) Strain
η	Coefficient of Viscosity
θ	Rate of Increase in Temperature
σ	Working Stress
σ_o	Initial Stress, Term in equation(2-2)
σ_i	Initial Pressure
σ_l	Long Term Strength
σ_t	Stress or Pressure retained after Time t
σ_{12}	Pressure retained after 12 hours
σ_{24}	Pressure retained after 24 hours
σ_{inst}	Instantaneous Strength
σ_{con}	Continuous Strength
σ_{init}	Initial Stress after relaxation
σ_{end}	Final Stress after relaxation
σ_{max}	Maximum Pressure developed

CHAPTER I

INTRODUCTION

The importance of studies on frozen soil becomes evident if one considers that nearly 26% of the dry surface of the globe (i.e. more than 1/4 thereof) is in a perennially frozen state. With the advancement of science and technology, man is venturing more and more into these permafrost regions in search of valuable minerals and oils etc. Hence, the Knowledge regarding the frozen soils is becoming more significant to scientists and engineers. However, the importance of studies on frozen soil is not limited to permafrost regions only. Rather it is more important in the land areas having a moderate climate, where during the winter, the top foot or more of soil becomes frozen; creating a challanging problem for the foundation engineers.

In many northern regions, such as the northern parts of North America, where there are no local construction materials, and the cost and trouble incurred in importing them is prohibitive, frozen soil and ice may very well serve as the main construction materials for structures like storehouses, shelters, ice roads, temporary river crossings, dams and piers for temporary use and even runways for temporary airfields. Frozen soils proved to be very much advantageous in the cases of underground structures, such as storage for oil or gas, cold

1

storage for agricultural products, underground research laboratories etc. About twenty years of effective research and experience lie behind the present knowledge of safer design, construction and maintenance of such structures under various climatic and other conditions. Considerable progress has also been made in the study of physical and mechanical properties of ice, snow and frozen soil, although much is yet to be known.

To use any material for construction purposes one must have sufficient knowledge about its mechanical as well as physical properties. Any relation between the physical and the mechanical properties can always be helpful. Unlike soil, a three phase system, frozen soil may be considered as a complicated four component system, or a system consisting of four interrelated bodies: solid (mineral particles) plastic (ice), liquid (unfrozen water) and gaseous (vapour and gases). It is expected that the relative amounts of these components should have marked effects on the mechanical behaviour of frozen soils. Some basic physical properties such as specific gravity of solid particles, porosity of soil mass, water content and temperature below freezing point may affect these relative amounts, and hence they may also influence the mechanical behaviour of frozen soils.

Mechanical properties are also of great importance for rating frozen soils as a material, environment and base of structures. However, the most characteristic mechanical property, which affects any design on frozen soil, is the tendency of frozen soil to weaken (i.e. to relax) under long term load

of any type. The instantaneous load capacity of a frozen soil mass may sometimes be as much as ten times its long term resistance capacity. Therefore, while calculating the safe load for a frozen soil, it is essential to consider, not only its temporary high resistance capacity for instantaneous external load, (to be prepared for construction difficulties resulting therefrom), but also its long term strength and possible deformation estimated by considering the relaxation characteristics of that particular soil under worst conditions of temperature, ice content, initial pressure and some basic changeable properties of soil itself. However, the worst condition can never be predicted unless the effect of change of the conditions in either direction is known.

The object of the investigation carried out in this research programme was to find out a general tendency in which the reduction of lateral stress with respect to time takes place in a 4" thick sand-ice layer subjected to radial pressure. The investigation was further extended to find out whether there was any correlation between the reduction in lateral stress with time and the variable parameters, namely, temperature, ice-saturation, porosity of soil and initial pressure.

To justify the importance of the present investigation, the following problems that may be faced by foundation engineers dealing with frozen soils are discussed briefly.

The first example is an anchored sheet pile having concrete

deadman for anchorage (fig. 1). In winter the sand layer, in which the anchor is located, may freeze and subsequently, when subjected to temperature increase, will produce lateral thrust against the sheet-piling wall and deadman [8] . The designer must decide whether the maximum expected thrust is to be used as a live load with full factor of safety or it should be treated as a temporary live load such as wind load or earthquake force, allowing the use of a smaller safety factor, if the maximum thrust is taken into consideration.

The second example of such problem is the case of a structure having a car park on the ground level. All the conditions that are required for the development of lateral thrust in soils due to temperature change [9] exist in this case. Frozen soil layer, restrained from expanding by confining walls (fig. 2) and subjected to consecutive cycles of cooling and warming will develop lateral pressure against the walls [8] creating the same problem as before.

The present investigation will probably be most helpful in the case of a cellular cofferdam, where the lateral thrust of frozen granular fill inside each cell, caused by the temperature change, will be radial and therefore similar to the experiments carried out.

The loading system in the experimental set up was chosen to simulate laterally induced radial pressure. Granular soil was chosen for the experimental work because, being non-suscep-

tible to frost action, it is considered by many engineers to
be a select material and is used in areas subjected to frost
action.

CHAPTER II

REVIEW OF LITERATURE

To the best of author's knowledge, no effort has been made to correlate the time dependent lateral stress reduction in frozen soil with the relevant parameters, such as temperature, degree of ice saturation, initial porosity of soil and initial pressure. Study of the time dependent behaviour of frozen soil subjected to lateral pressure seems to have escaped the notice of most of the prominent investigators in this field. Probably the only literature on this topic (Laba, 1970) dealt with the lateral thrust exerted by frozen granular soils due to temperature change. Majority of other investigators were mostly concerned with the vertical loads of constant magnitude applied to the frozen soil mass, studying its strength properties.

Before going into the actual works done in this field, some definitions of basic rheological properties of frozen soil are given below.

      a) Creep: It is defined as the gradual deformation
         of a body over a period of time taking place
         at a constant stress.

      b) Relaxation: It is the diminution (weakening) of
         stress in a body required to maintain a constant
         deformation.

6

c) Loss of strength: It is the decrease of that
stress level in a frozen soil mass which causes
failure of the mass with an increase in the
time of load action in frozen soil.

Understanding of relaxation and long term strength charac-
teristics of frozen soil were helpful for the present investi-
gation. Also the phenomenon of development of lateral thrust
in frozen soil served as a basis for the present research work.
Hence literature related to these two topics is emphasized in
the following review as being of significant value to the re-
search work undertaken.

Relaxation and Long Term Strength

Among the few investigators who are well known for their
works in the fields of frozen soil mechanics, Tsytovich, N. A.
[11, 12] should probably be considered as a pioneer. He pre-
sented a brief but informative introduction to the works done
on rheological properties of frozen soil in one of his publi-
cations [11] , along with other topics on frozen soil. Later
on he concentrated his attention on the basic mechanics of
freezing, frozen and thawing soils [12]. However, Tsytovich
did not mention any record of study regarding lateral stress
in frozen soil.

In order to explain the internal mechanics of soil-ice
system, Tsytovich considered it as a complicated four-component

system, or a system consisting of four interrelated bodies: solid (mineral particles), plastic (ice), liquid (unfrozen water) and gaseous (vapour and gases). The strength or load resistance of such a system depends on the strength of a complex type of internal bonds between individual particles, which form aggregate of frozen soils, and the strength of bonds between these aggregates. These bonds, known as cohesion, may be regarded as consisting of three components as follows:

a) Cohesion by cementation, which is the most important component, results from bonds between ice crystals and mineral particles. It depends on the ice content and temperature of freezing as well as the mechanical and minerological composition of frozen soil.

b) Molecular cohesion results from forces of molecular attraction between mineral particles. It depends on the area of contact surfaces of these particles and the distances between them which in turn depends on the compactness of soil and applied pressure.

c) Structural cohesion reflects the effects of diverse physical, physico-chemical, mechanical and other processes in increasing the total cohesion.

Krausz, A. S. [7] maintained that natural fresh water ice, when formed unidirectionally and free of snow, usually consists of long pencil-like grains. Each grain is one crystal in which the oxygen and hydrogen atoms are arranged in a regular geometrical pattern. This pattern is built up from simple hexagonal prism units as shown in figure 3. The plane perpendicular to the axis of hexagonal symmetry i.e. the C axis, is called the basal plane and plays an important role in the plastic deformation of ice. According to the well-established fact that crystalline materials deform plastically by slip on preferred crystallographic planes, slip in ice occurs most easily on the basal plane in the manner illustrated in figure 4. In each grain, there is only one system of slip planes (the basal planes) and the deformation will depend on the shear stress component in this plane rather than on maximum shear stress.

Tsytovich [12] explained that any load applied to frozen soil causes a concentration of stresses at the contacts between mineral particles and ice crystals, inducing plastic flow of ice. As increased pressure decreases the melting point of ice, the equilibrium between film water and ice is disturbed. Ice, melted under increased pressure flows to regions of lower pressures and regelates (Vyalov, 1954). This phenomenon is accompanied by a decrease in structural cohesion and cohesion by cementation which results in irreversible deformation. With gradual displacement of film water, the phenomenon of creep is observed.

This explanation is acceptable at temperatures near melting point or at very high pressures. But for very low temperatures and low pressures it is more probable that ice crystals undergo plastice deformation along the basal plane due to components of contact pressure parallel to the basal plane as explained by Krausz.

A rise in molecular cohesion occurs as soil particles come closer under pressure. Thus under a pressure not exceeding certain threshold value, weakening (relaxation) of structural cohesion and cohesion by cementation will be compensated by strengthening of molecular cohesion and a state of equilibrium will be re-established in the soil with time. However, under greater load, the destruction of internal bonds is no longer compensated by strengthening and plastic viscous flow due to creep occurs.

A long term force, which if exceeded results in unattenuating deformation, is known as the ultimate long term strength. The relation between such failure force and its required duration to cause failure was investigated by Tsytovich, Berezantsev and Vyalov as cited by Tsytovich [11] . Relationship between tensile stress causing failure and the time until failure, as obtained by Tsytovich for clayey sand samples with a total moisture-ice content of about 30 percent, is shown in figure 6a. The values of failure tensile forces are shown on the ordinate while the abscissa shows the duration of the load to cause

failure. Tsytovich obtained similar curves for long term strength of frozen bond between wooden wedges and fine sandy loam at $-3.6\,^{\circ}C$. The curves showing decrease in cohesive forces in frozen soils with time were also of similar shape as obtained by him [12]. He also studied the relationship between ultimate compressive strength (under rapidly increasing load at the rate of 20 kg/cm^2 per minute) of frozen soils and the temperature below freezing point. He found that the ultimate compressive strength was proportional to the decrease in temperature [11].

Tsytovich [11] derived an analytical expression for the curve of stress relaxation (fig. 5) in frozen soil at constant temperature and at a constant deformation. He considered the frozen soil mass as a perfect elastic viscous body.

The total strain, ϵ, which is constant in the case of relaxation, is composed of two components, namely, elastic component, ϵ_{el}, and plastic component, ϵ_{pl}. Hence,

$$\epsilon = \epsilon_{el} + \epsilon_{pl} = constant \qquad (2\text{-}1a)$$

From Newton's law, assuming that velocity of the plastic deformation is proportional to the working stress, the value of plastic deformation is given by,

$$\frac{d\epsilon_{pl}}{dt} = \frac{1}{\eta}\sigma \qquad (2\text{-}1b)$$

where, η = coefficient of viscosity,

and δ = working stress.

The value of elastic deformation may be written as,

$$\epsilon_{el} = \frac{1}{E} \delta \qquad (2\text{-}1c)$$

in which, E = modulus of elasticity.

Differentiating equation (2-1a), one obtains

$$\frac{d\epsilon_{el}}{dt} + \frac{d\epsilon_{pl}}{dt} = 0 \qquad (2\text{-}1d)$$

Substituting values from equations (2-1b) and (2-1c) this becomes,

$$\frac{d\delta}{dt} + \frac{E}{\eta} \delta = 0 \qquad (2\text{-}1e)$$

Integrating and finding the constants one gets,

$$\delta = \delta_0 \exp\left(-\frac{t}{\eta/E}\right) \qquad (2\text{-}2)$$

where, δ_0 = stress at $t = 0$ i.e. initial stress.

Setting $\eta/E = t_r$ (so called time of relaxation) and introducing Shvedov's correction, which implies that not the whole stress relaxes, but only its excess above the value of the continuous resistance, i.e. $\delta_{inst} - \delta_{con}$ (fig. 5), the following equation can be written,

$$\delta_1 = \delta_{con} + (\delta_{inst} - \delta_{con}) \exp(-t/t_r) \qquad (2\text{-}3)$$

Putting $Z = \exp(-t/t_r)$, the value of δ_{con} may be obtained from

the equation,

$$\delta_{con} = \frac{\delta_1 - \delta_{inst}. Z}{1 - Z} \qquad (2\text{-}4)$$

In order to compute from equation (2-4) the value of continuous resistance, δ_{con}, it is necessary to know the value of Z. Tsytovich proposed that the value of Z may be calculated from the equation

$$Z = \frac{\delta_1 - \delta_2}{\delta_{inst} - \delta_1} \qquad (2\text{-}5)$$

in which, $\quad \delta_1 =$ strength corresponding to time t_1

$\qquad\qquad \delta_2 =$ strength corresponding to time t_2

$\qquad\qquad$ wherein $t_2 = 2t_1$

and $\qquad\qquad \delta_{inst} =$ Instantaneous strength.

However, according to Tsytovich long duration testing of frozen clayey soils indicated that experimental curves of stress relaxation differ from the theoretical curves computed for an ideal elastic-viscous body. The experimental data indicated that the actual relation has a logarithmic character. This discrepancy may be attributed to the fact that coefficient of viscosity, η, and modulus of elasticity, E, for frozen soils are not constant quantities as assumed in the derivation of above equations.

Considering the variation of modulus of elasticity, E, in frozen soil, the equation denoting the state of stress in a deformed, ideal elasto-viscous body is as follows (Rzhanitsyn,

1949, Rebinder, 1951);

$$r . E_{init} \frac{d\epsilon}{dt} + E_{end} = \sigma + r . \frac{d\sigma}{dt} \qquad (2\text{-}6)$$

Integrating equation (2-6) at E = constant, gives the Maxwell-Shvedov equation of relaxation,

$$\sigma_t = \sigma_{end} + (\sigma_{init} - \sigma_{end}) \exp (-t/r) \qquad (2\text{-}7)$$

where, σ_t = Stress at time t

σ_{init} = Initial stress before relaxation

σ_{end} = Final stress after relaxation

E_{init} = Initial modulus of elasticity

E_{end} = Final modulus of elasticity

$r = \eta/(E_{init} + E_{end})$ = relaxation time.

Substituting σ_{end} by σ_l and σ_{init} by σ_{inst} one can get the equation for reduction in strength, wherein σ_l denotes the long term strength and σ_{inst} denotes the instantaneous strength.

The above equations are based on the assumption of ideal elasto-viscous body which obeys the law of linear deformation and possesses constant viscous properties. This does not fully reflect the real properties of such a complex body as frozen soil. Consequently the above formulae do not represent a sufficiently accurate quantitative description of processes taking place in frozen soil. Hence experimental stress relaxation curves differ considerably from the theoretical curves as shown in figure 6b. This discrepancy is explained by the fact that

in the ideal case the time of relaxation, r, in equation (2-6) is taken to be constant, but in reality this factor is found to be variable, because of the variation of coefficient of viscosity during relaxation. Besides the ideal case is based upon the law of linear deformation which is not quite true as far as frozen soil is concerned.

Lateral pressure in frozen soil

As the basis of present investigation, the work of Laba [8, 9] on lateral thrust exerted by frozen granular soils due to temperature change may be mentioned here. He has establi- shed that with increase in temperature, sand-ice system exerts lateral pressure against confining boundaries when all the following conditions exist.

a) The frozen soil layer is restrained from expanding by retaining structures.

b) Consecutive cycles of cooling and warming occur in the frozen soil layer during winter and spring.

c) Ice-wedges form in the soil layer itself or along the contact area between the soil mass and retaining structure.

At a constant rate of temperature rise, this lateral pre- ssure increases rapidly, reaches a maximum value and then drops steadily with time. A typical pressure time curve, as obtained

by Laba [8] is shown in figure 7. The following empirical equation was proposed for the pressure time curves,

$$\delta = At. \exp(-t/t_m) \qquad (2\text{-}8)$$

where, A = coefficient psi/min

t = time [min.]

t_m = time required to reach the maximum pressure [min.]

The value of maximum pressure, δ_{max}, was given by the following relation,

$$\delta_{max} = \frac{n}{46.6}\left[0.475\ S_i\ (1 - T_0/30)\ \theta^{\,m} + c\right] \qquad (2\text{-}9)$$

where, δ_{max} = Maximum pressure developed

m = $0.225 + 0.00075\ S_i$

c = 0 for $T_0 \leqslant 25^\circ F$

c = $\dfrac{(T_0 - 25)\theta\ S_i}{2500}$ for $25^\circ F < T \leqslant 30^\circ F$

n = Sand porosity [%]

θ = Rate of temperature rise [$^\circ F/hr$]

T_0 = Initial sample temperature [$^\circ F$]

Time required to reach this maximum pressure, t_m, can be found out from the proposed equation,

$$t_m = \frac{n+60}{106.6}\left[Ke^{\,L\theta}. (S_i)^{0.85} (\theta)^{P}\right] \qquad (2\text{-}10)$$

where for $T_0 \leq 20°F$

$$K = 4.95 - 0.11\, T_0$$

$$L = -(0.076 - 0.015\, T_0/20)$$

$$p = -(0.06 + 6.5\, T_0/1500)$$

and for $20°F < T_0 \leq 30°F$

$$K = 6.9\, (1 - T_0/31.8)$$

$$L = -(0.183 - 0.0061\, T_0)$$

$$p = -(0.113 + T_0/750)$$

From equation (2-8) it follows that

$$A = \frac{\delta_{max}}{0.3679\, t_m} \qquad (2\text{-}11)$$

Thus δ in equation (2-8) can be found out from the five known parameters, namely, porosity, n, degree of ice saturation, S_i, initial temperature, T_0, rate of temperature rise, Θ, and time of temperature rise, t.

However, if the change in temperature is similar to that shown in figure 8, i.e. if the temperature increases at a constant rate up to a time t_1 and then remains constant up to the time t_2 before changing again, a different situation arises. The above mentioned equations are sufficient to predict the lateral thrust produced up to the time t_1 as shown in figure 9. However as the temperature remains constant instead of increasing, the " pressure time " curve will not follow the dotted line (fig. 9), instead, it is more likely to follow the continuous line up to time t_2 as will be shown later.

CHAPTER III

SAMPLE, APPARATUS AND TEST PROCEDURE

Sample

The experimental investigations were limited to granular non-cohesive soil. Two different types of sand were used to prepare test specimens of various combinations of initial porosity and degree of ice saturation. Sand No. 1 was a crushed uniform sand from Ottawa, Illinois (Uniformity Coefficient 1.5 and Specific Gravity 2.65) while Sand No. 2 was a natural variety of well graded sand from Paris, Ontario (Uniformity Coefficient 3.8 and Specific Gravity 2.67). The grain size distribution of both the sands are shown in figure 10.

Apparatus

The main apparatus used in this research work (which will henceforth, be referred to as the " pressure unit "), was designed by Laba (1970) following the idea originated by Wilmot (1956), who had conducted studies on pure ice. The pressure unit (fig. 11) consisted of an outer steel cylinder encasing an inner concentric rubber diaphragm with a thin annular void of 1/16" between them. The 1/8" thick rubber diaphragm was provided with circular outer flange at both the ends which were sealed with the ends of steel cylinder by using steel rings. The void, thus made air tight, was provided with an

18

inlet for pressure line and an outlet for releasing excess oil or entrapped air; both being secured by valves. The pressure line was connected to a hydraulic pressure pump so that the desired amount of radial lateral pressure could be applied through the flexible diaphragm to the frozen specimen. The oil pressure exerted could be measured by means of an external pressure gauge connected to the pressure line. The steel cylinder was insulated all around except for the top surface of the sample so that the freezing and thawing of the sand mass followed the pattern existing in nature. However, the top of the steel cylinder was covered with a thin polythene sheet to avoid loss or increase of moisture content in the sample. Figure 12 shows the pressure unit with the pump connected to it.

To measure the strain in the frozen sand SR-4 (Type A-9) resistance strain gauges, (fig. 14) having nitrocellulose impregnated bond paper backing (Manufactured by BLH Electronic) were embedded in the sand and were connected to a portable digital 8-channel strain indicator (strainsert, Model TN8C). Strain in microinch per inch could be read directly from the strain indicator (fig. 13). The strain gauges were coated on both sides with Eastman 910 Adhesive cement and were covered with sand particles, as shown in figure 14, to ensure proper bond between the frozen sand and the strain gauges. To compensate the effect of temperature on strain measurements, a " dummy gauge " was used; it was a strain gauge from the same

lot loosely attached to a flat wooden bar and was buried in a box containing dry sand of the same type as the specimen under investigation. The dummy gauge was kept at the same tempera-ture environment as the active gauges, but was free from any sort of mechanical strain.

The pressure unit with soil sample and embedded strain gauges was placed inside a freezing chamber having thermostatic temperature control (fig. 15). Soil samples could be brought to and kept at the required constant temperature inside the freezer.

The temperature at various depths of the sample was meas-ured by means of four copper-constantan thermocouples inserted into the specimen at three different levels and connected to a temperature potentiometer through a multipolar rotary switch (fig. 16).

Preparation of Sample

The sand ice specimens were prepared as follows. A known weight of dry sand and a measured amount of water were thorough-ly mixed together to provide the desired water content and hence the desired degree of ice saturation when frozen. The moist sand thus prepared was placed in the pressure unit in four equal layers; each layer being compacted gently to form finally a 9 5/8 inches in diameter and 4 inches high sample of a certain porosity. After the second layer was compacted, two 6 inches long sand coated strain gauges (as described before) were placed

crosswise, horizontally and symmetrically about the specimen's centroidal axis (fig. 12). The strain gauges were thus half way down the depth of the sample.

The pressure unit was then placed into the freezing chamber. Four copper constantan thermocouples were penetrated inside the sample; one was located 1/4 inch below the top surface near the centre of the sample; two were placed 2 inches below the top surface (one near the centre, the other 1 inch away from the side); and the fourth was embedded near the centre 1/4 inch above the bottom. In addition to these, a fifth thermocouple was used to record the air temperature just above the sample and a sixth one measured the sand temperature around the dummy gauge.

On completion of the sample preparation and necessary wire connections to strain indicator and temperature potentiometer, the freezer was closed and the specimen was frozen to the required temperature. Before being tested, each frozen sample was left at the selected constant temperature for not less than 6 hours to ensure uniform temperature distribution throughout the frozen sample.

Test Procedure

Each test was started by checking the temperature indicated by the potentiometer for each of the six thermocouples. Same temperature readings for different levels of sample indicated uniform temperature distribution throughout the sample and the

specimen was ready to be tested. The strain reading was set at zero and the active channels were balanced by using the respective balancing knobs. A selected initial pressure was then quickly applied to the frozen sample and the pressure valve was closed instantaneously. The initial pressure as indicated by the pressure dial and corresponding initial strain from strain indicator were recorded against zero hour. The pressure, indicated by pressure gauge, and strain given by strain indicator were recorded after definite intervals of time. The temperature was kept constant throughout the test and was frequently checked. After 24 hours one set of readings was completed. A few tests were continued up to 30 hours or more, but no considerable change in readings were observed. After each test, the specimen was unloaded and was allowed to recover at $32^{\circ}F$ for not less than 24 hours before refreezing for another set of readings. A typical observation sheet used for recording data is shown in Appendix C.

As equivalent sand ice specimens having same combination of variables were likely to differ in orientation of ice crystals, frequent change of specimens was to be avoided. On the other hand, a sample, previously loaded, was likely to undergo some small permanent changes in the orientation and shape of ice matrices. Hence using the same sample for a large number of tests was also not advisable. Number of tests carried out on one sample was varied from one to three to minimize systematic error, i.e. to distribute the error, resulting from either

of the above two cases, arbitrarily among the test data.

More than sixty specimens were included in the programme and the variables selected were the temperature of the frozen sample, initial soil porosity, degree of ice saturation and the initial pressure. The experiment was designed partly in a systematic pattern (factorial design) and partly in randomized block so as to obtain maximum reliable information from the limited number of tests. The levels of the quantitative factors were taken to be fixed. Initial pressure was selected from 25 psi, 50 psi, 75 psi and 100 psi; temperature was limited to $30^{\circ}F$, $25^{\circ}F$, $15^{\circ}F$ and $0^{\circ}F$; degree of ice saturation used were 33.33%, 50%, 66.67% and 100% while porosity was fixed at 46.0%, 40.0%, 36.0% or 30.0%. The selected soil temperatures and degree of ice saturation cover most of the range which is common in areas subjected to moderate climate.

CHAPTER IV

DISCUSSION OF TEST RESULTS

A discussion of the results of experimental investigations is presented below in the sequence in which it was developed.

Reduction of Lateral Stress with Time

The main purpose of this research work was to study the nature in which the reduction of induced lateral stress in a frozen sand mass takes place when left to itself for a certain period of time at constant temperature as well as the effect of several relevant parameters on the magnitude of the aforesaid reduction.

The lateral radial pressure (equal to the induced lateral stress in the frozen sample) σ_t, retained by the sand ice specimens at any time was investigated as a function of five variables: the initial lateral pressure applied on the sample, σ_i, the value of constant sample temperature, T_F, the initial soil porosity, n, the degree of ice saturation, S_i, and the time, t, during which reduction of stress took place.

The first set of experiments consisted of twenty seven tests performed on nine sand ice specimens of sand No. 1, all with a constant initial soil porosity of 46.0%. The selected ice contents of 10%, 15% and 30% corresponded to the degree of

24

ice saturations of approximately 33.33%, 50% and 100% respectively. [As the unfrozen water content in granular soil is negligible, as pointed out by Tsytovich (1960), the ice content in each frozen sand specimen was assumed to be equal to its water content before the freezing took place. However, the degree of ice saturation was based on a 9% volume expansion of the pore water upon freezing [9]. Levels of temperature were fixed at $0^\circ F$, $15^\circ F$ or $30^\circ F$ and initial lateral pressure applied was 25psi, 50psi or 100psi. Tests were performed under conditions obtained by all possible combinations of the above mentioned selected values of each variable.

In the next set of experiments sand No. 1 and sand No. 2 were used to obtain porosities of 46%, 40%, 36% and 30%. Degree of ice saturation was selected from the set of 33.33%, 50%, 66.67% and 100%. Levels of temperature were $0^\circ F$, $15^\circ F$, $25^\circ F$ and $30^\circ F$ and initial pressure was selected from 25psi, 50psi, 75psi and 100psi. Combinations of these variables were planned in such a manner that sufficient data were available from the total of sixty tests performed. Test data were studied in the form of graphs which are described below.

Figures 18 to 26 show the relationship between the lateral pressure, σ_t, retained by the frozen sand specimen, and the corresponding elapsed time for different values of n, S_i, T_F and σ_i. Time elapsed, t, after the application of initial lateral pressure is shown along the abscissa and the pressure σ_t, is shown along the ordinate. The results from all the experi-

ments show the same tendency; i.e. all the "pressure time" curves drop rapidly during the first hour or so and then keeps on decreasing at a slow rate. It may be of interest to mention here that these lateral "pressure-time" curves resemble the "relaxation curve" for tensile stress shown by Tsytovich [11]. Each of figures 18 to 26 shows "pressure-time" curves obtained for different initial pressures but under the same porosity, ice saturation and temperature conditions.

For convenience of interpretation a new term "Reduction in stress", R_t, expressed as a precentage of initial pressure is introduced at this stage. It is defined as

$$R_t = \frac{\sigma_i - \sigma_t}{\sigma_i} \times 100 \qquad (4\text{-}1)$$

where, R_t = Reduction in lateral stress after time t expressed as a percentage of initial pressure.

σ_i = Initial pressure at t = 0 [in psi]

σ_t = Actual pressure retained after time t. [in psi]

Figures 27 to 41 show the "R_t vs t" curves for different combinations of n, S_i, T_F and σ_i. In each of figures 27 to 35 magnitudes of n, S_i and σ_i are kept the same to get some idea about how the "R_t vs t" curves tend to change with change of temperature. Similarly figures 36 to 38 show the effect of change of initial pressure on the behaviour of "R_t vs t" curves. Figures 39 and 40 show the effect of n on the "R_t vs t" curves and figure 41 shows the effect of S_i on the same,

while the rest of the variables remain unchanged. In the above mentioned figures " R_t vs t " curves were plotted by taking time t along abscissa and corresponding value of R_t along the ordinate.

For each of " R_t vs t " curve, the relation between reduction in lateral stress and the corresponding time could be approximated by the following empirical equation:

$$R_t = A \exp (-B/t) \qquad (4-2)$$

where, $A = f(n, S_i, T_F, \sigma_i) =$ Reduction factor,

and $B = f(S_i, \sigma_i) =$ Time factor.

For each "R_t vs t" curve the values of n, S_i, T_F and σ_i are constant. Hence for each combination of these values, there are unique values for reduction factor, A, and time factor, B, giving a unique theoretical " R_t vs t " curve.

Putting t = 0 in equation (4-2), R_t is found to be zero which gives the initial condition. When t is taken to be very large, R_t approaches A, which gives the maximum reduction in lateral stress that may be expected under certain known conditions.

From equation (4-1),

$$\sigma_t = \sigma_i - \frac{R_t \times \sigma_i}{100} \qquad (4-1a)$$

Putting value of R_t from equation (4-2) value of the

reduced lateral pressure at a certain time may be written as

$$\sigma_t = \sigma_i - \frac{A}{100} \sigma_i \exp(-B/t) \tag{4-3}$$

Taking $C = \frac{A}{100}$, equation (4-3) can be written as

$$\sigma_t = \sigma_i - C \sigma_i \exp(-B/t) \tag{4-4}$$

Values of the coefficients A and B in terms of the variables mentioned earlier, were found out in the forms of empirical equations by searching systematically for unknown functions by means of an electronic computer.

The proposed values of A and B are given below

$$A = M\sigma_i + 100 \, e^k + 8 \, T \, (0.46 - n) \tag{4-5}$$

with a maximum value of 100

in which, $M = 0.245 \log_{10} T + 0.035$

$k = -0.00717 \, S_i \, (\sqrt{T} - 1.15)$

$T = 32 - T_F = $ Temperature below freezing point in Fahrenheit scale

and $n =$ initial soil porosity written in decimal form.

For $T > 5$,

$$B = 0.46 \, (S_i)^{0.185} - 0.33 \log_{10} \sigma_i \tag{4-6a}$$

where, $S_i =$ degree of ice saturation in percentage.

while for $T \leqslant 5$ corrected value of B is proposed to be B'

where $B' = B \times T/5 \tag{4-6b}$

Knowing the values of n, S_i, T and σ_i the values of A
and B can easily be calculated from the above equations. Using
the values of A and B in equation (4-2) the percent reduction
in lateral stress at any time may be estimated. Equation (4-3)
or (4-4) may be used to estimate the magnitude of reduced pres-
sure retained by the frozen sand mass after any given period
of time. From equation (4-4), taking t to be very large, the
long term stable lateral stress capacity of the frozen sand can
easily be calculated as follows:

$$\sigma_{end} = \sigma_i - c\,\sigma_i = (1 - c)\,\sigma_i \qquad (4-7)$$

Experimental results show a wide range of percent reduction
in stress within the range of parameters used in the investiga-
tion. The minimum value of R_t after 24 hours, R_{24}, was found
to be 12% at porosity, ice saturation, temperature and pressure
of 46%, 100%, 0°F and 25 psi respectively. On the other hand
the maximum reduction in lateral stress after 24 hours, i.e.
R_{24} was found to be 99% at levels of n, S_i, T_F and σ_i of 46%,
33.33%, 30°F and 100 psi respectively. However, the value of
R_{24} would increase a little with the decrease of porosity to
30% as will be shown later.

All the empirical curves, shown by continuous lines in
figures 27 to 41 and dotted lines in figures 18 to 26 show good
agreement with the experimental results. Tables 1 to 5 show
the comparison between the calculated and experimental values
of pressure after 24 hours, σ_{24}. Calculated values of R_{24},

A and B are given in tables 6 to 10.

To evaluate the effects of porosity, ice saturation, temperature and initial pressure on the reduction of lateral stress in frozen soil, the percent reduction in stress after 24 hours, R_{24}, is taken as the basis of comparison. The observed effects are given below under separate headings.

Effect of Initial Pressure, σ_i:

Figures 42 to 44 show the variation of R_{24} with the initial pressure σ_i; σ_i being shown along the abscissa and R_{24} along the ordinate. From these figures it is evident that with the increase in initial applied pressure, the percent reduction in stress increases. Theoretical curves came very close to straight lines within the experimental range. Slope of " R_{24} vs σ_i " line depends on temperature level only whereas the magnitude of intercept of the line seems to depend on all the four variables.

In fact, the empirical equation shows the relation between R_{24} and σ_i as follows:

$$R_{24} = (C_1 \sigma_i + C_2) \exp (-C_3 + C_4 \log_{10} \sigma_i) \qquad (4\text{-}8)$$

where, C_1, C_2, C_3 and C_4 are constant for a particular case.

Within the experimental range of σ_i, the value of $(-C_3 + C_4 \log_{10} \sigma_i)$ varies very little so that $\exp(-C_3 + C_4 \log_{10} \sigma_i)$ remains almost constant.

Hence between $\sigma_i = 25$ psi and $\sigma_i = 100$ psi, it can be

written that

$$R_{24} = C_6 \, \acute{o}_i + C_7 \qquad\qquad (4\text{--}8a)$$

where $C_6 = M \exp\,(-B/24)$

and $\quad C_7 = \left[100 \; e^k + 8T \,(0.46 - n) \right] \;\; \exp\,(-B/24)$

Figure 42 shows the correlation between R_{24} and $\acute{o}_i$ at constant porosity, ice saturation and temperature as well as the effect of temperature on such correlation. At temperature well below the freezing point, say at $0^\circ F$, the rate of increase in R_{24} with $\acute{o}_i$ is relatively high. From the graph it is seen that at $n = 46\%$, $S_i = 50\%$ and $T_F = 0^\circ F$ the value of R_{24} increases from nearly 30% at $\acute{o}_i = 25$ psi to nearly 60% at $\acute{o}_i = 100$ psi. At the temperature of $15^\circ F$, the rate of increase of R_{24} with $\acute{o}_i$ decreases but very slightly. But at temperature near freezing point i.e. $30^\circ F$, the relation between R_{24} and $\acute{o}_i$ no more remains visibly linear as can be seen from the figure. Theoretical curve shows a very flat initial slope of a curve slightly convex upwards and assymptotic with the 100 percent reduction line. This change in shape of " R_{24} vs $\acute{o}_i$ " curve is due to the correction of time factor B for higher temperatures.

Figure 43 shows the effect of ice saturation on the correlation between $\acute{o}_i$ and R_{24} at constant porosity of 46% and temperature of $15^\circ F$. From the graph it is evident that higher the ice saturation, lower is the value of R_{24} corresponding to a certain value of $\acute{o}_i$ in " R_{24} vs $\acute{o}_i$ " plot. It seems

that ice saturation has no effect on the slope of the " R_{24} vs δ_i " curve.

Figure 44 shows the effect of porosity on the " R_{24} vs δ_i " plots at 50% ice saturation and a temperature of $15^{\circ}F$. As porosity is decreased from 46% to 40%, the " R_{24} vs δ_i " curve shows nearly 8% upward shift. Porosity also has no effect on the slope of " R_{24} vs δ_i " curves.

Effect of Temperature below Freezing Point, T:

Figures 45 to 47 show the correlation between reduction of lateral stress after 24 hours, R_{24}, and the temperature below freezing point, T. In the plots R_{24} is taken along the ordinate while T is shown along the abscissa. R_{24} decreases non-linearly from a high value near freezing point to a lower value as T increases, i.e. T_F decreases. " R_{24} vs T " curves are concave upwards and tend to merge at higher values of R_{24} i.e. low values of T. Figure 45 shows the " R_{24} vs T " curves at $n = 46\%$ and $S_i = 50\%$ and at three levels of δ_i, namely 25 psi, 50 psi and 100 psi. Higher the initial pressure, higher is the " R_{24} vs T " curve. Figure 46 shows the " R_{24} vs T " curves for $n = 46\%$ and $\delta_i = 25$ psi at three levels of ice saturation i.e. 100%, 50% and 33.33%. High ice saturations tend to increase the curvature of the plots and bring them lower. Figure 47 shows the effects of porosity on the " R_{24} vs T " curves. In all the cases, however, the effects of variables seem to be more pronounced at lower temperatures. Also the slope of each " R_{24} vs T " curve is steep-

er near the freezing point and becomes flat at lower temperature.

Effect of Degree of Ice Saturation, S_i:

Figures 48 to 50 show the non-linear relation between the reduction of lateral stress after 24 hours R_{24}, and degree of ice saturation S_i, as well as the intereffects of initial pressure, σ_i, temperature, T_F, and porosity, n, on such relationship. The " R_{24} vs S_i " curves are somewhat similar to " R_{24} vs T " curves but have lesser and more or less uniform curvature. The effects of σ_i and n is same as in the previous case (figures 48 and 49). But with increased temperature, i.e. at temperature near freezing point, the curve becomes flat (fig. 30).

Effect of Porosity, n:

Figures 51 to 53 show the porosity, n, vs reduction in lateral stress after 24 hours, R_{24} curves for different values of S_i, T_F and σ_i. The " R_{24} vs n " curves are straight lines with negative slope, indicating linear decrease of R_{24} with increase in n. Figures 51 and 52 show that the slope of the straight lines representing " R_{24} vs n " plot does not depend on σ_i or S_i. Increase in σ_i increases the intercept of such lines on ordinate showing R_{24}, while an increase in S_i decreases that. Temperature seems to have a marked effect on the slope of the " R_{24} vs n " curves. Figure 53 shows an interesting fact from the " R_{24} vs n" curves for $S_i = 50\%$, and $\sigma_i = 50$psi. When temperature changes from 0°F to 15°F, value of R_{24} increases

if porosity is above 36.5%; while R_{24} decreases if porosity is below 36.5%.

Reproducibility of Apparatus and Technique

When the same sand ice specimen was tested twice under the same conditions of variables, some difference was observed between two sets of data. Check tests were run on several samples to determine the reproducibility of the apparatus and technique used. Table 11 shows the tabulated values of pressure recorded after 12 hours as obtained from a number of frozen sand specimens subjected to duplicate tests. Five duplicate tests were performed and the results were compared.

To draw a reasonable comparison for each set of experiments, the following items were recorded: the measured value of δ_{12}, the Range, $\bar{R}$, indicating the possible difference between the highest and the lowest observations, standard deviation, S, and the coefficient of variation, V, expressing the dispersion of results on a percentage basis.

Observed range $\bar{R}$, varied from 0.6 psi to 2.7 psi whereas the coefficient of variation varied from 2.88% to 11.4%. The dispersion of the test results could be caused by the following factors.

      a) The reproducibility of the apparatus and the experimental technique used.

      b) Mechanical properties of the sand-ice system,

especially the formation and behaviour of

the ice matrices in the sand-ice system.

As it is impossible to produce two specimens with identical
formation and orientation of ice matrices, and as any applied
load will cause permanent changes, no matter how small, in the
ice matrices of the specimen, the second factor may be assumed
to contribute considerably to the dispersion of results. Hence
for practical purposes the reproducibility of apparatus and
technique used in this research work may be considered to be
of satisfactory precision on the basis of information given in
table 11.

Strain Time Curves

Strain measurements were also taken for each test as addi-
tional data to observe the deformation behaviour of the frozen
granular soil under lateral radial pressure. Although it is
beyond the scope of this thesis to discuss compressive strain-
time relationship in frozen sand in detail, a few representative
strain-time curves are presented in Appendix B. Figures 54 to
58 show some of the " strain-time " curves which were plotted
from experimental data. A brief discussion on these curves is
given below as an introduction to the strain-time behaviour of
frozen granular soils under lateral pressure.

The " strain-time " curves (fig. 54 to 57) show a tendency
to increase in magnitude rapidly during the first few hours,

but the slope of the curves decreases with time and the magnitude of strain increases very slowly after some time. This tendency however, seems to be valid for lower temperature only. At higher temperature near the freezing point, the curves indicate a different tendency as can be seen in figure 58. In this case the curves rise to a maximum value of compressive strain with a rather steep slope and then drop to maintain a mild slope almost parallel to the time axis. This phenomenon is no doubt interesting and may be taken as a clue to further investigations. This tendency of rapid initial flow of sand-ice system at temperature near freezing point, before attaining a slow rate of deformation may be explained as follows. As was mentioned earlier in Chapter II, any load applied to frozen granular soil causes a concentration of stresses at the contact points between the mineral particles and ice crystals. At a temperature near the melting point of ice, such concentration of stress may cause the melting of ice in contact with soil particles, due to the reduction of freezing point at higher pressure. Thus a rapid flow occurs as indicated by the rapidly increasing compressive strain. Afterwards, the melted ice regelates at places of lower pressure and increases in volume showing a decrease in total compressive strain. However, more strain-time curves for longer time period is to be studied for more elaborate explanation.

Like " pressure-time " curves, the " strain-time " curves were also found to be affected by temperature to a great extent;

the magnitude of strain being higher at higher temperature.
Increase in initial pressure also increased the compressive
strain, which is obvious. Magnitude of compressive strain in
the sand-ice system was also affected by the degree of ice
saturation and porosity, but no definit tendency could be
predicted as it was possible in the case of the pressure-time
relationship in frozen granular soil.

CHAPTER V

CONCLUSIONS AND RECOMMENDATIONS

On the basis of experimental results and the analysis of these results presented in the previous chapter, the following conclusions can be drawn:

1. Reduction in lateral induced pressure in frozen granular soil at constant temperature was found to be a function of five variables; the magnitude of temperature below freezing point (T) of the sample, the initial lateral pressure ($\acute{\sigma}_i$) applied to the sample, the time (t) elapsed after the application of initial pressure, initial porosity (n) of the soil and degree of ice saturation (S_i) of the specimen.

2. Reduction in lateral stress in frozen granular soil is highly dependent on the temperature of the frozen sand. Reduction of lateral stress in sand ice samples after 24 hours, R_{24}, were found to be above 90% of the initial pressure in most cases when the temperature was constant at $30^\circ F$. The value of R_{24} was found to be much lower at relatively lower temperature. Hence, where lateral thrust is to be avoided, internal heating arrangements, to keep the surrounding frozen sand temperature as high as possible, may serve the purpose. On the other hand,

38

where lateral strength is a requirement, the possible rise in temperature is to be guarded against.

3. The percent reduction of lateral stress was found to be inversely proportional to the initial porosity of the frozen granular soil, provided that the other variables affecting the reduction remain constant. The rate of increase in R_{24} with the decrease in initial soil porosity was found to be dependent on temperature only.

4. The value of percent reduction of lateral stress in frozen granular soil increases with the increase of initial pressure; the increase being approximately linear for practical range. The rate of increment in R_{24} with the increase in initial pressure depends on the temperature of the frozen sample.

5. Degree of ice saturation in a sand-ice system has a nonlinear effect on R_{24}; the latter decreases with the increase of the former. The rate of decrease in the value of R_{24} is greater at lower magnitude of S_i.

6. In this particular case the type of sand did not have any appreciable effect on the reduction rate of lateral stress in frozen sand. However, this conclusion may need further experimental evidence.

7. A general equation was developed for predicting the value of lateral pressure retained by the 4 inches thick sand-

ice layer at any selected time after the application of
known initial pressure, provided that the temperature
remains constant and the initial porosity and degree of
ice saturation of the sample is known.

The proposed general equation may be used to determine
the percent reduction of lateral stress at any particular
time, as well as to predict the stable long term pressure
that can be retained by the sand-ice system.

8. The general shape of the " pressure-time " curves for
    lateral pressure in frozen granular soil resembles the
    " relaxation curve " or " long term strength " curves for
    any other type of stresses. In general, the major part
    of the reduction of lateral stress in sand ice system
    occur during the first few hours after the application
    of initial pressure. The reduction that occurs after-
    wards is only a fraction of the total reduction in stress.

9. The lateral thrust produced by frozen sand may be taken as
    a temporary live load for design purposes and a smaller
    safety factor may be assumed when the maximum thrust is
    taken into consideration.

Recommendations for Further Works

1. Reduction in lateral stress with time may be investigated
    for soils other than granular soil.

2. Effect of particle size and shape of grains in granular

soil on the reduction of lateral stress in frozen sand should be investigated.

3. Lateral pressures, other than radial pressure should be used to find out the effect of the type of restraint on the " pressure-time " characteristics of frozen soil.

4. Effect of vertical restraint or overburden pressure may also be investigated as an extension of this work.

5. Strain-time relationship in laterally stressed frozen soil may be investigated, and the effect of temperature, initial pressure, soil porosity and degree of ice saturation on such relationship may be thoroughly studied.

REFERENCES

1. Andersland, O. B., and Akili, W., " Stress Effect on Creeprates of a Frozen Clay Soil " - Geotechnique, V. 14, No. 1, March 1967, p. 27-30, (1967).

2. Brown, R. J. E., " Relation Between Mean Annual Air and Ground Temperatures in the Permafrost Regions of Canada " - N.R.C., Canada, Division of Building Research, Research paper No. 296, (1963).

3. Gold, L. W., " Some Bulk Properties of Ice " - N.R.C. Canada, Division of Building Research, Technical Paper No. 256, (1967).

4. Gold, L. W., " Elastic and Strength Properties of Fresh-Water Ice " - N.R.C. Canada, Division of Building Research, Technical Paper No. 283, (1968).

5. Goughnour, R. R., and Andersland, O. B., " Mechanical Properties of Sand Ice System " - A.S.C.E. Proc. V. 94, Journal of the Soil Mechanics and Foundation Division No. SM4, July 1968, Paper 6030, p. 923-50, (1968).

6. Jumikis, A. R., " Thermal Soil Mechanics " - Rutgers University Press, New Brunswick, New Jersey, (1966).

7. Krausz, A. S., " An Experimental Investigation of Strain Relaxation in Ice " - N.R.C. Canada, Division of Building Research, Research Paper No. 387, (1969).

8. Laba, J. T., " Lateral Thrust in Frozen Granular Soils Due to Temperature Change " - Highway Research Record 304, H.R.B. National Academy of Sciences, Washington D.C. (1970).

REFERENCES (continued)

9.   Laba, J. T., " Lateral Thrust Exerted by Frozen
       Granular Soils due to Temperature Change " - Ph.D.
       Thesis, Department of Civil Engineering, Faculty of
       Graduate Studies, University of Windsor, (1970).

10.   Penner, E., " The Importance of Freezing Rate in
       Frost Action in Soils " - Proceedings of the A.S.T.M.
       V. 60, (1960).

11.   Tsytovich, N. A., " Bases and Foundations on Frozen
       Soil " - Highway Research Board, Special Report 58,
       (1960).

12.   Tsytovich, N. A., Et. Al., " Basic Mechanics of Free-
       zing, Frozen and Thawing Soils " - N.R.C. Canada,
       Division of Building Research, Technical Translation
       1239, (1966).

13.   Voitkovskii, K. F., and Krylov, M. M., " Use of Ice,
       Snow and Frozen Soil in Engineering Structures " -
       N.R.C. Canada, Division of Building Research, Technical
       Translation 1267, (1967).

14.   Vyalov, S. S., Et. Al., " Methods of Determining
       Creep, Long Term Strength and Compressibility Charac-
       teristics of Frozen Soils " - N.R.C. Canada, Division
       of Building Research, Technical Translation 1364,
       (1966).
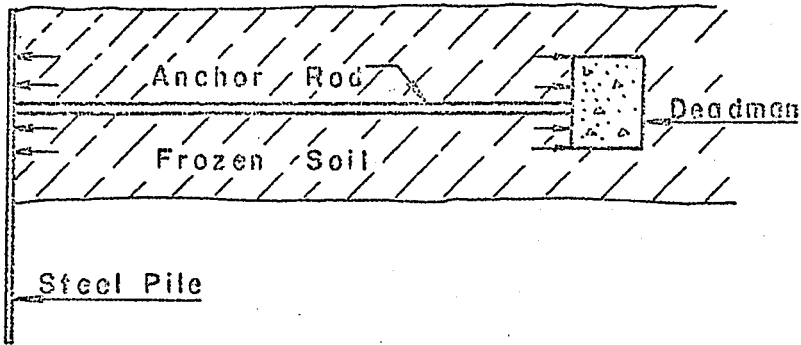
APPENDIX A

MISCELLANEOUS FIGURES

Fig. 1   Lateral Thrust Exerted by Frozen Soil

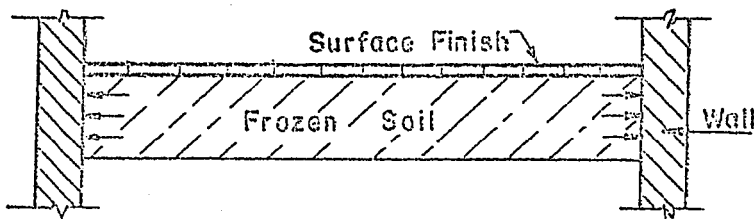Against Sheetpile and Deadman.

Fig. 2   Lateral Thrust Against the Confining

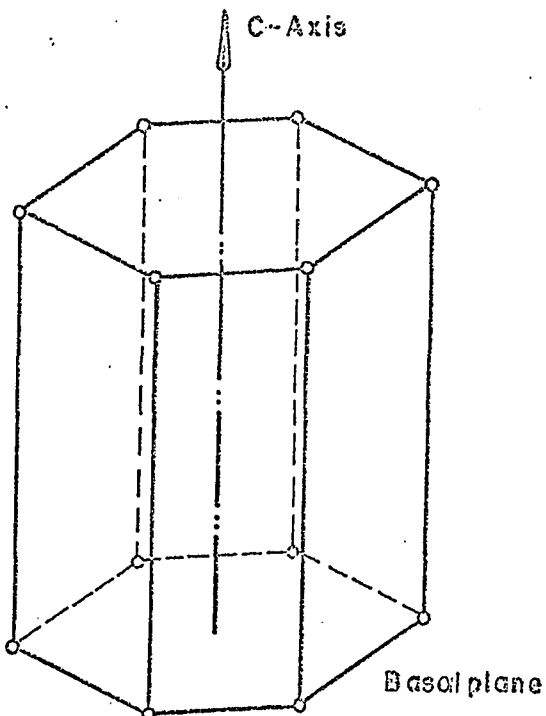Walls of a Car Park.

Fig. 3   A Simplified Model of a Hexagonal Prism
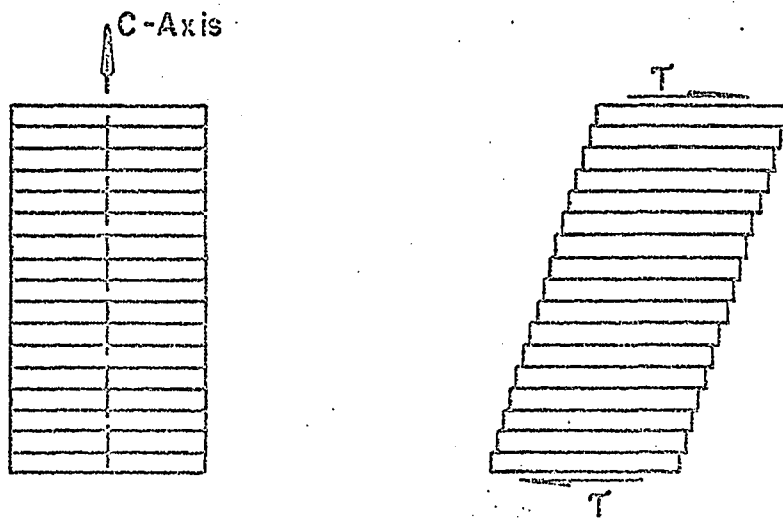   Unit. (after Krausz)

Fig. 4   Plastic Deformation Under the Effect of
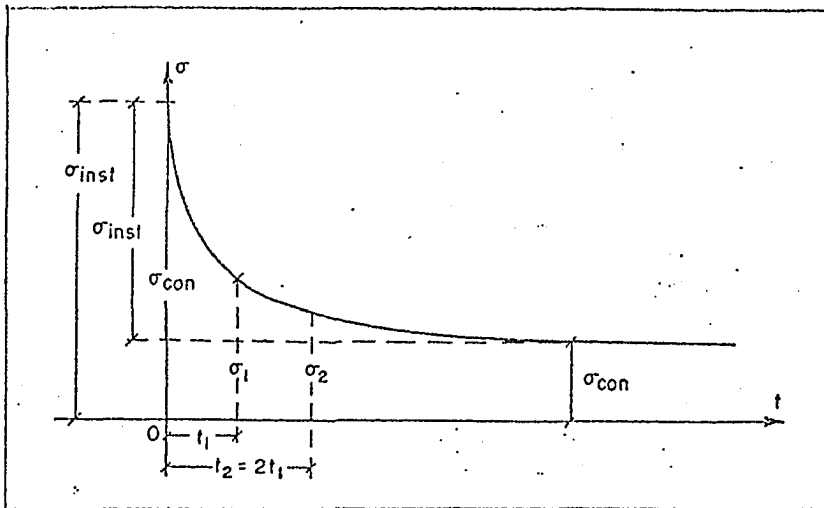   Shear Stress   (after Krausz).

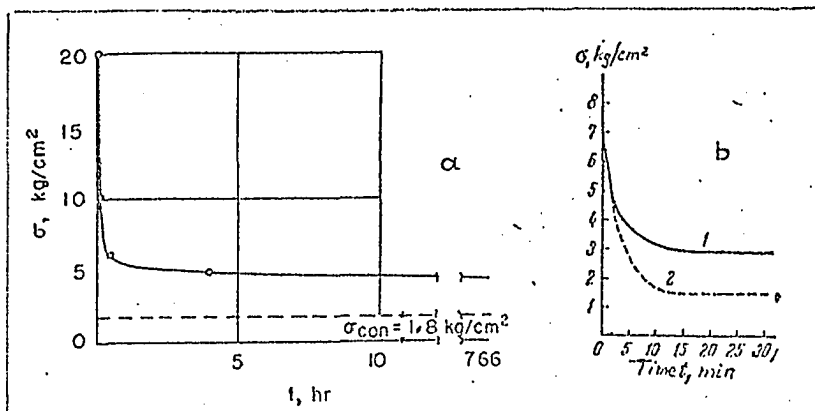Fig. 5 The Curve of the Relaxation of Stresses
in Frozen Soils. (after Tsytovich)

Fig. 6 a) Long Term Strength Characteristics of
. Frozen Soil Under Tensile Stress.
b) Experimental (1) and Theoretical (2)
Curves Illustrating Relaxation Character-
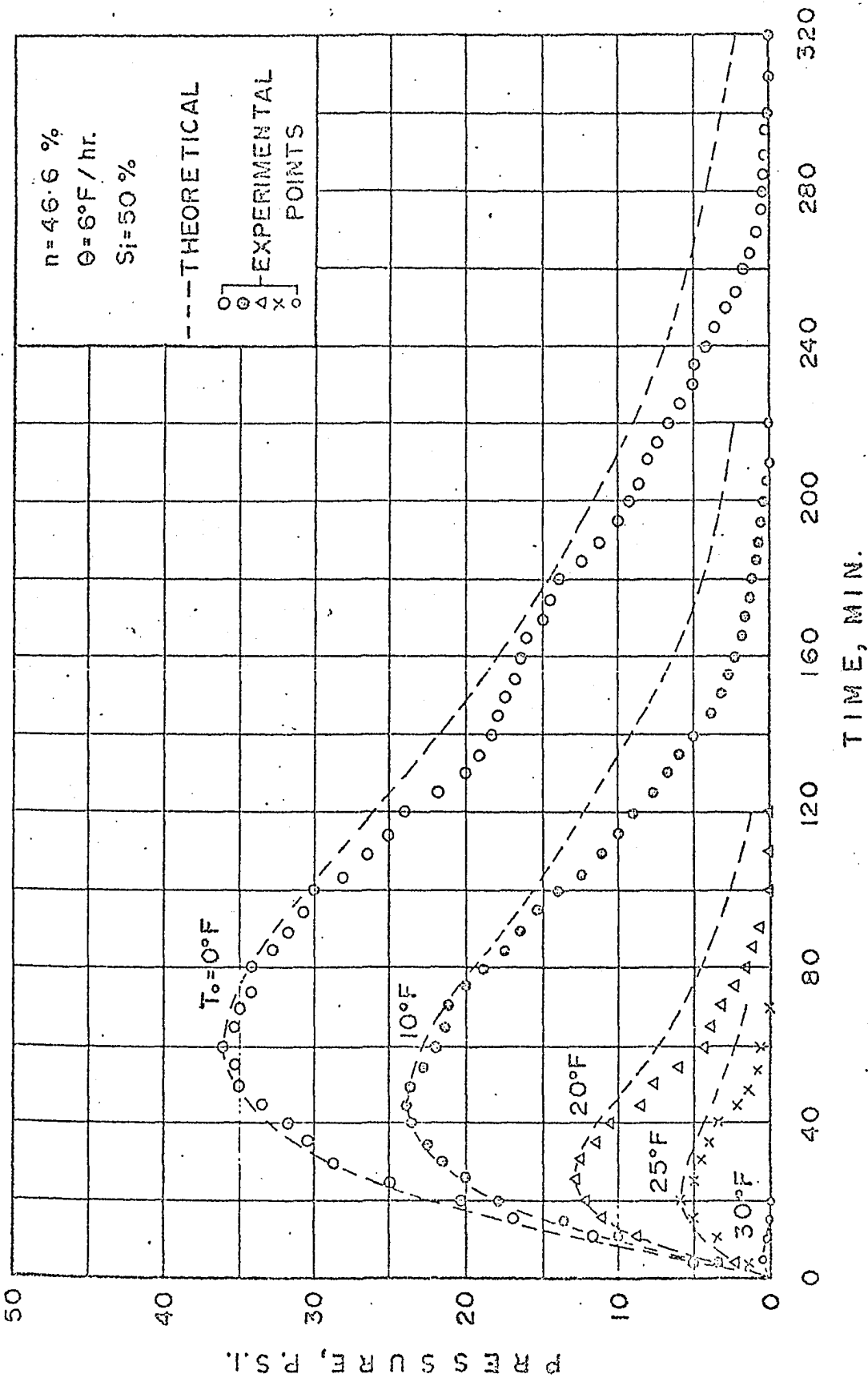istics of Frozen Fine Sandy Loam.
(after Tsytovich)

n = 46·6 %
Θ = 6°F / hr.
Si = 50 %

——— THEORETICAL

⊖⊖ △ × ○ ⟩ EXPERIMENTAL POINTS

PRESSURE, P.S.I.

50   40   30   20   10   0

TIME, MIN.

0   40   80   120   160   200   240   280   320

$T_o = 0°F$

10°F.

20°F

25°F

30°F.

Fig. 7   Typical Pressure-Time Curves for Temperature Rise of 6°F/hr
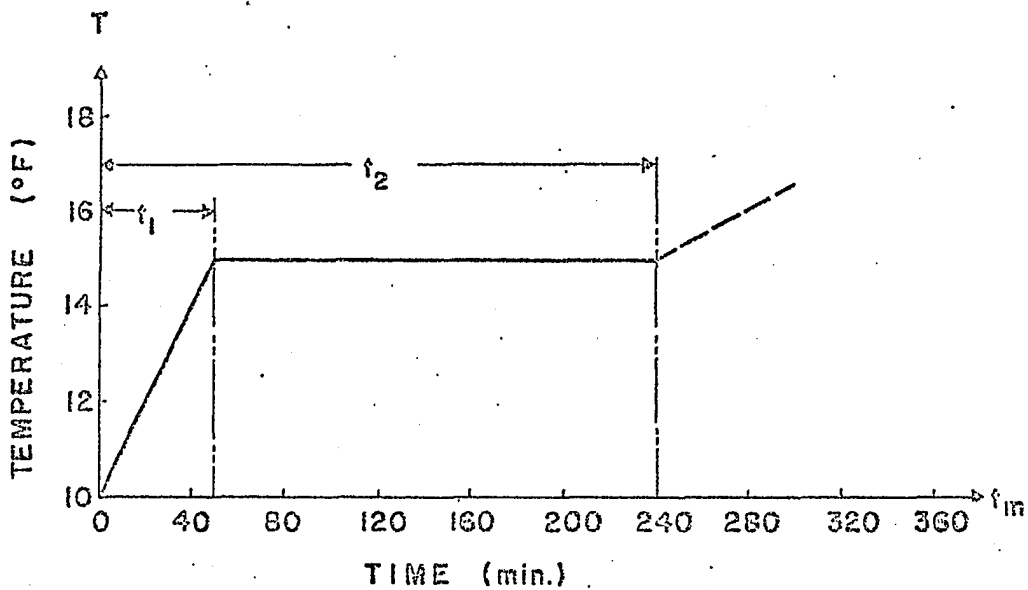From the Indicated Initial Temperatures T_o (after Laba)

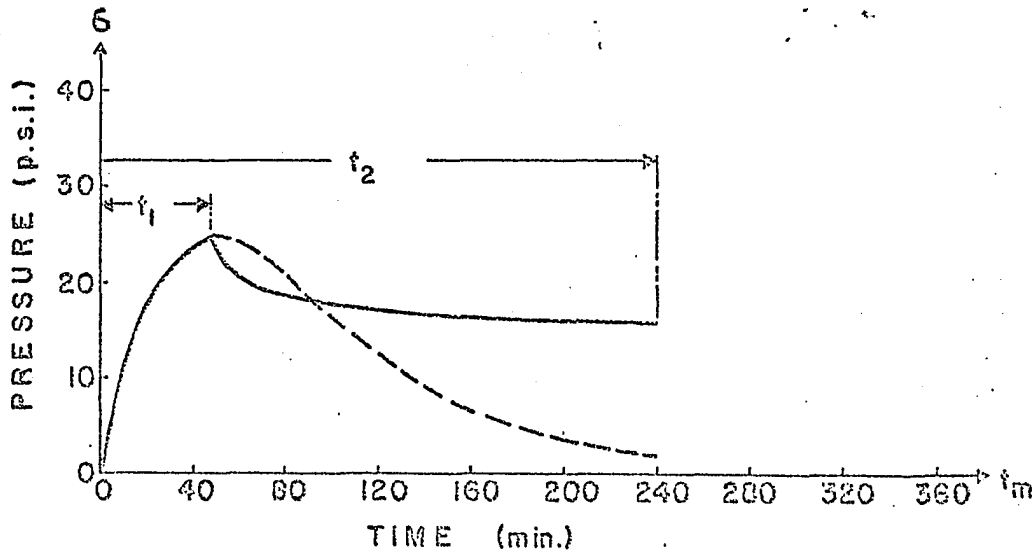Fig. 8 Possible Temperature Variation in Nature.

Fig. 9 Expected Pressure-Time Curve For Temperature
Condition Shown in Fig. 8.
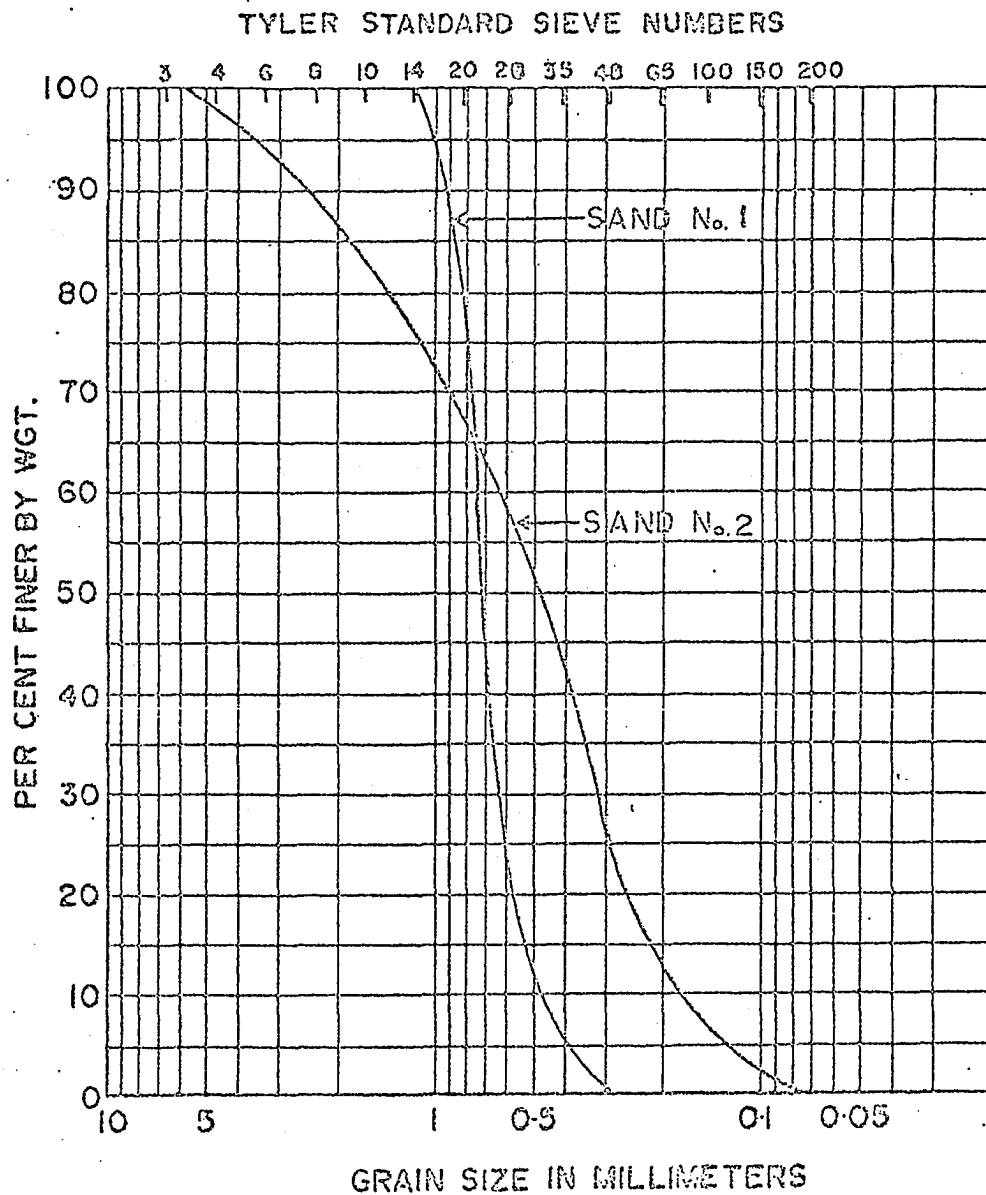
Fig. 10 Grain Size Distribution Diagram.
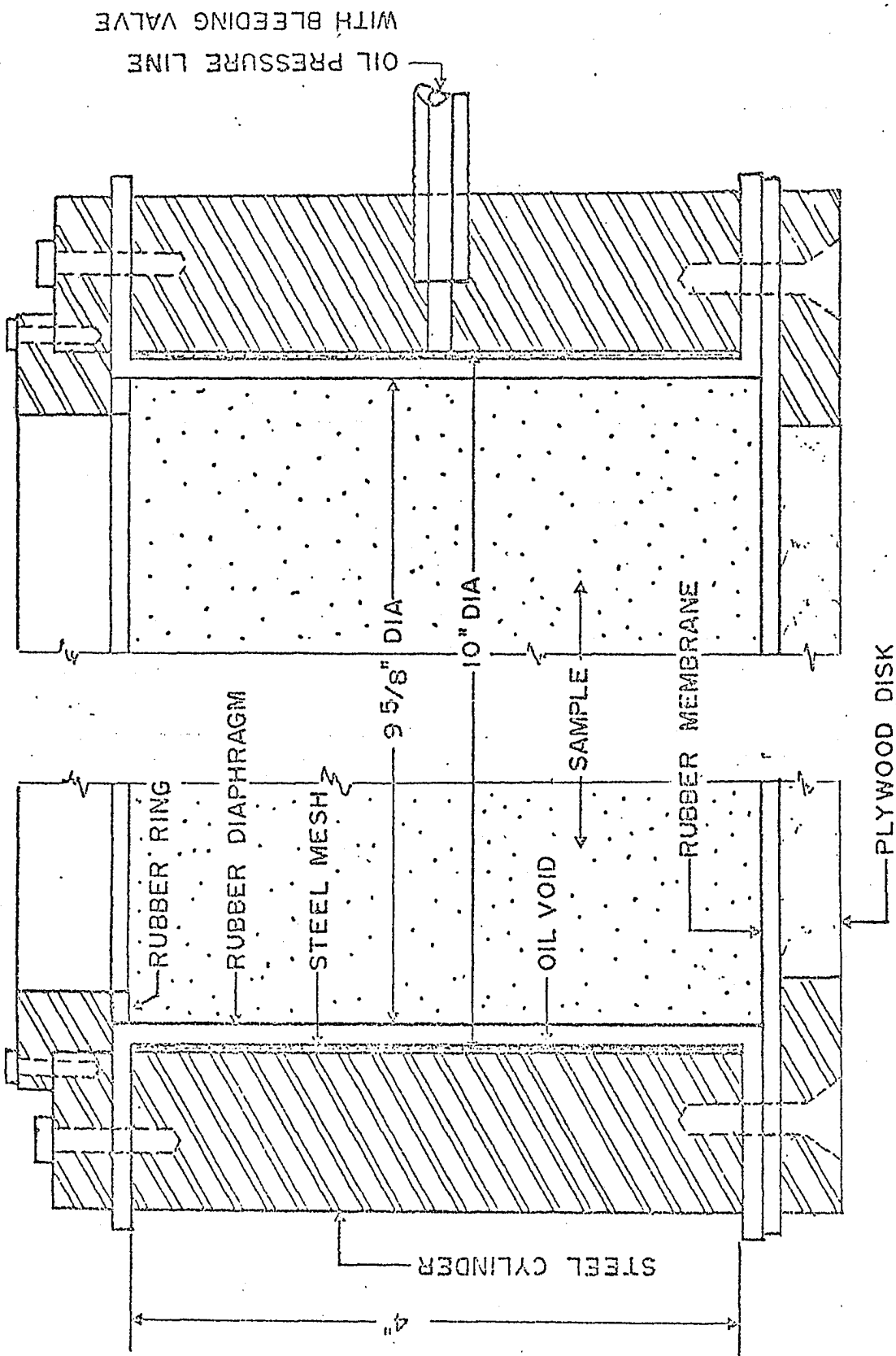
Fig. 11 Cross-Sectional View of the Pressure Unit Showing the Steel Cylinder and Rubber Diaphragm.
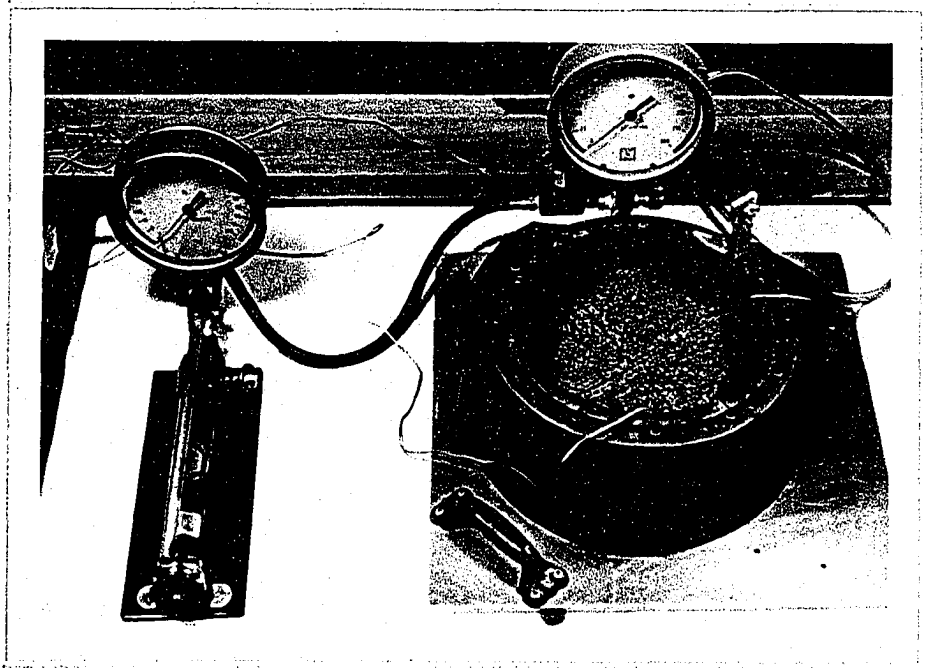
Fig. 12   The Pressure Unit with the Pressure Pump.

Fig. 13   Temperature Potentiometer (Left) and Strain
          Indicator (Right).
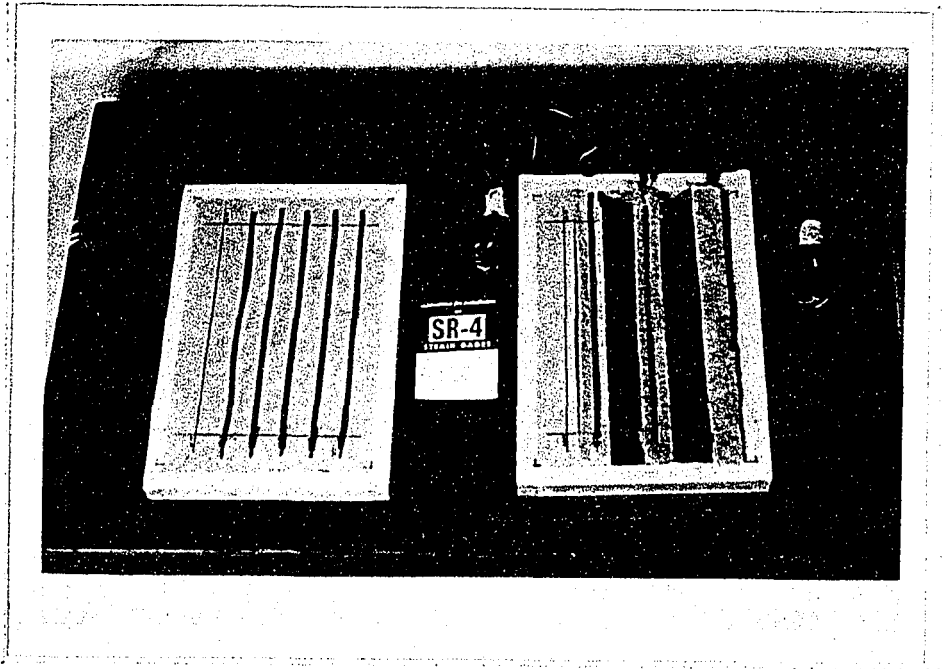
Fig. 14 Strain Gauges as Manufactured (Left) and Coated with Sand (Right).
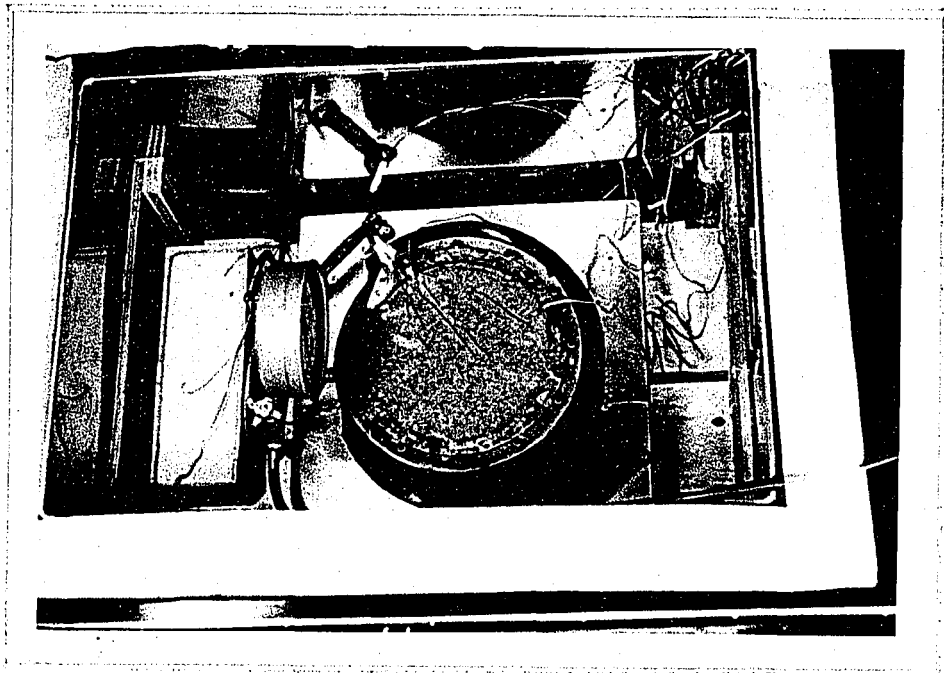
Fig. 15 Pressure Unit Inside the Freezer.
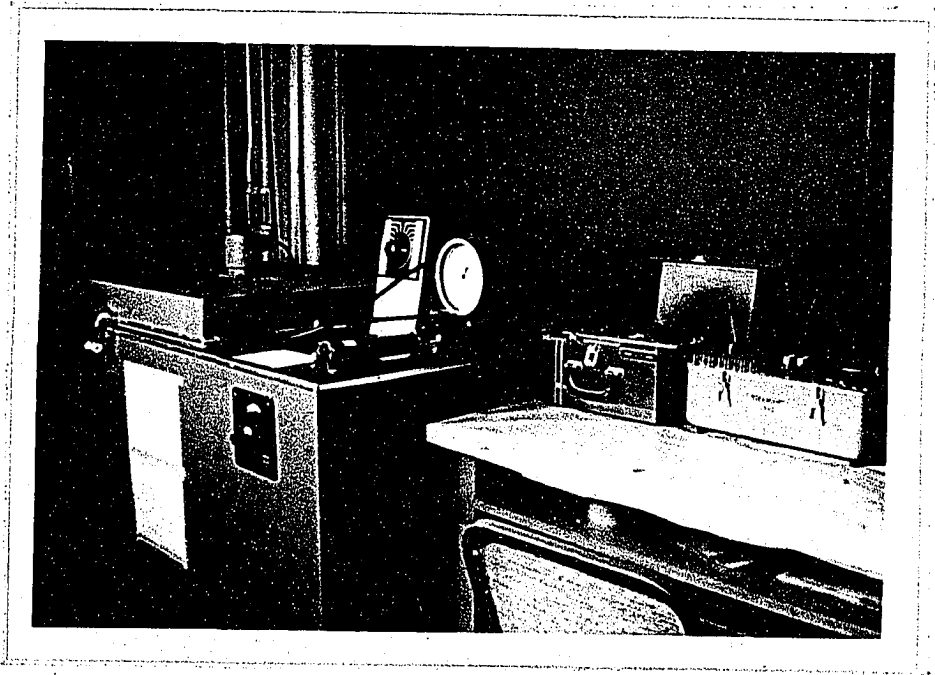
Fig. 16   Complete Experimental Set Up.
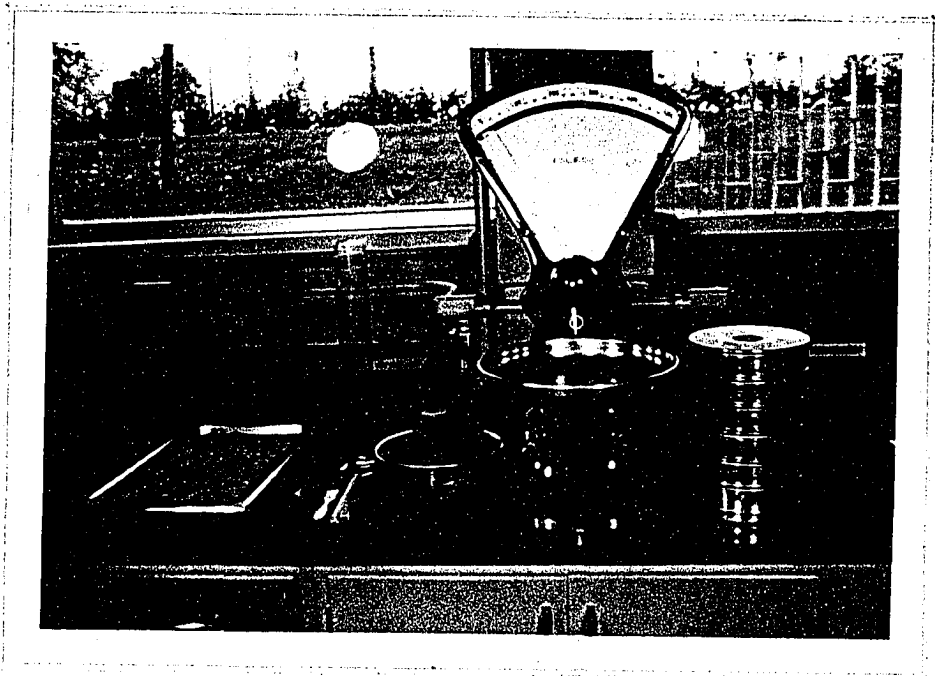
Fig. 17   Accessories Used in the Tests.

APPENDIX B

FIGURES SHOWING

TEST DATA IN GRAPHICAL FORM
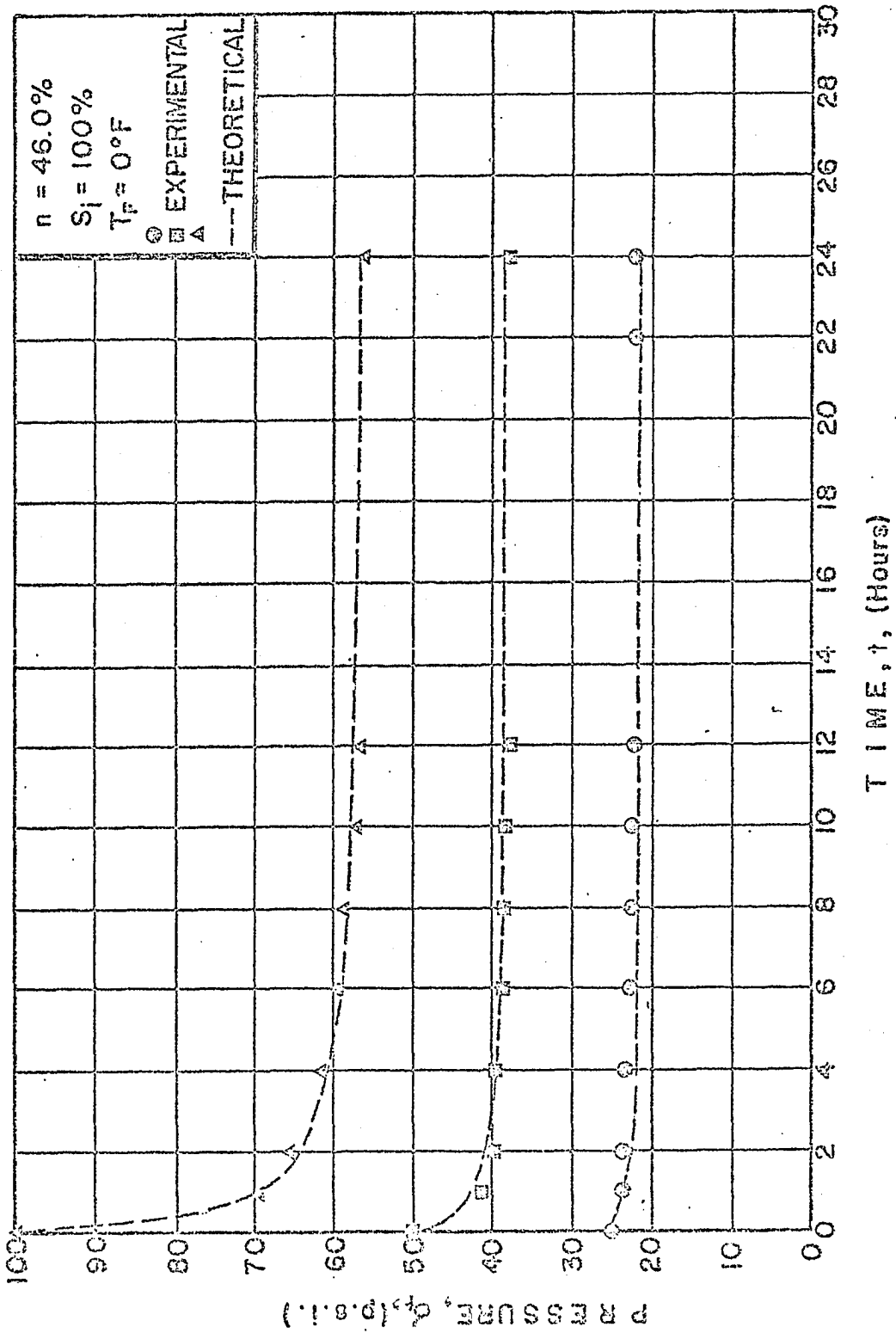
Fig. 18 Comparison Between Experimental and Calculated Values for Pressure-Time Curves at Three Different Initial Pressures.
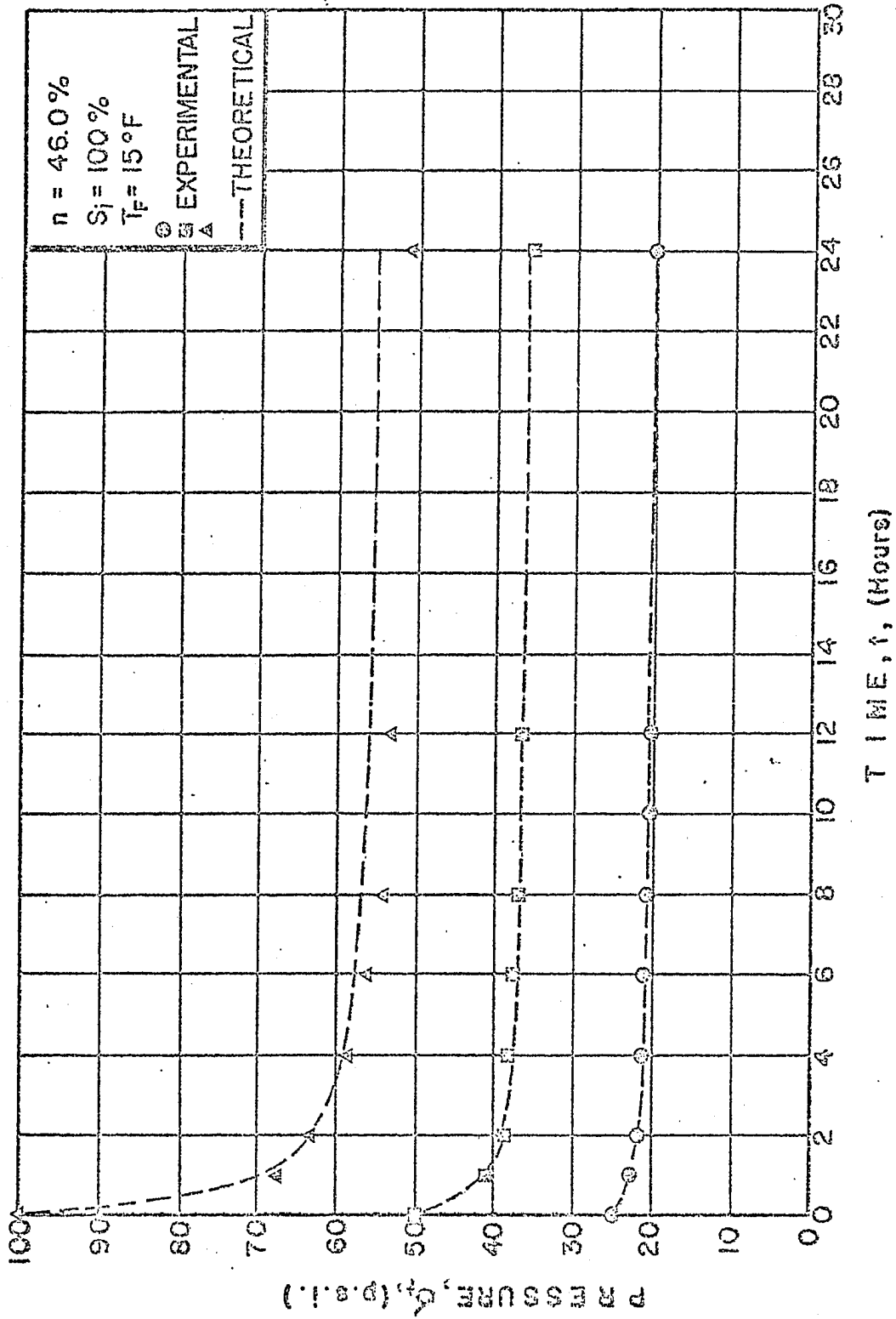
Fig. 19 Comparison Between Experimental and Calculated Values for Pressure—Time Curves at Three Different Initial Pressures.
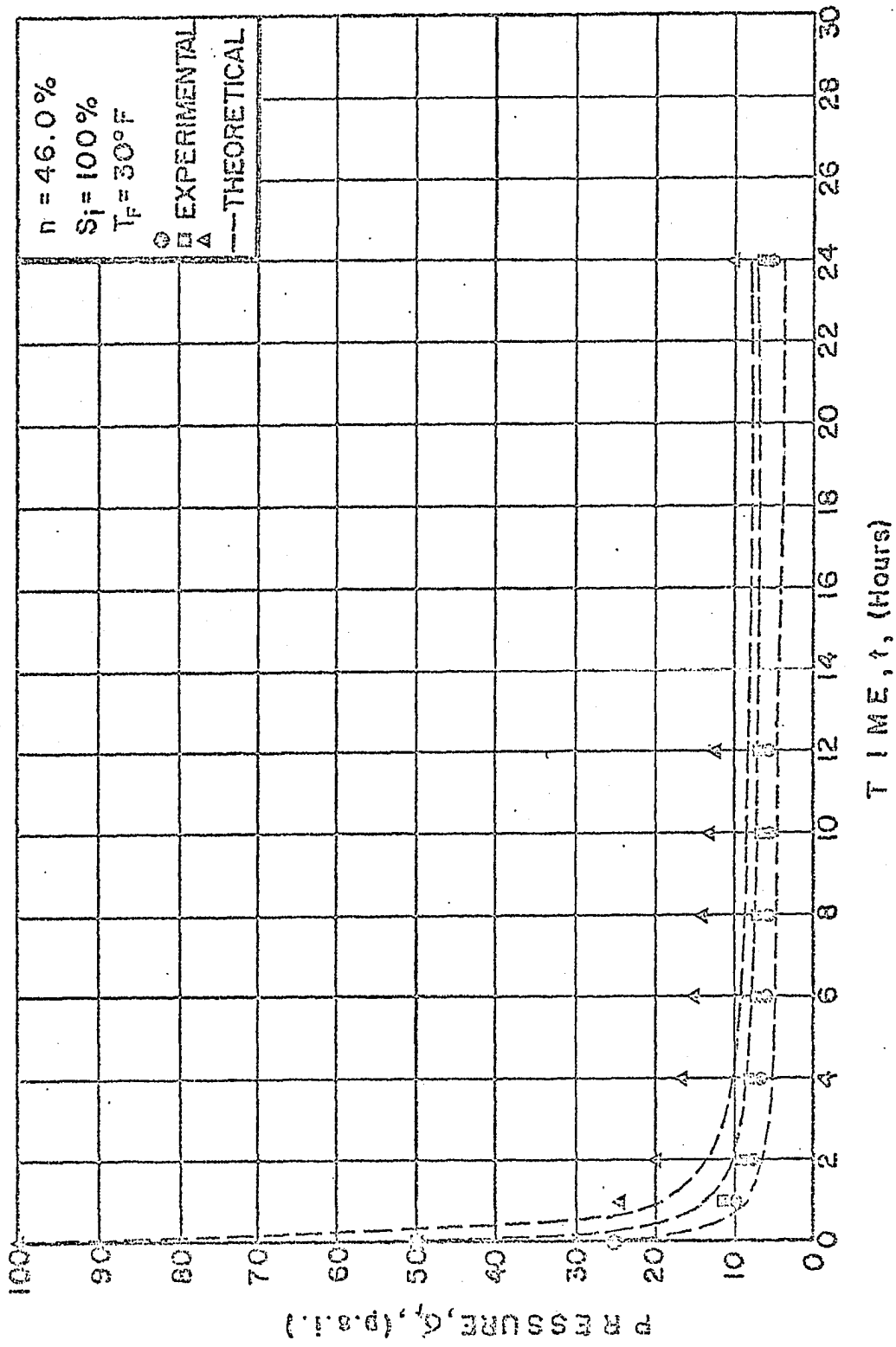
Fig. 20 Comparison Between Experimental and Calculated Values for Pressure-Time Curves at Three Different Initial Pressures.
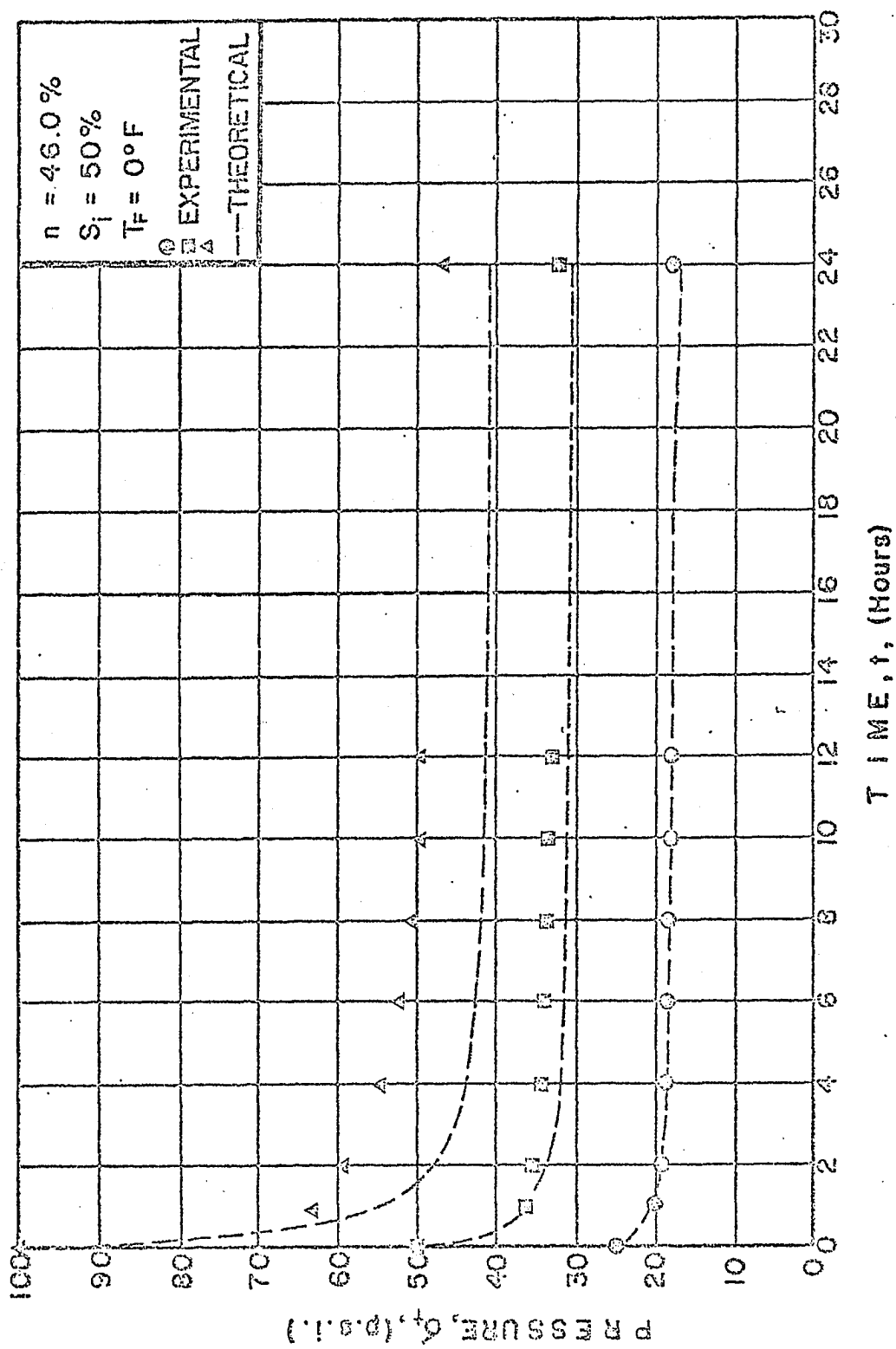
Fig. 21 Comparison Between Experimental and Calculated Values for Pressure-Time Curves at Three Different Initial Pressures.
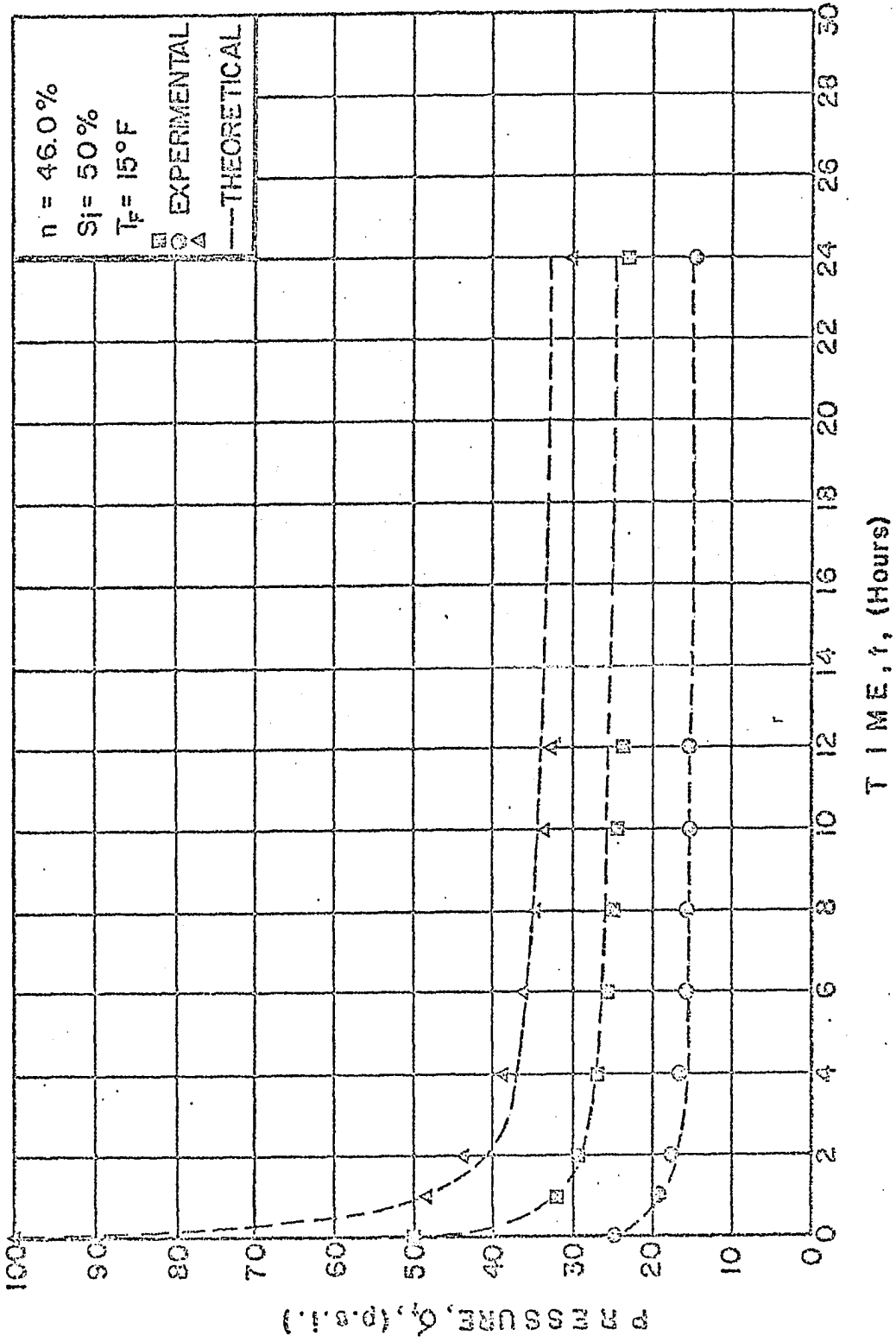
Fig. 22 Comparison Between Experimental and Calculated Values for Pressure-Time Curves at Three Different Initial Pressures.
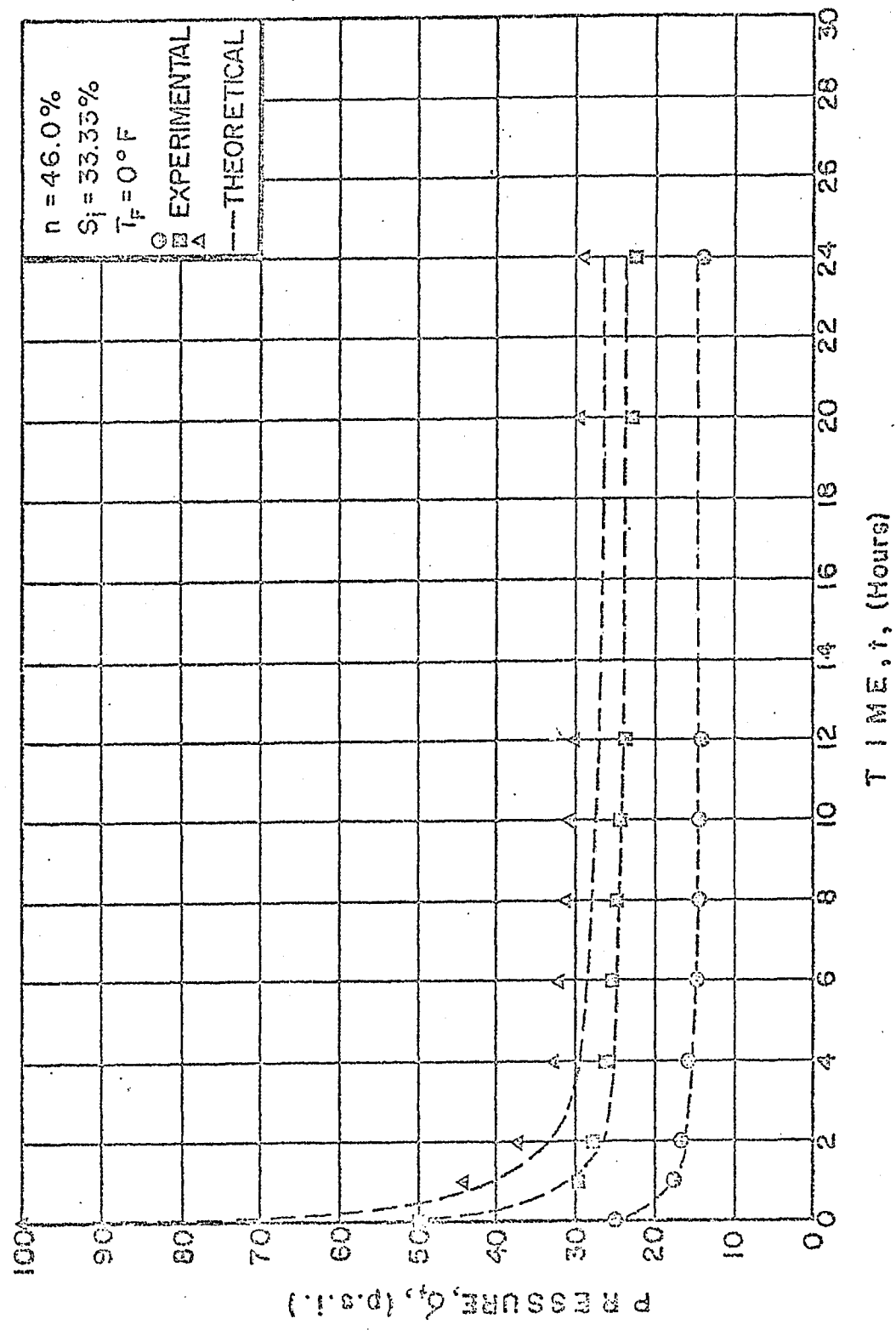
Fig. 23 Comparison Between Experimental and Calculated Values for Pressure-Time Curves at Three Different Initial Pressures.
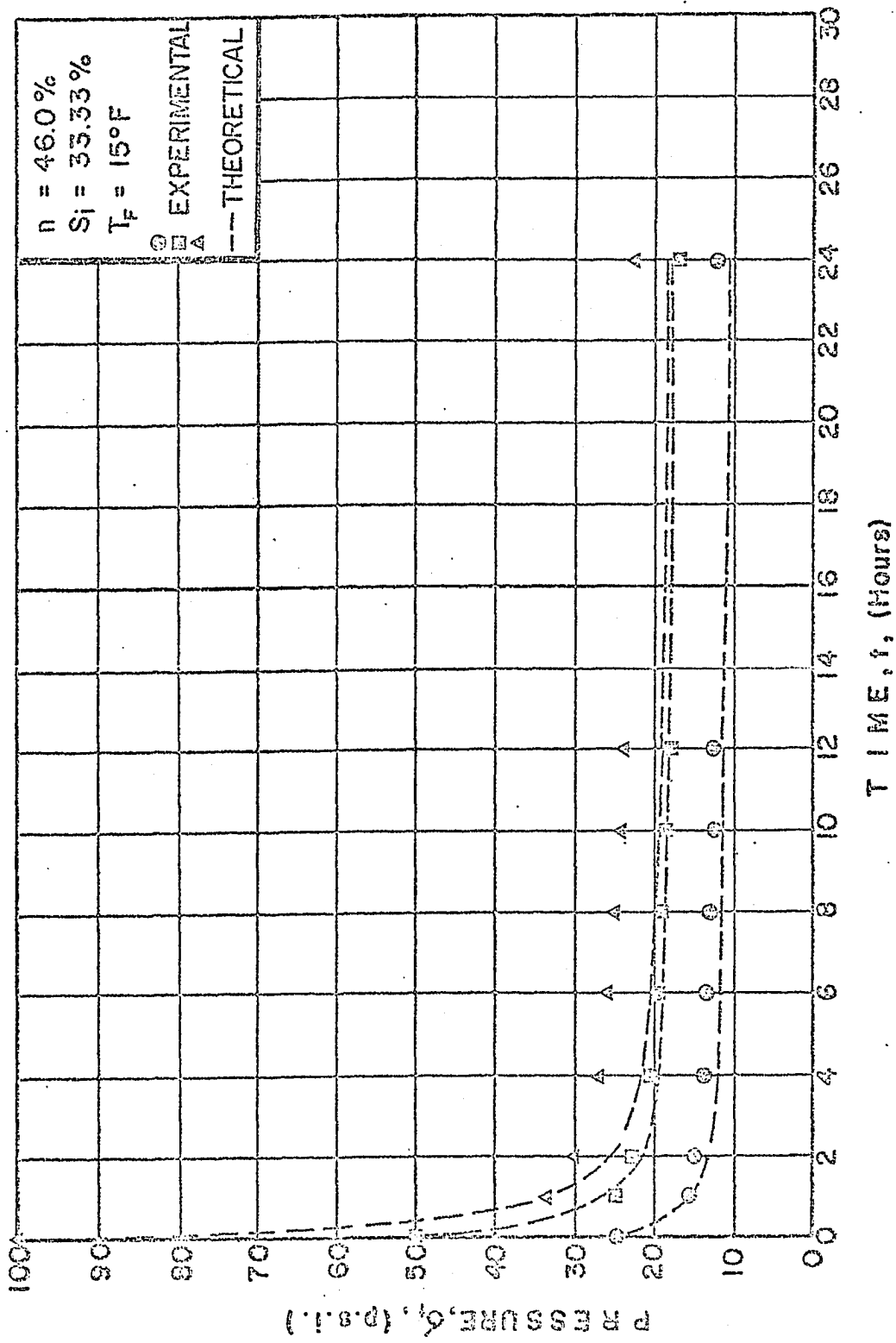
Fig. 24 Comparison Between Experimental and Calculated Values for Pressure-Time Curves at Three Different Initial Pressures.
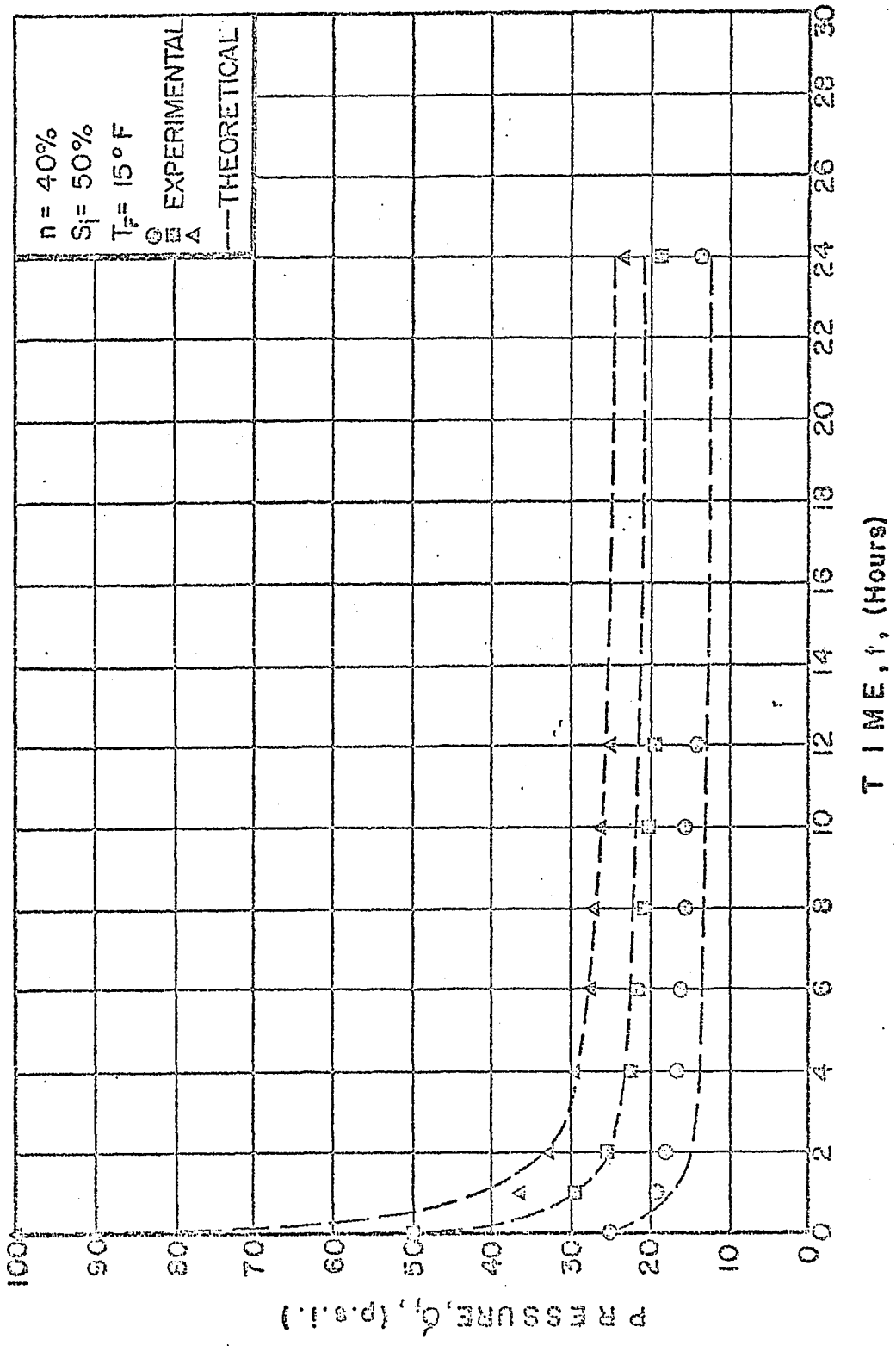
Fig. 25 Comparison Between Experimental and Calculated Values for Pressure—Time Curves at Three Different Initial Pressures.
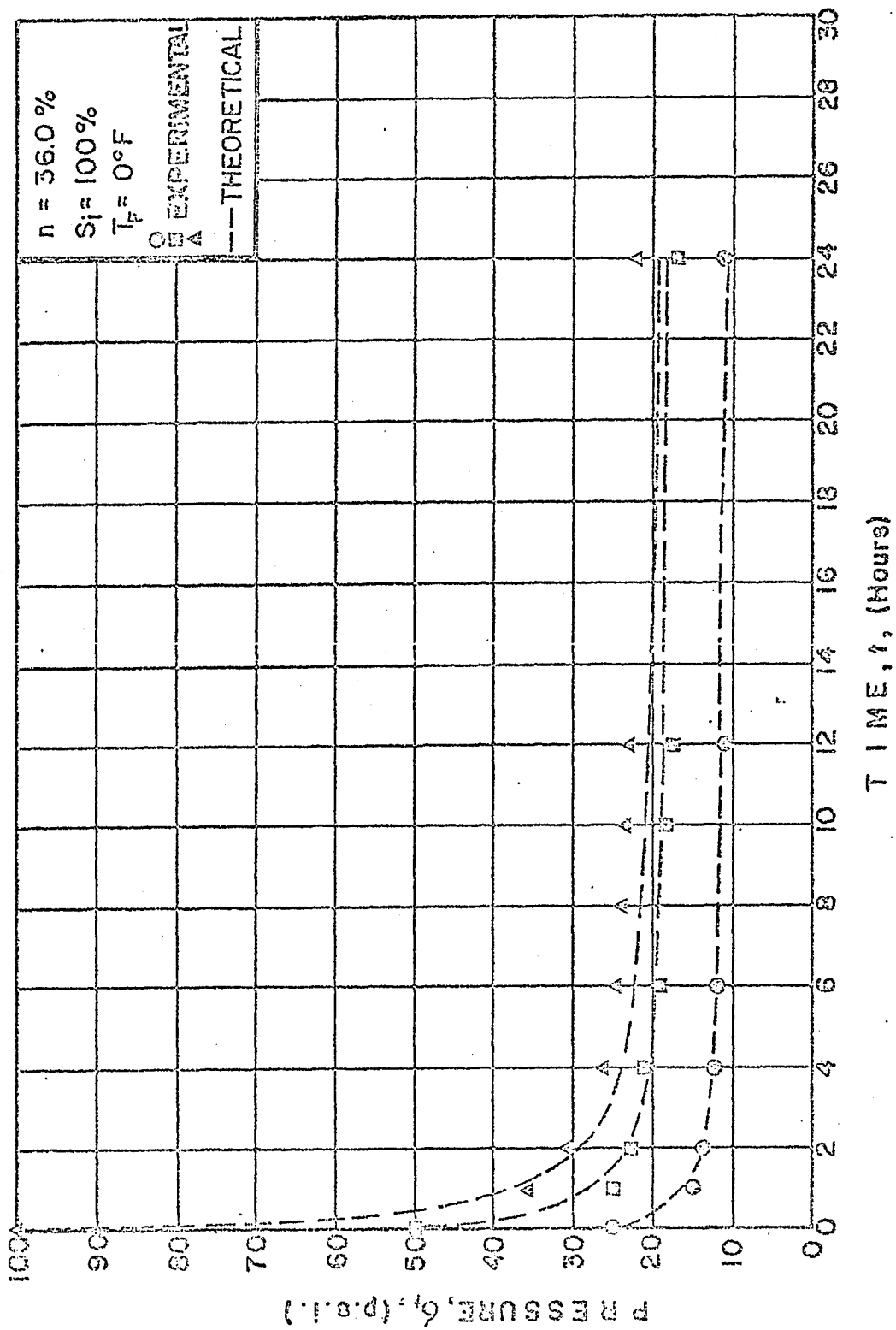
Fig. 26   Comparison Between Experimental and Calculated Values for Pressure.
Time Curves at Three Different Initial Pressures.
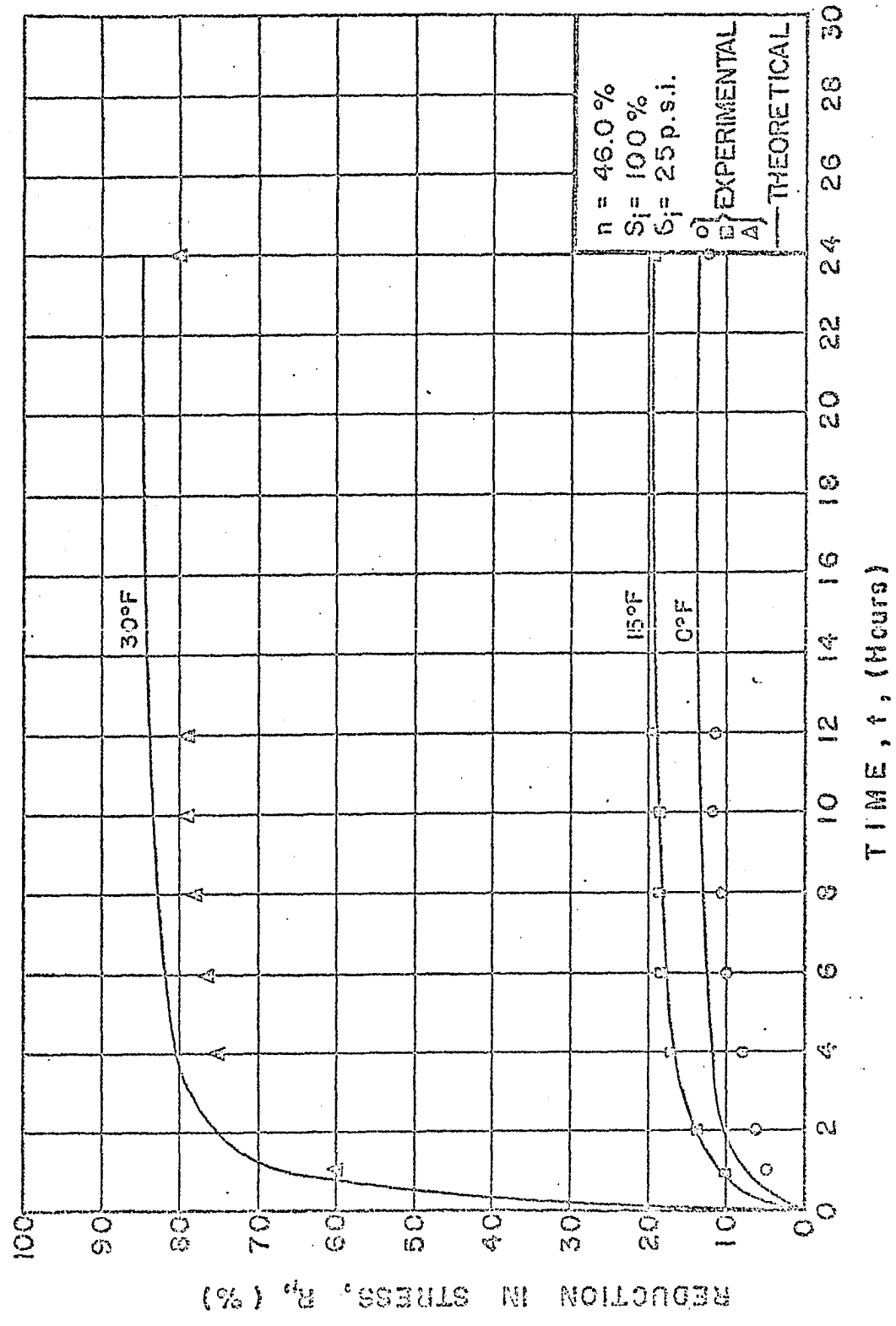
Fig. 27 Reduction in Lateral Stress vs Time at Selected Constant
Temperatures Under Indicated Conditions.
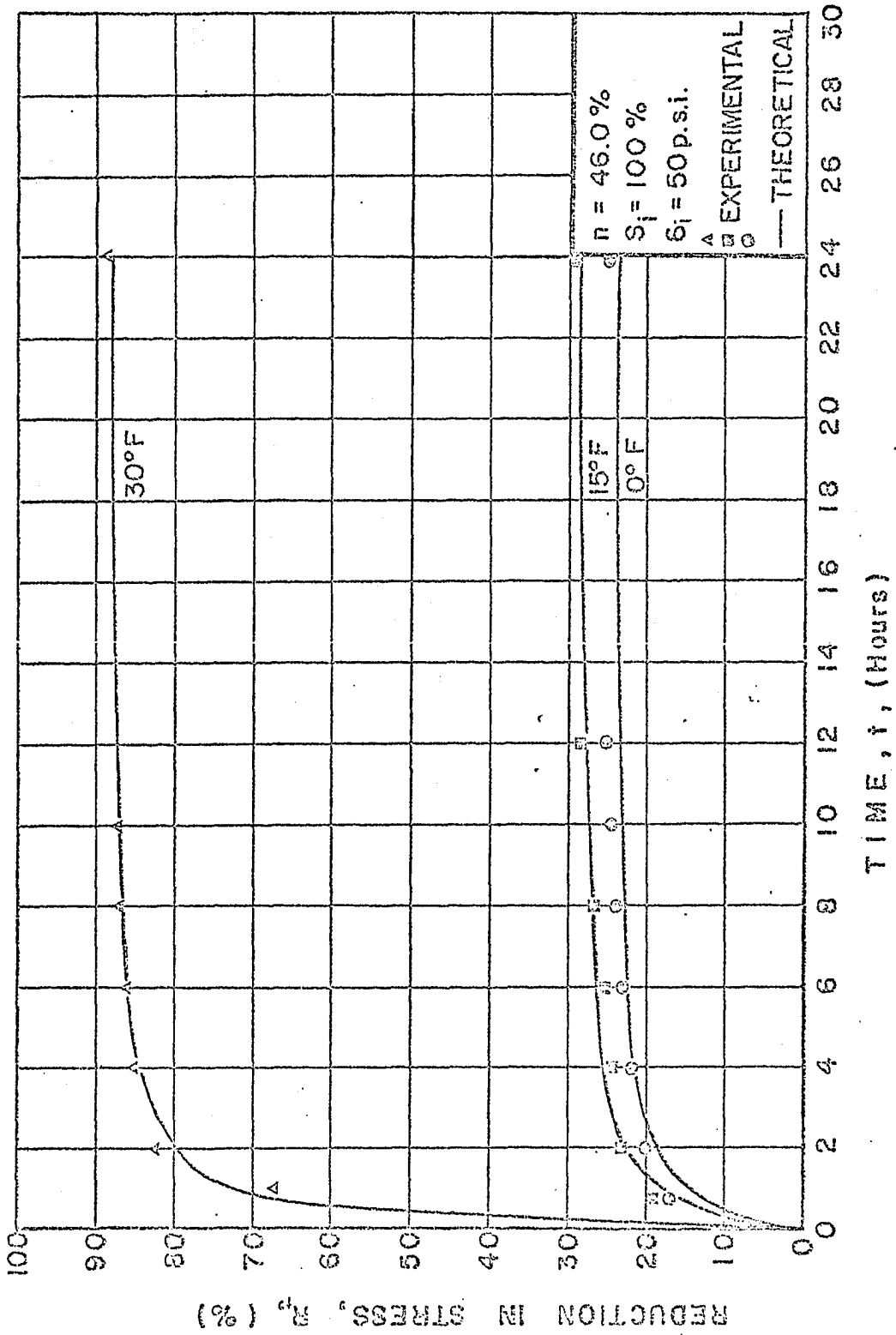
Fig. 28 Reduction in Lateral Stress vs Time at Selected Constant Temperatures Under Indicated Conditions.
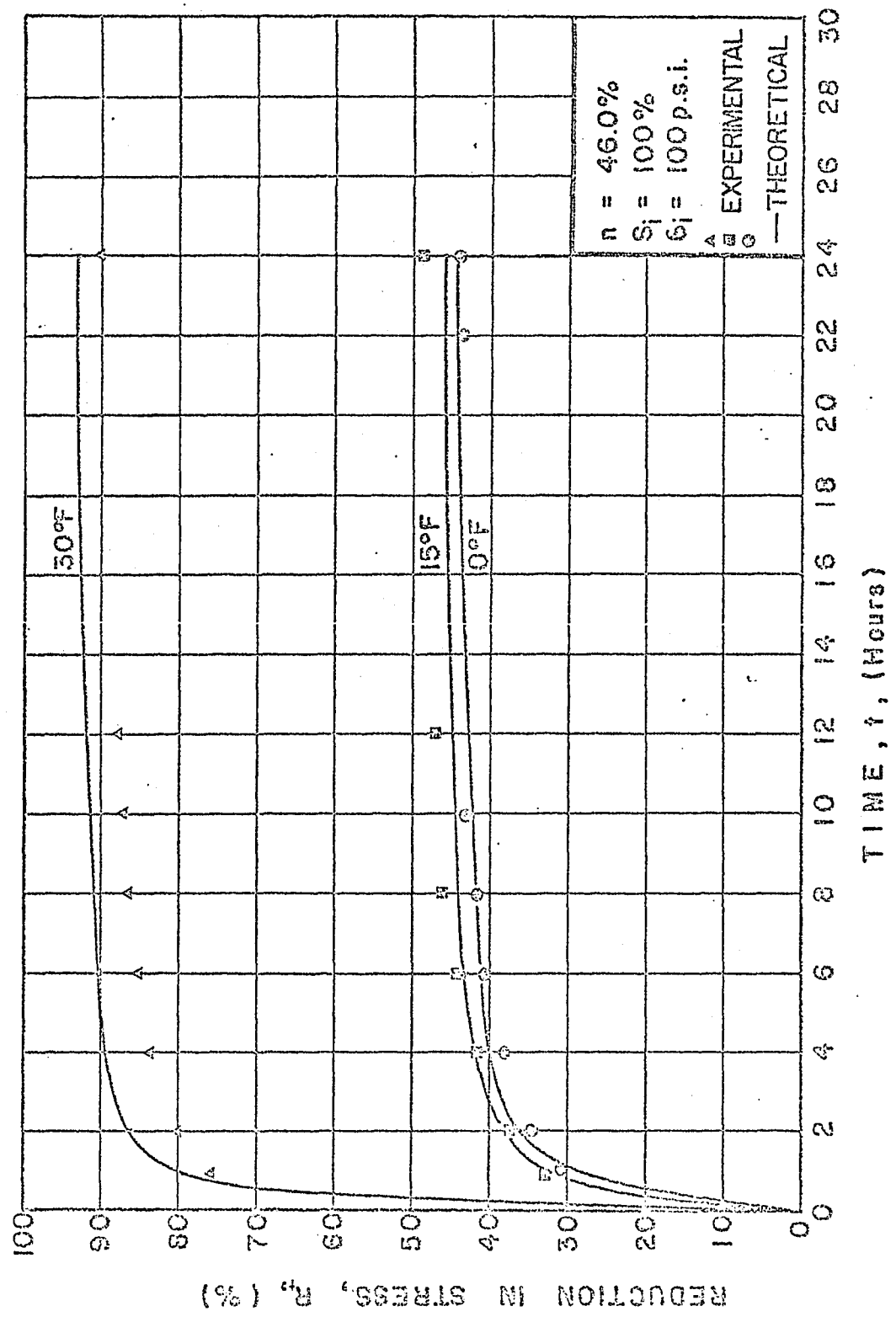
Fig. 29 Reduction in Lateral Stress vs Time at Selected Constant Temperatures Under Indicated Conditions.
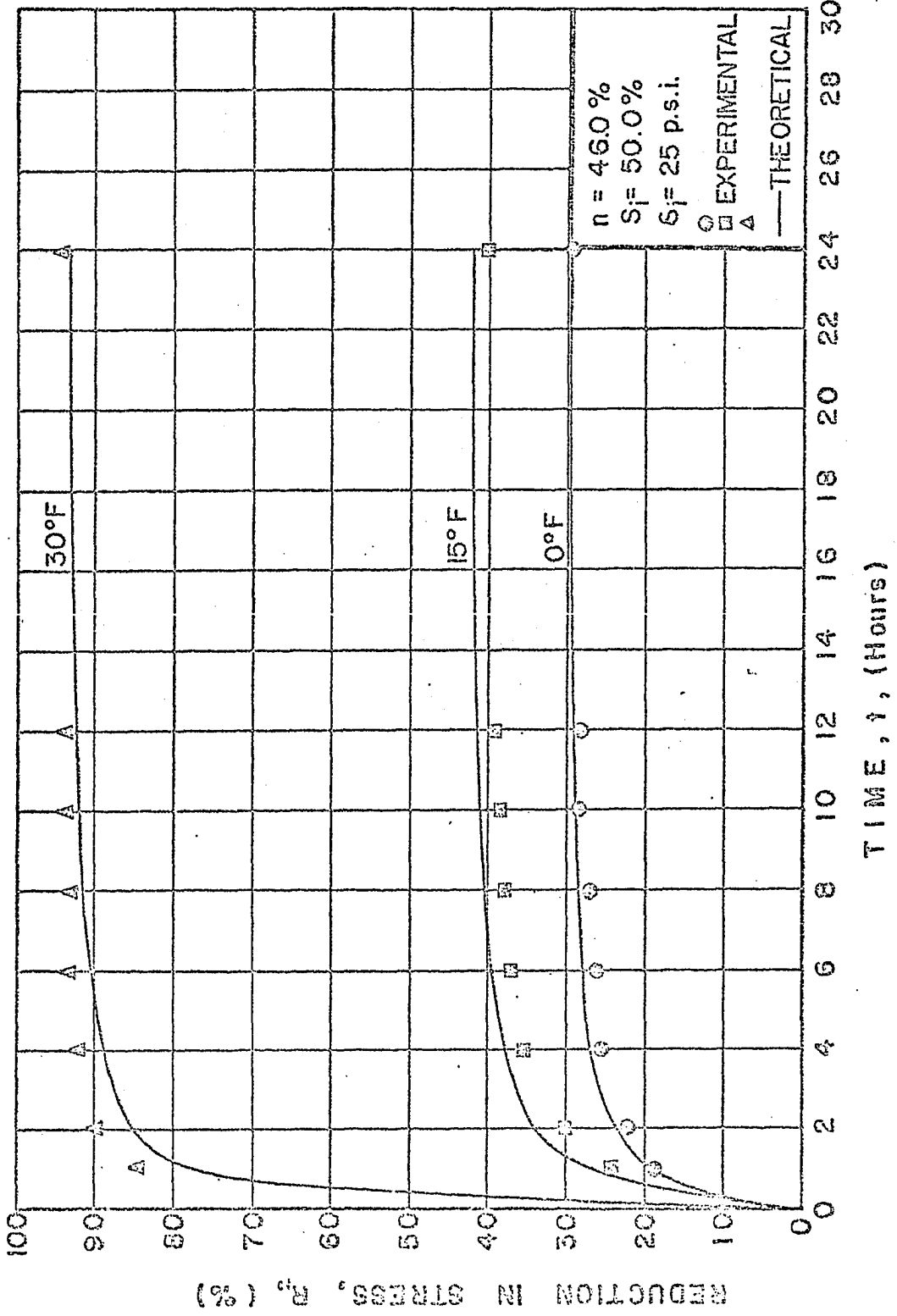
Fig. 30 Reduction in Lateral Stress vs Time at Selected Constant Temperatures Under Indicated Conditions.
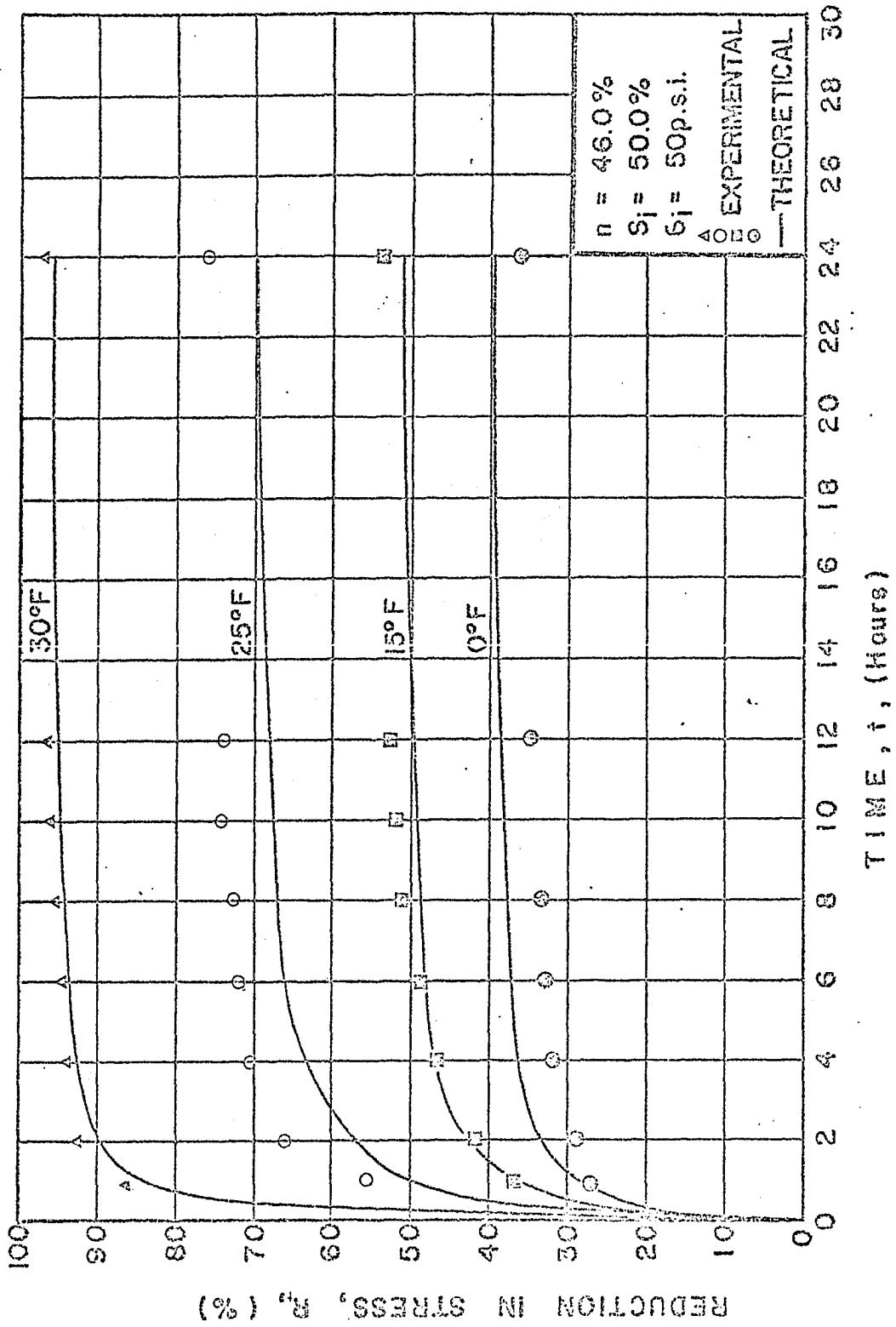
Fig. 31 Reduction in Lateral Stress vs Time at Selected Constant Temperatures Under Indicated Conditions.
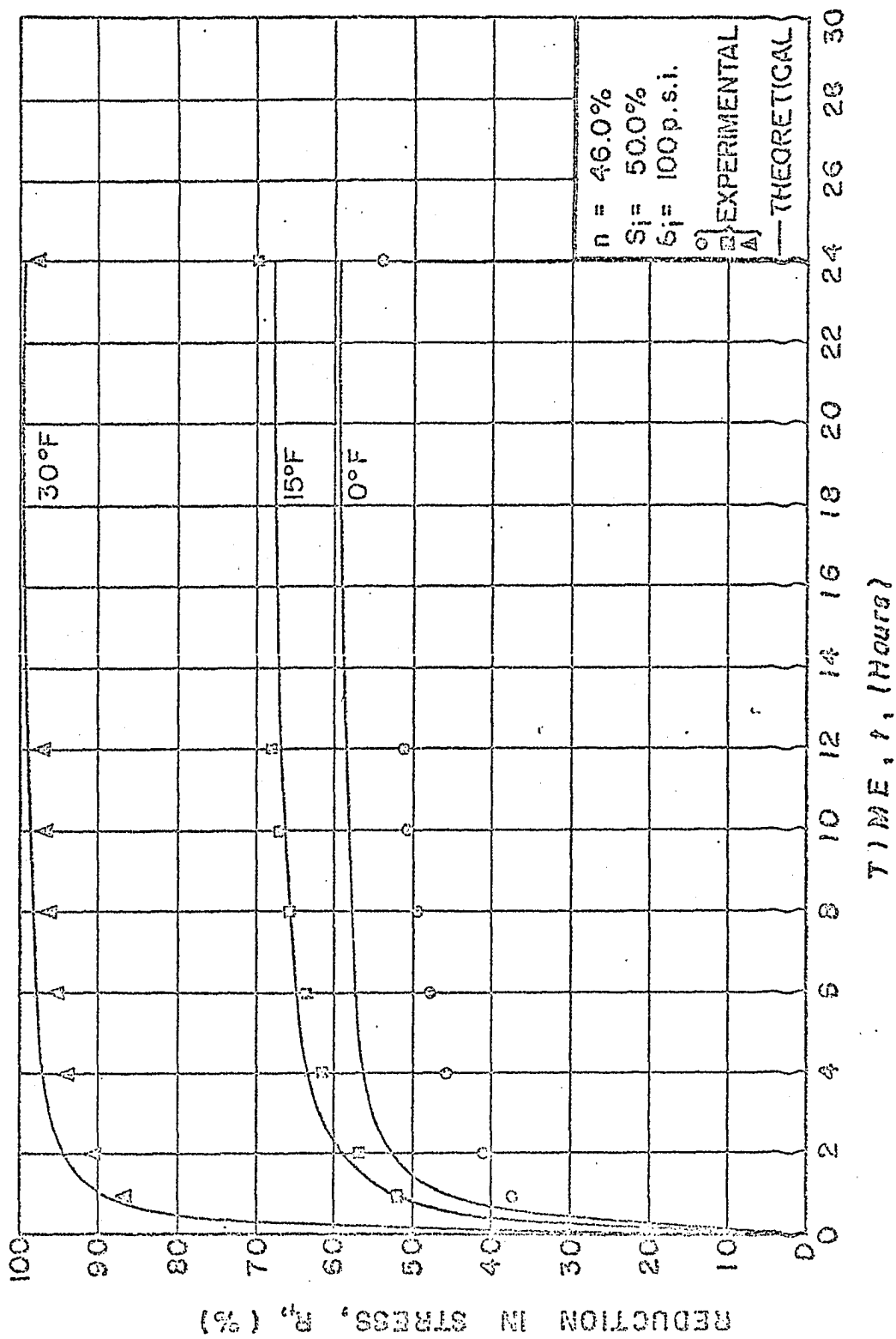
Fig. 32 Reduction in Lateral Stress vs Time at Selected Constant
Temperatures Under Indicated Conditions.
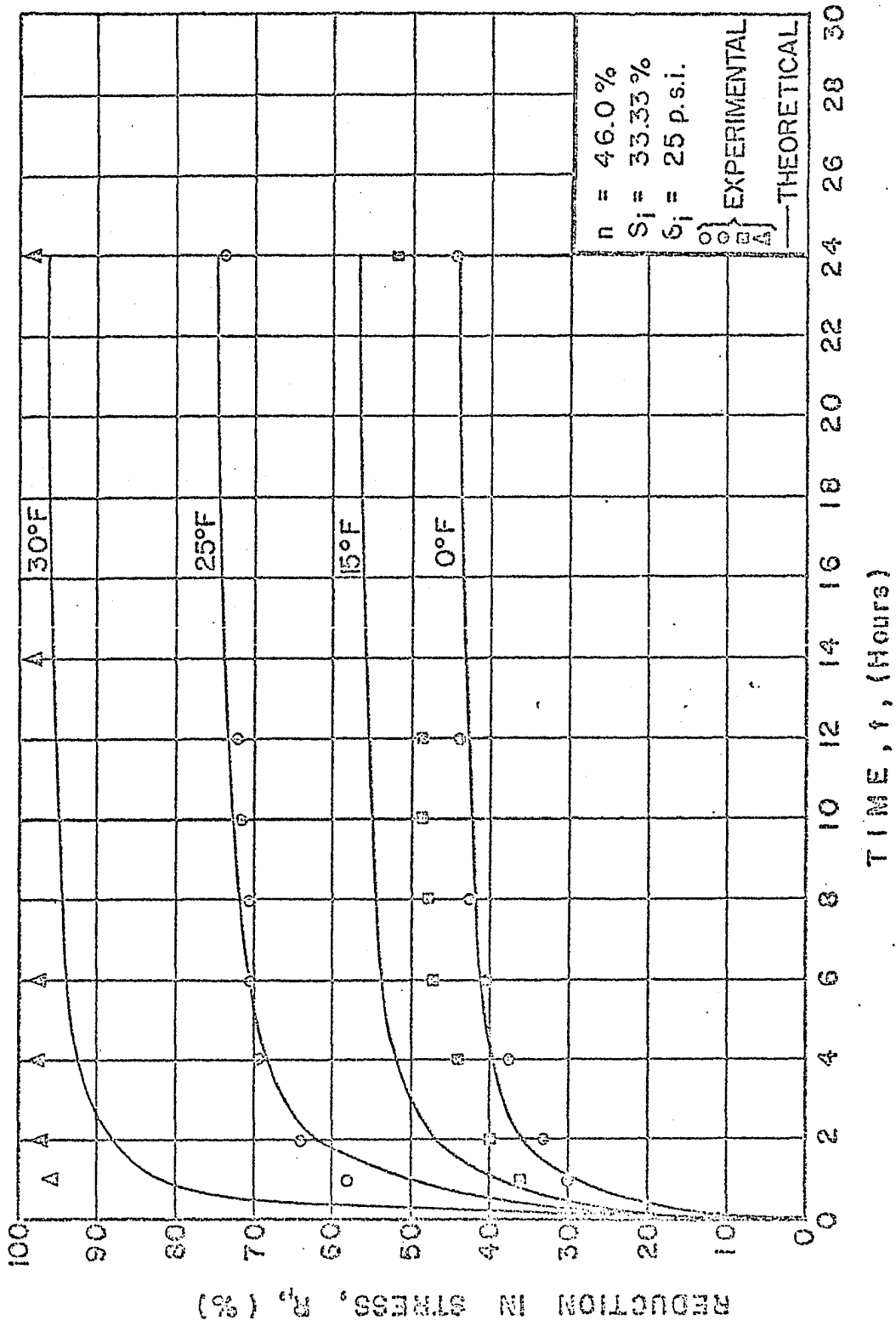
Fig. 33 Reduction in Lateral Stress vs Time at Selected Constant Temperatures Under Indicated Conditions.
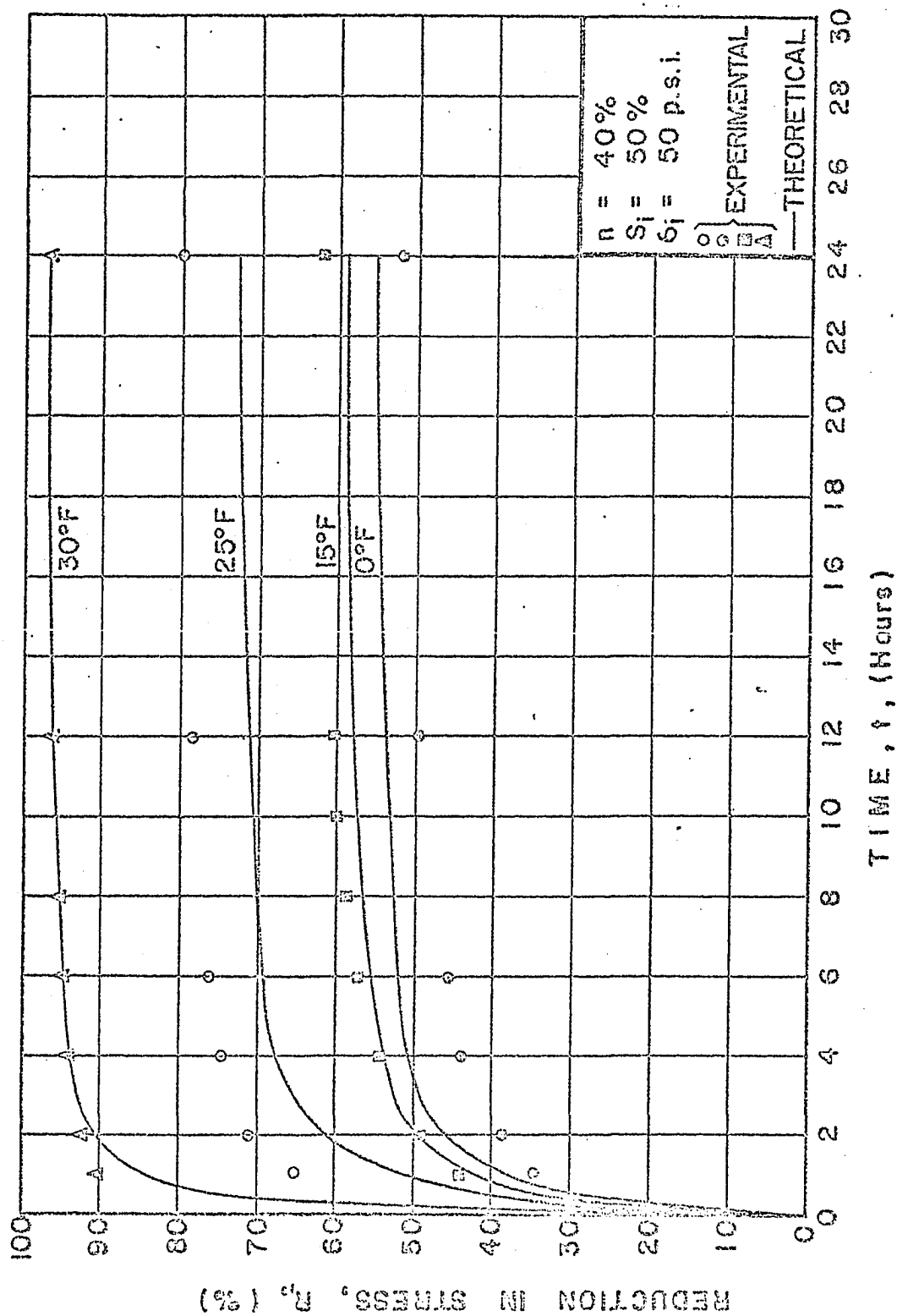
Fig. 34 Reduction in Lateral Stress vs Time at Selected Constant Temperatures Under Indicated Conditions.
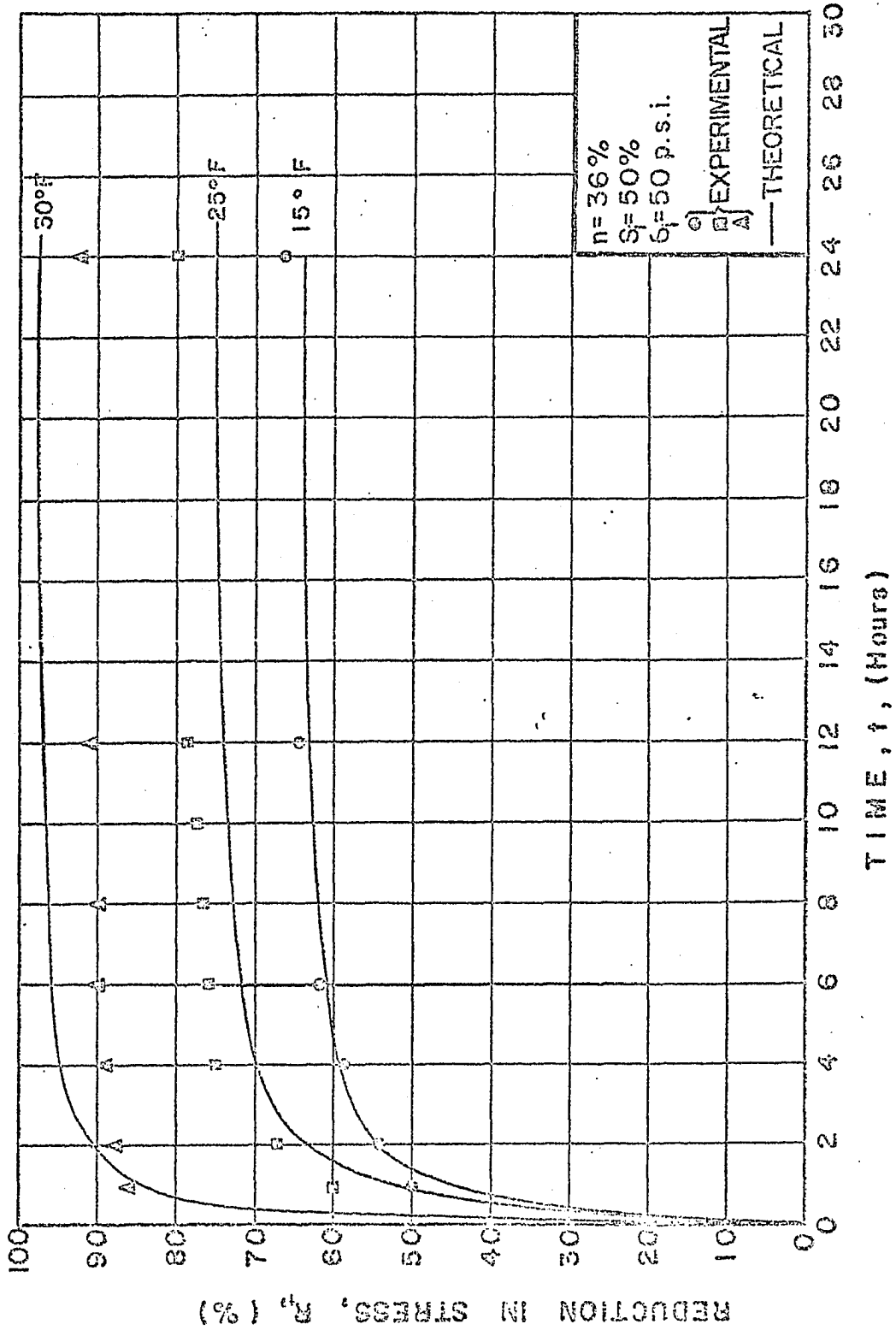
Fig. 35 Reduction in Lateral Stress vs Time at Selected Constant Temperatures Under Indicated Conditions.

74
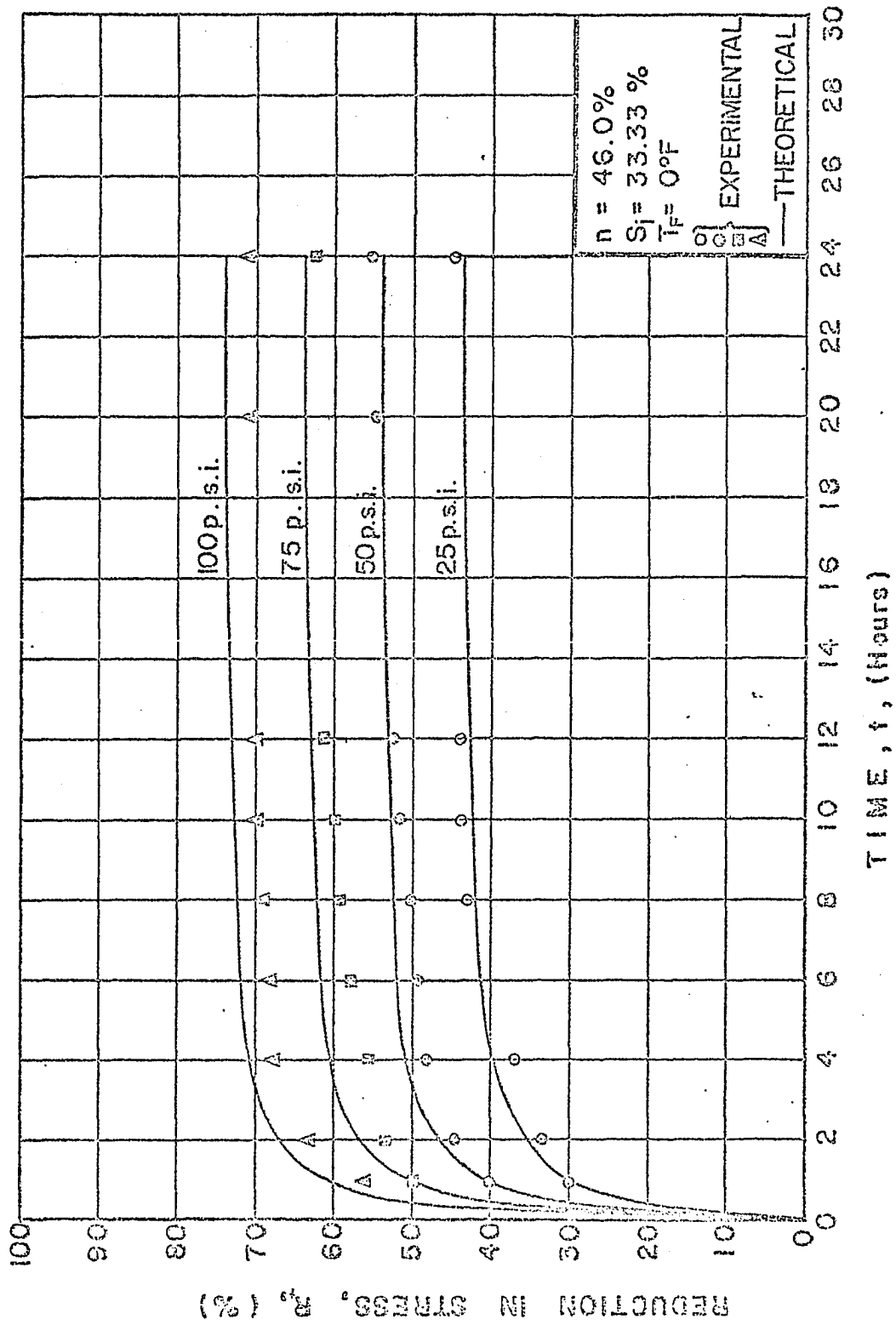
Fig. 36 Reduction in Lateral Stress vs Time at Selected Initial
Pressures Under Indicated Conditions.
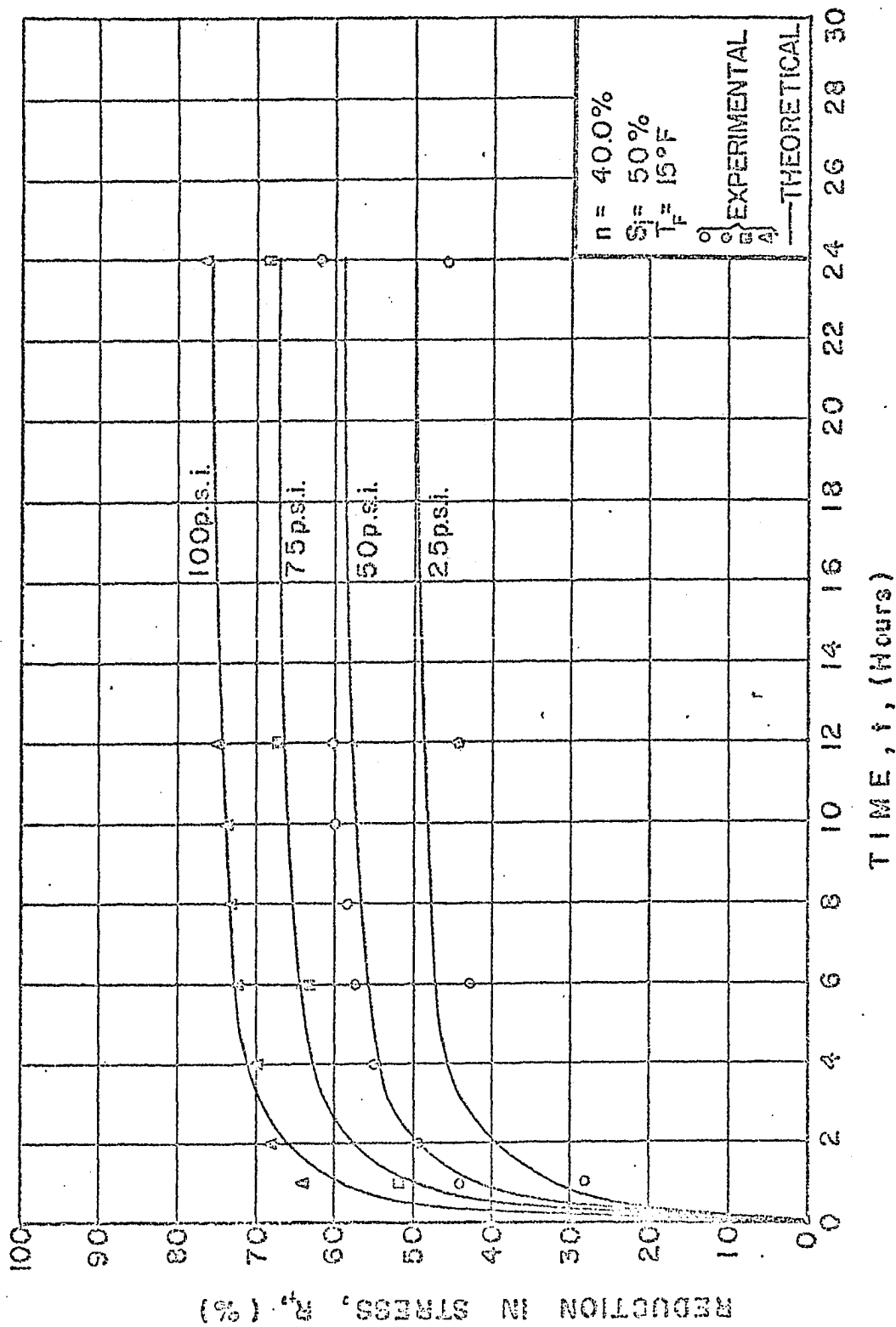
Fig. 37 Reduction in Lateral Stress vs Time at Selected Initial Pressures Under Indicated Conditions.
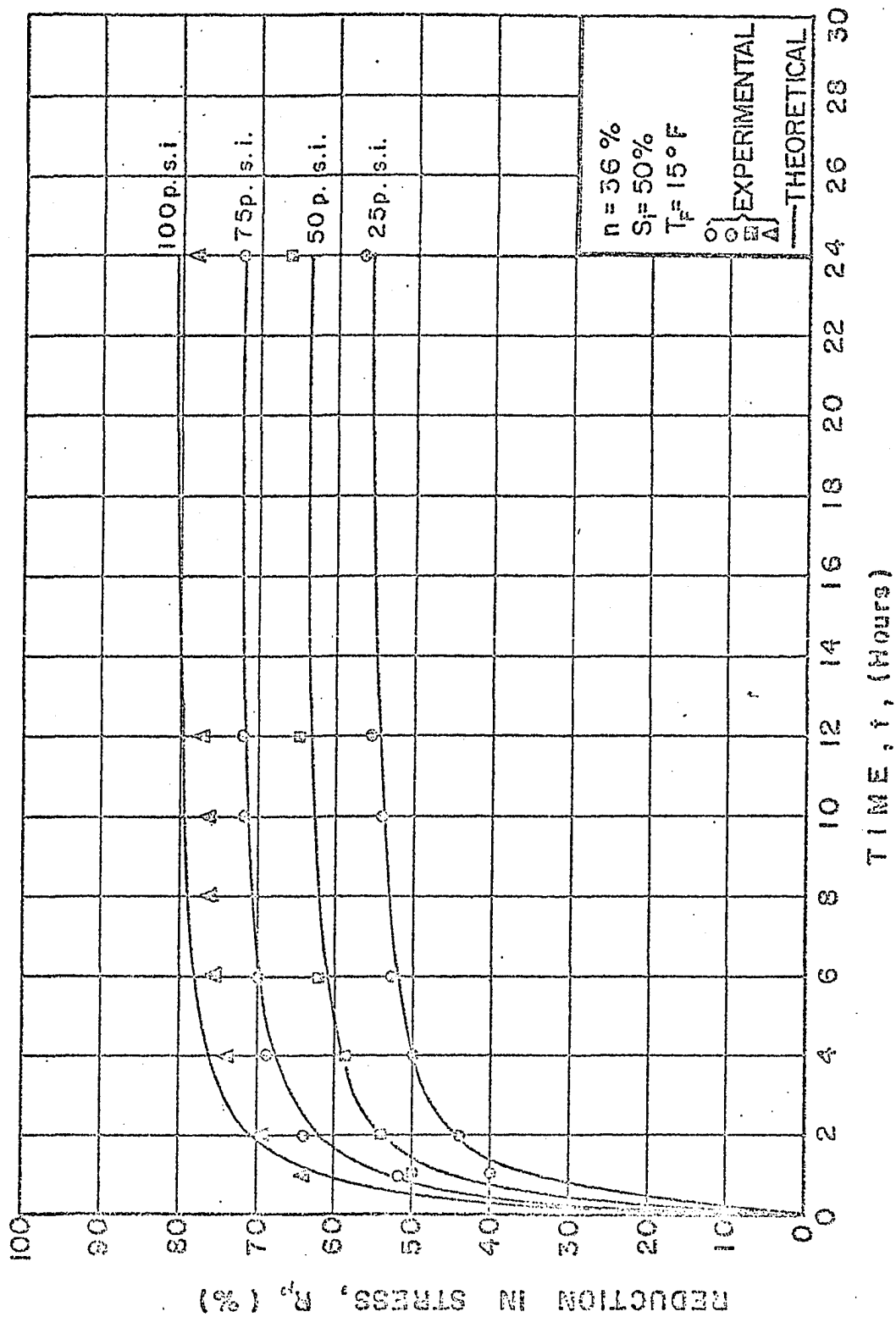
Fig. 38 Reduction in Lateral Stress vs Time at Selected Initial Pressures Under Indicated Conditions.
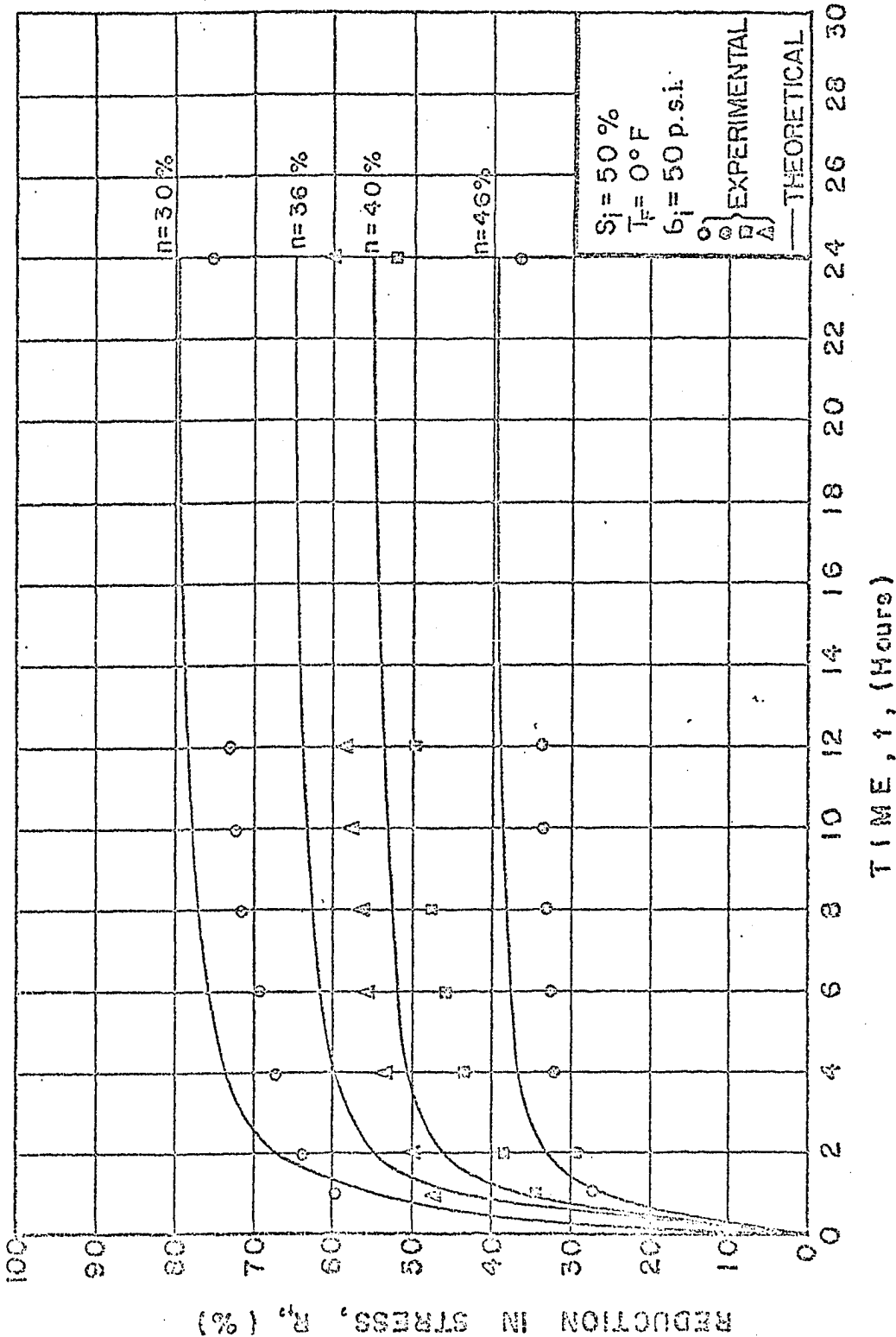
Fig. 39 Reduction in Lateral Stress vs Time at Selected Initial Porosities Under Indicated Conditions.
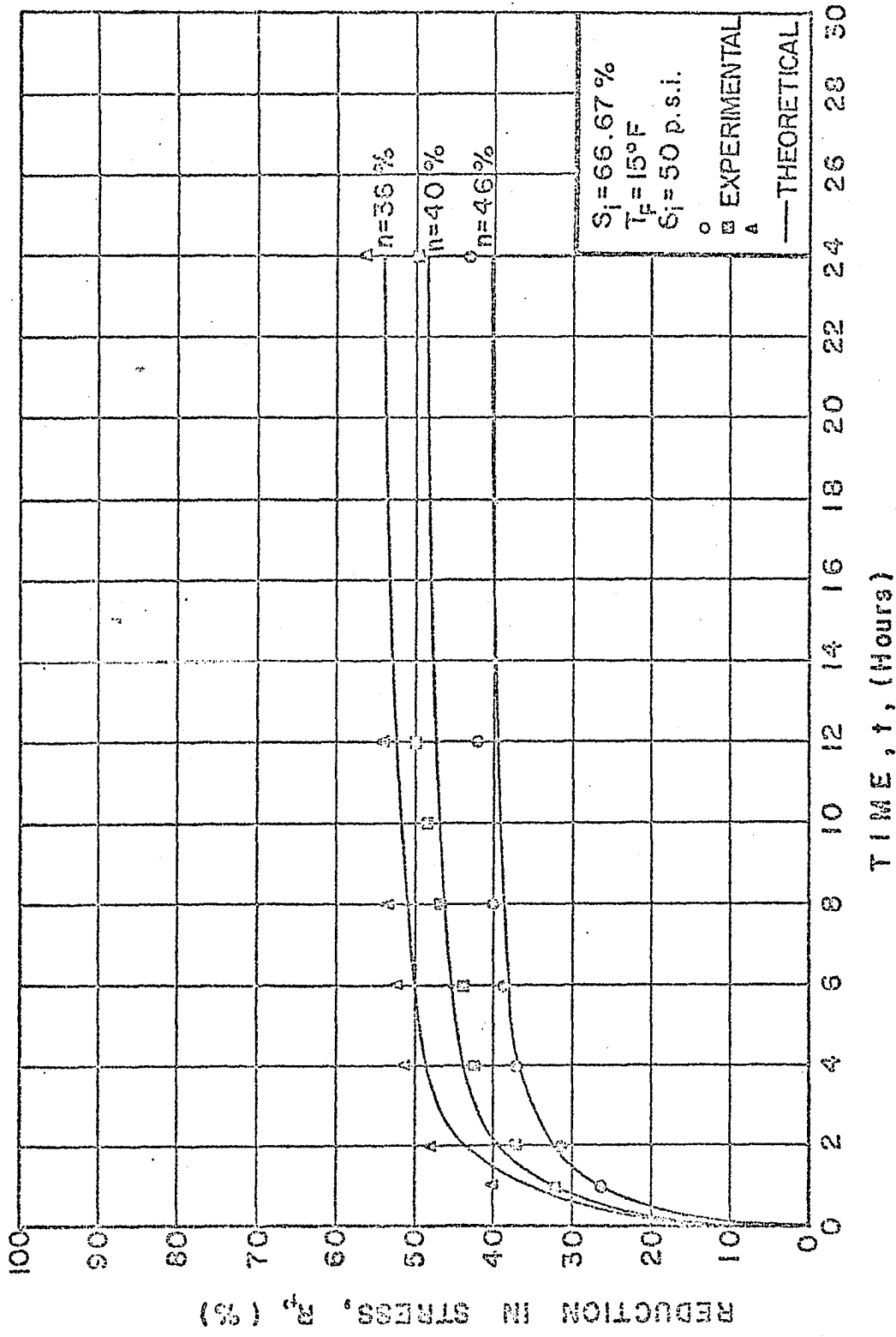
Fig. 40 Reduction in Lateral Stress vs Time at Selected Initial Porosities Under Indicated Conditions.
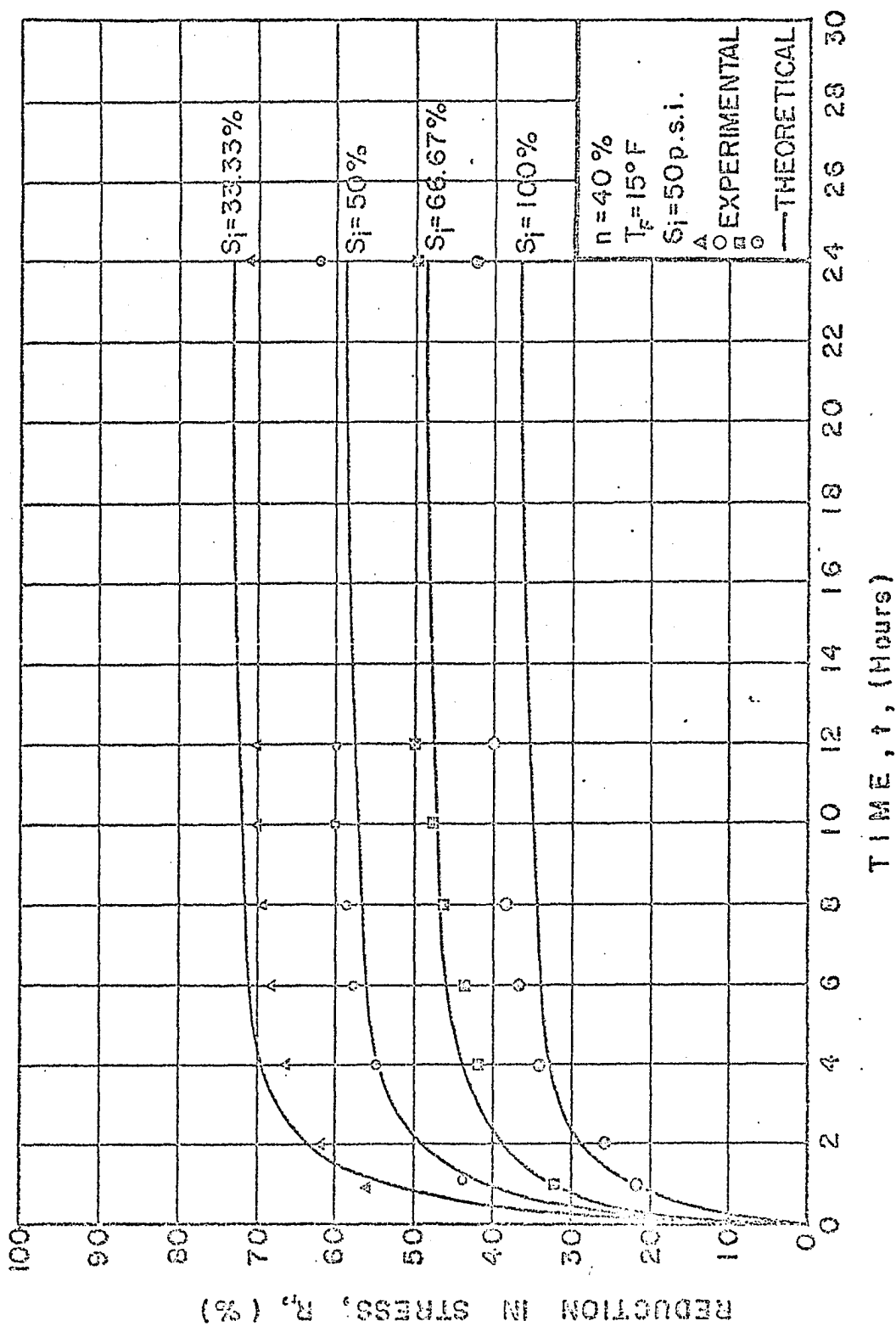
Fig. 41 Reduction in Lateral Stress vs Time at Selected Degrees of Ice Saturation Under Indicated Conditions.
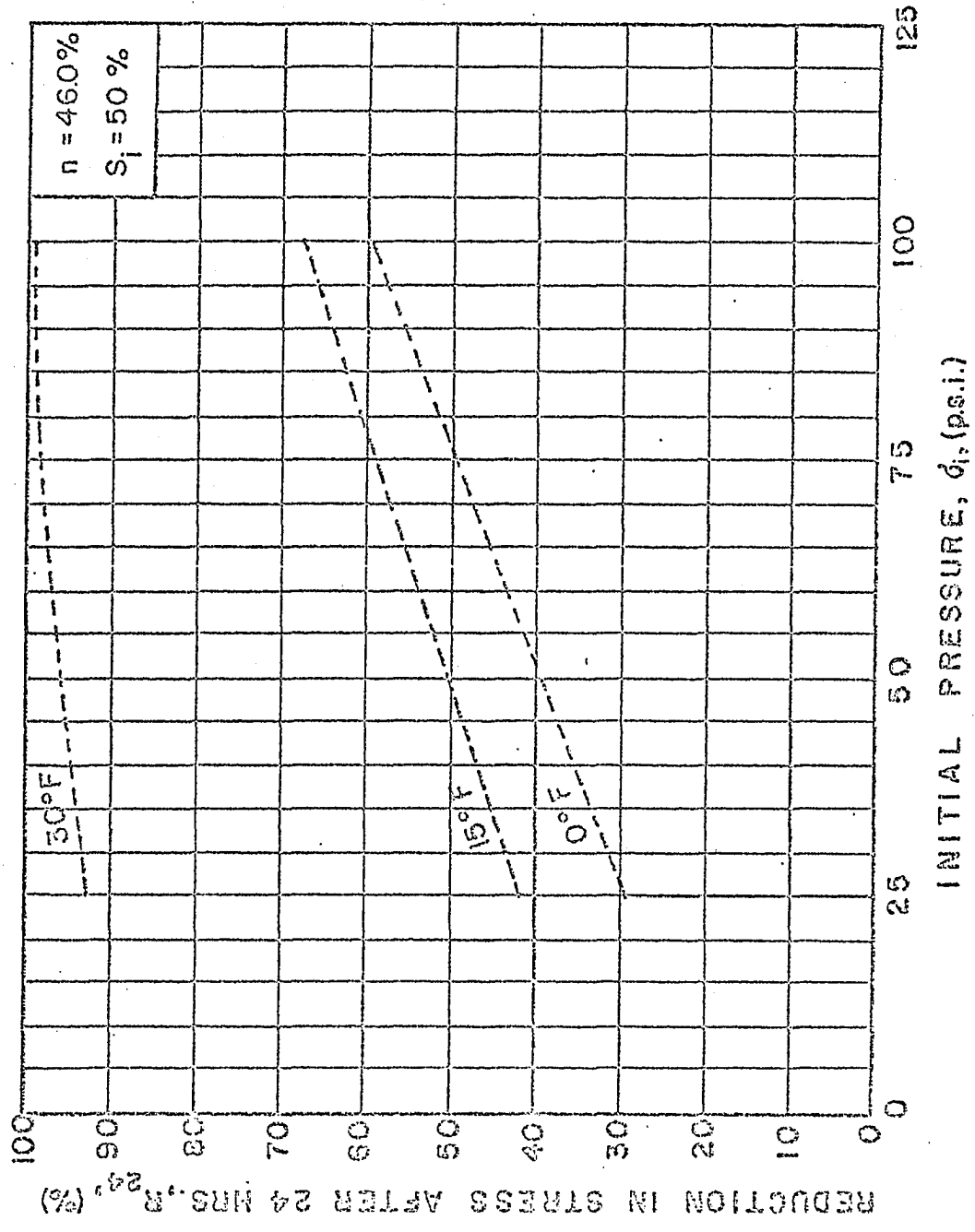
Fig. 42 Theoretical Curves Showing the Relationship Between Reduction in Lateral Stress after 24 Hours and Initial Pressure at Different Indicated Temperatures.
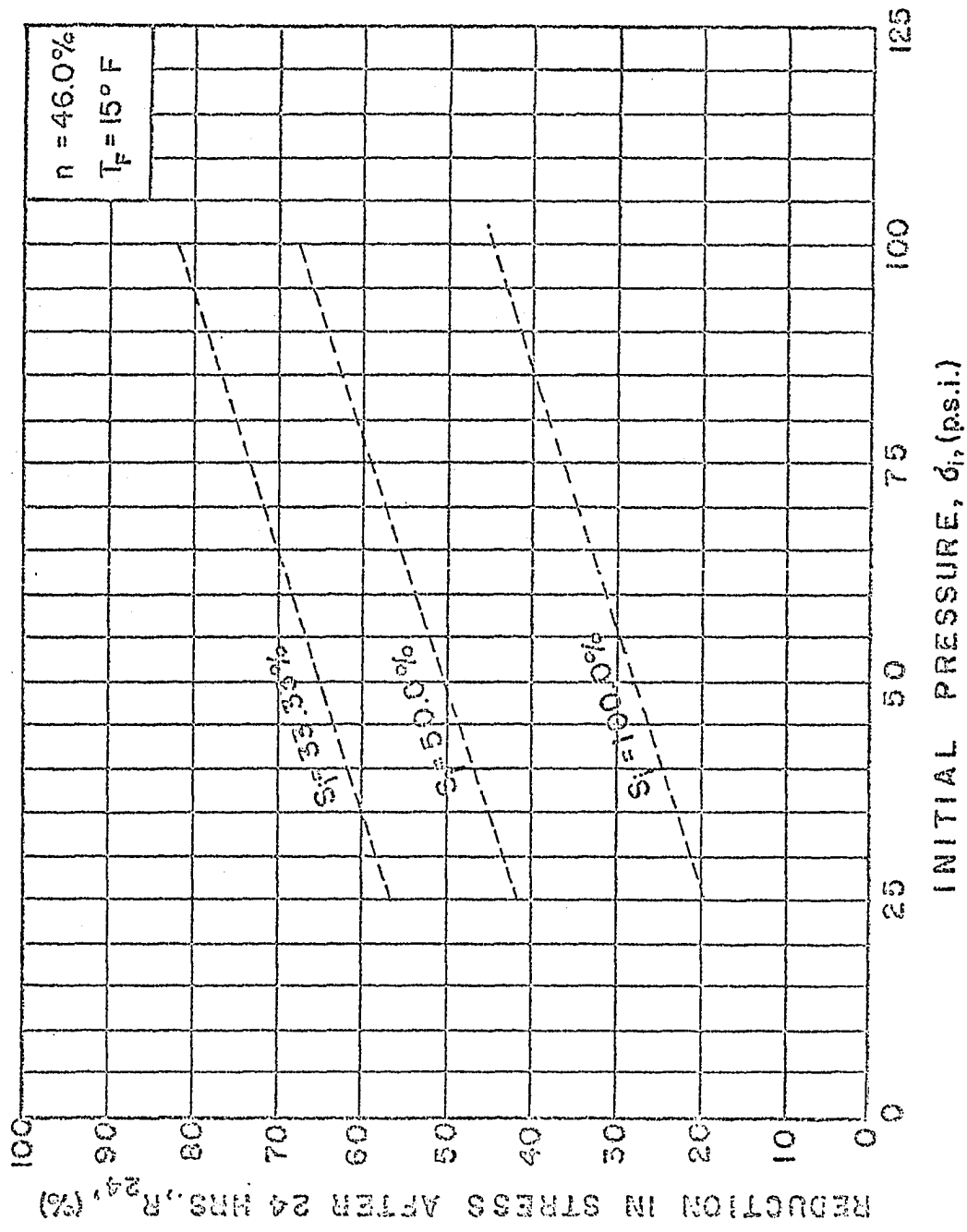
Fig. 43 Theoretical Curves Showing the Relationship Between
Reduction in Lateral Stress after 24 Hours and Initial
Pressure at Different Indicated Degrees of Ice Saturation.
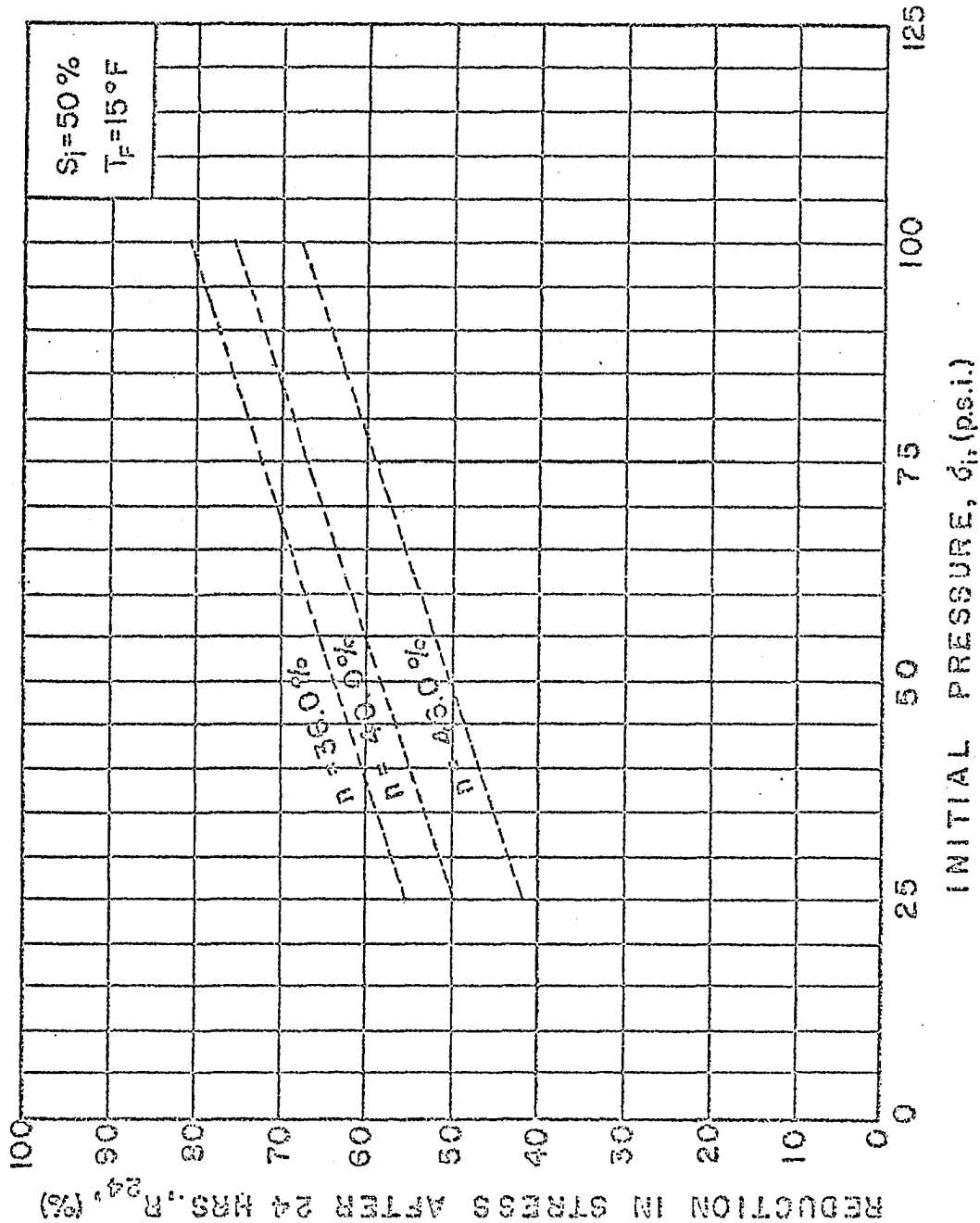
Fig. 44   Theoretical Curves Showing the Relationship Between Reduction in Lateral Stress after 24 Hours and Initial Pressure at Different Indicated Initial Porosities.
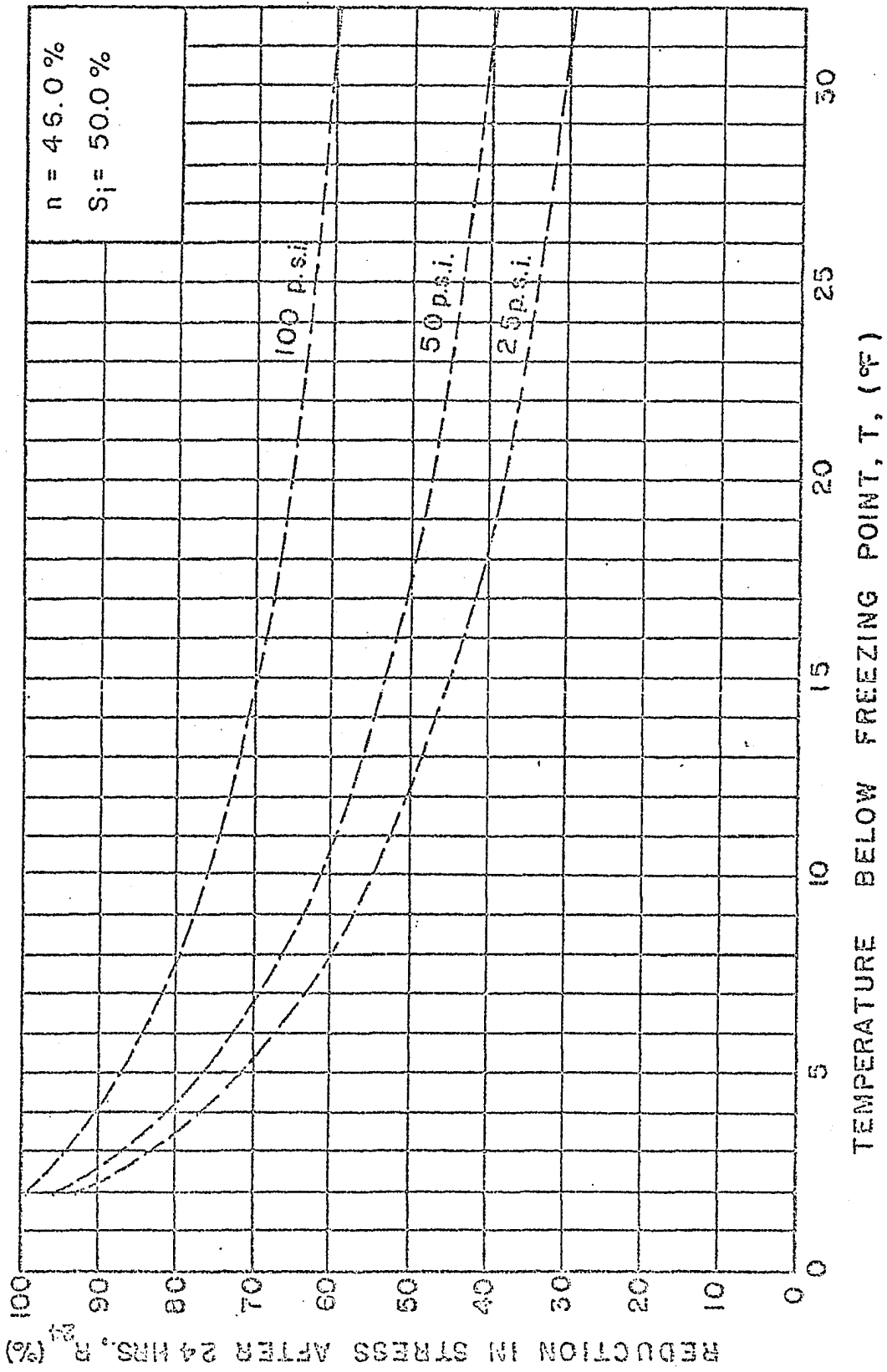
Fig. 45 Theoretical Curves Showing Reduction in Lateral Stress after 24 Hours vs Temperature Below Freezing Point at Different Indicated Initial Pressures.
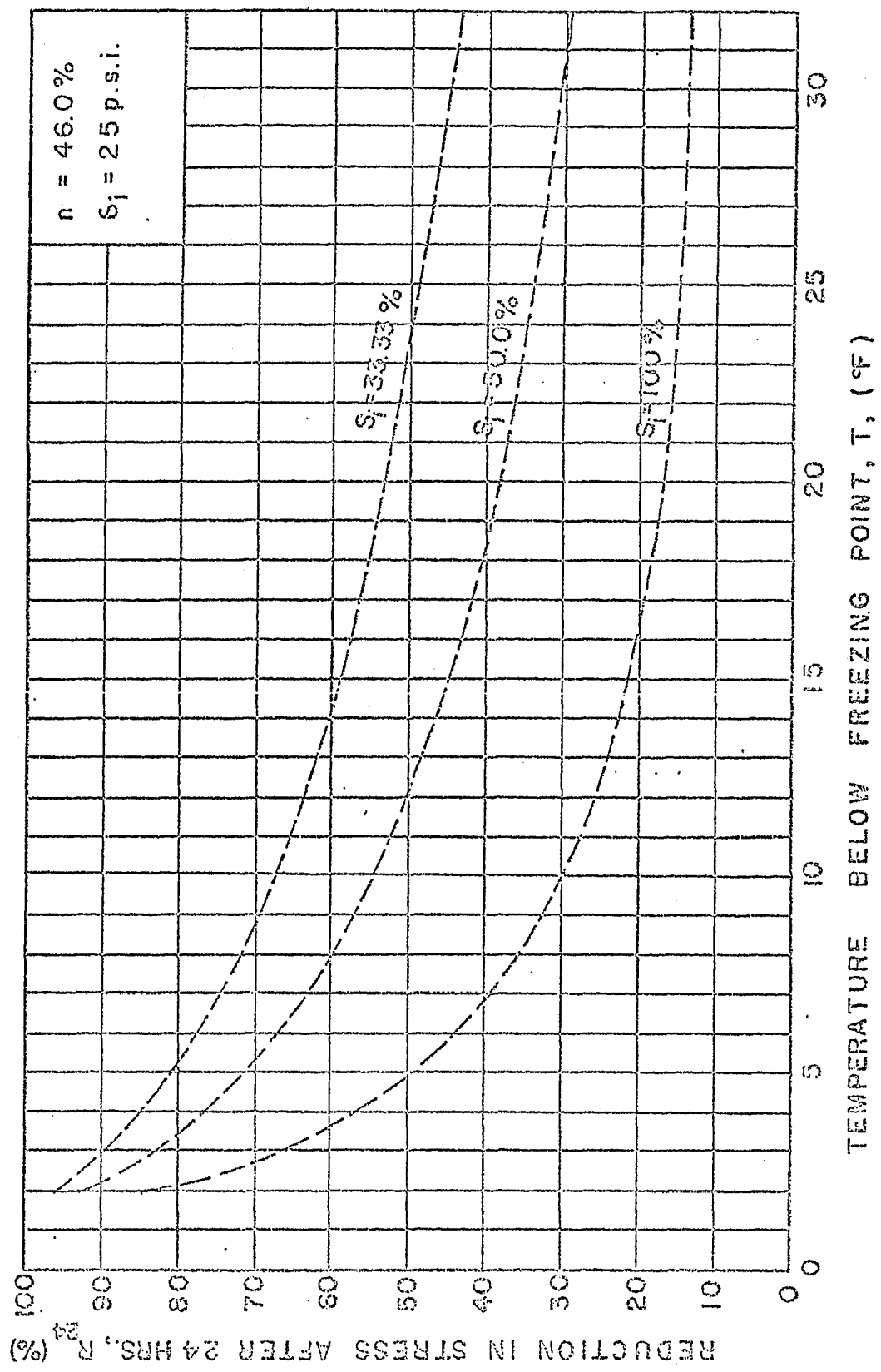
Fig. 46 Theoretical Curves Showing Reduction in Lateral Stress after 24 Hours vs Temperature Below Freezing Point at Different Indicated Degrees of Ice Saturation.
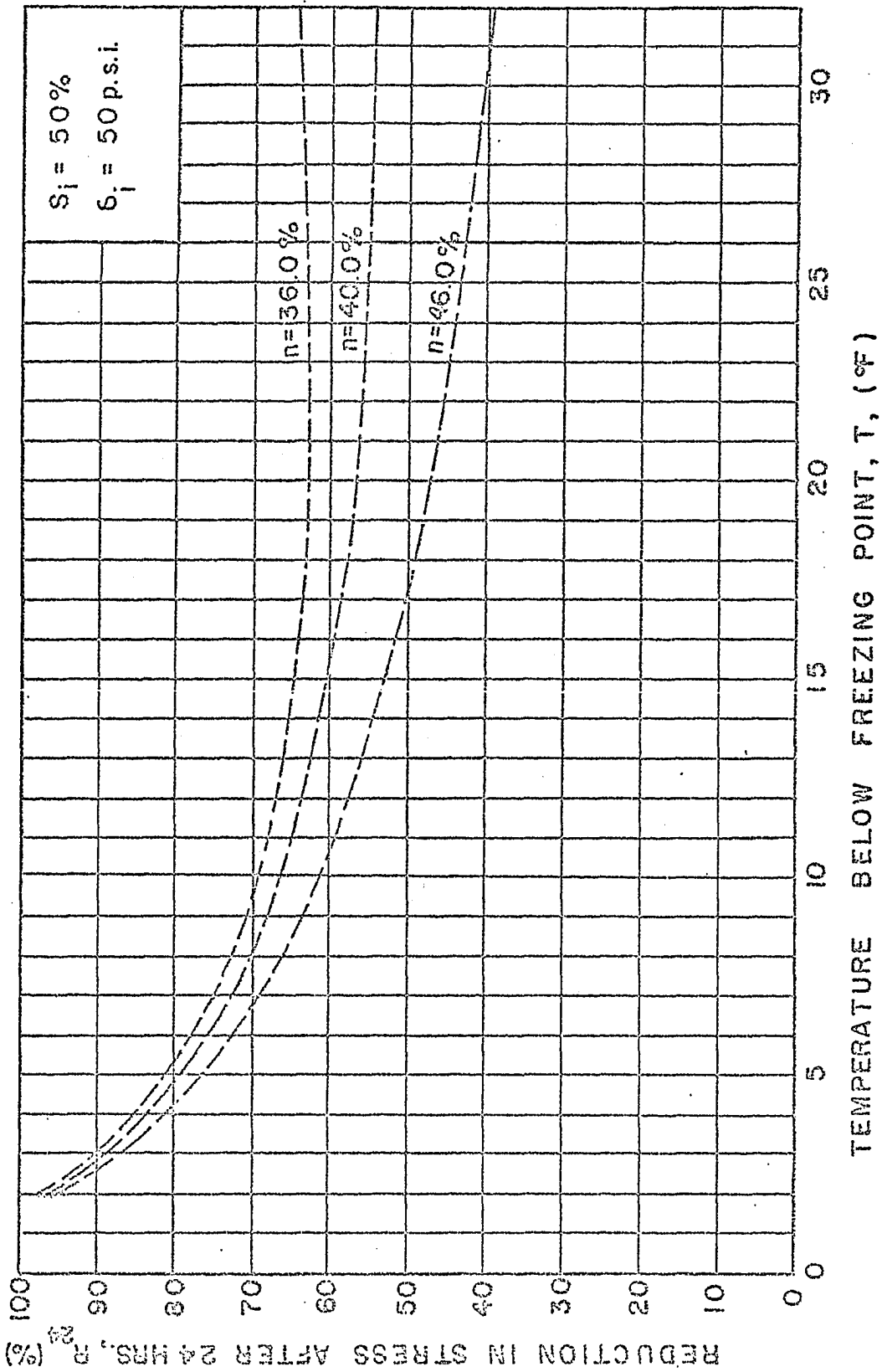
Fig. 47 Theoretical Curves Showing Reduction in Lateral Stress after 24 Hours vs Temperature Below Freezing Point at Different Indicated Initial Porosities.
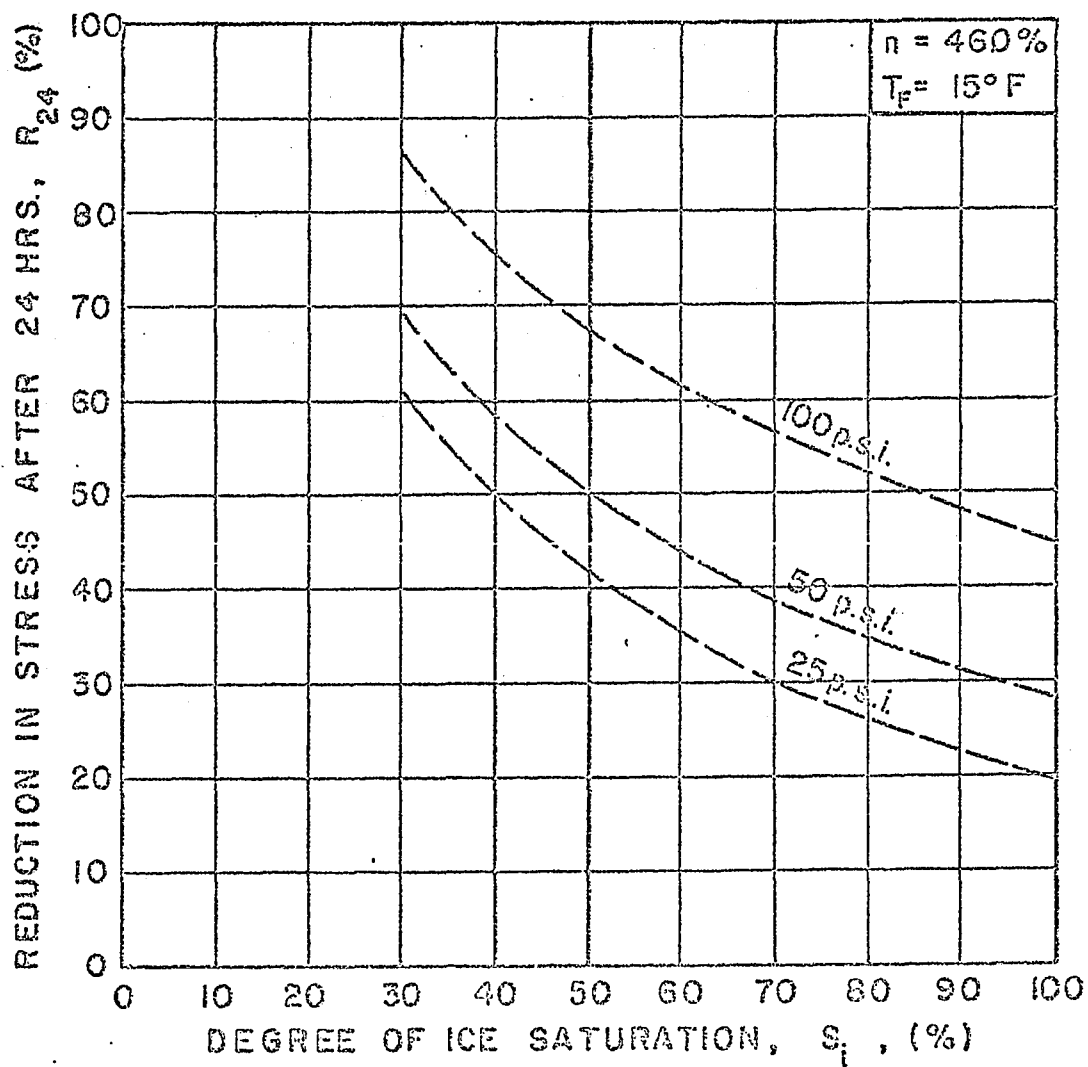
Fig. 48   Theoretical Curves Showing Reduction in
Lateral Stress after 24 Hours vs Degree
of Ice Saturation at Indicated Initial
Pressures.
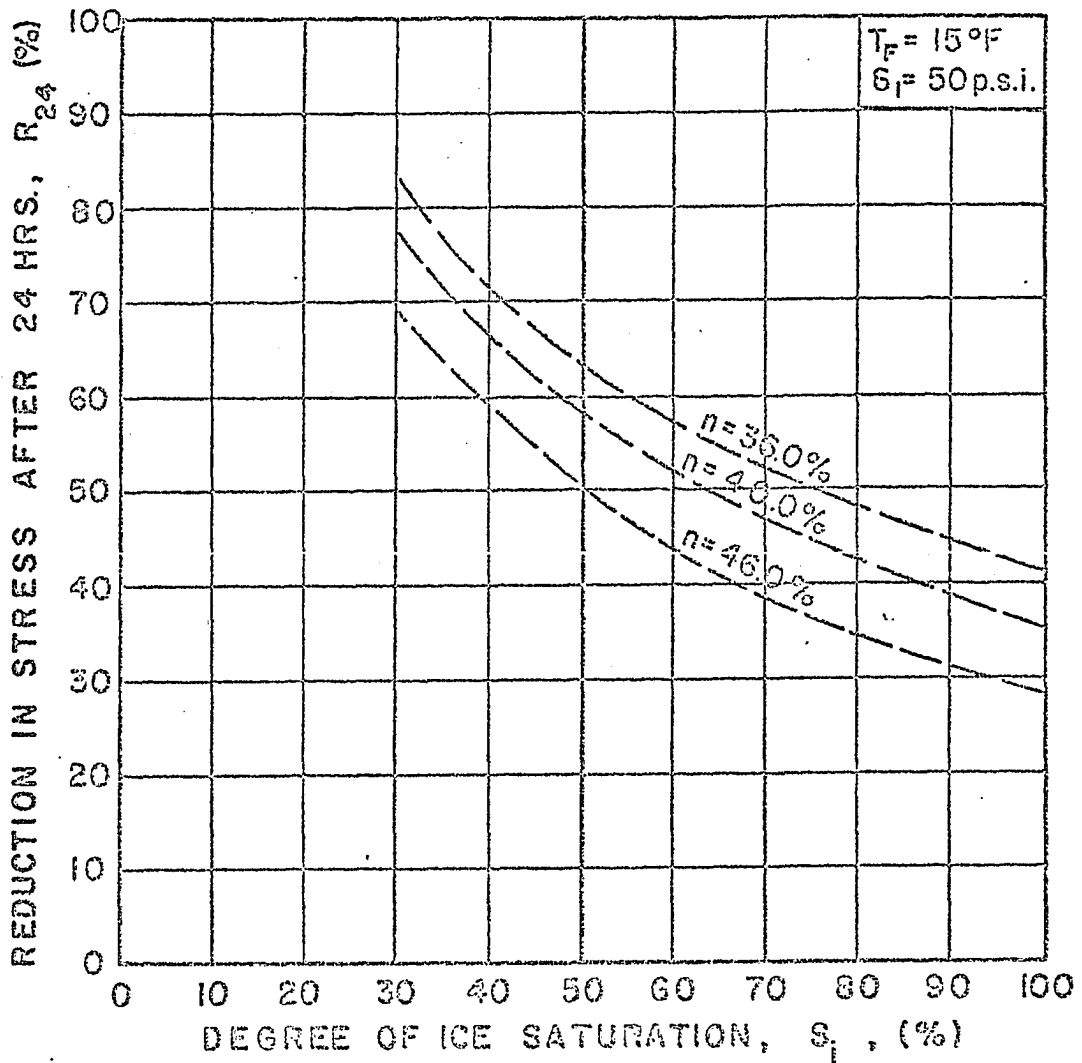
Fig. 49   Theoretical Curves Showing Reduction in
           Lateral Stress after 24 Hours vs Degree
           of Ice Saturation at Indicated Initial
           Porosities.
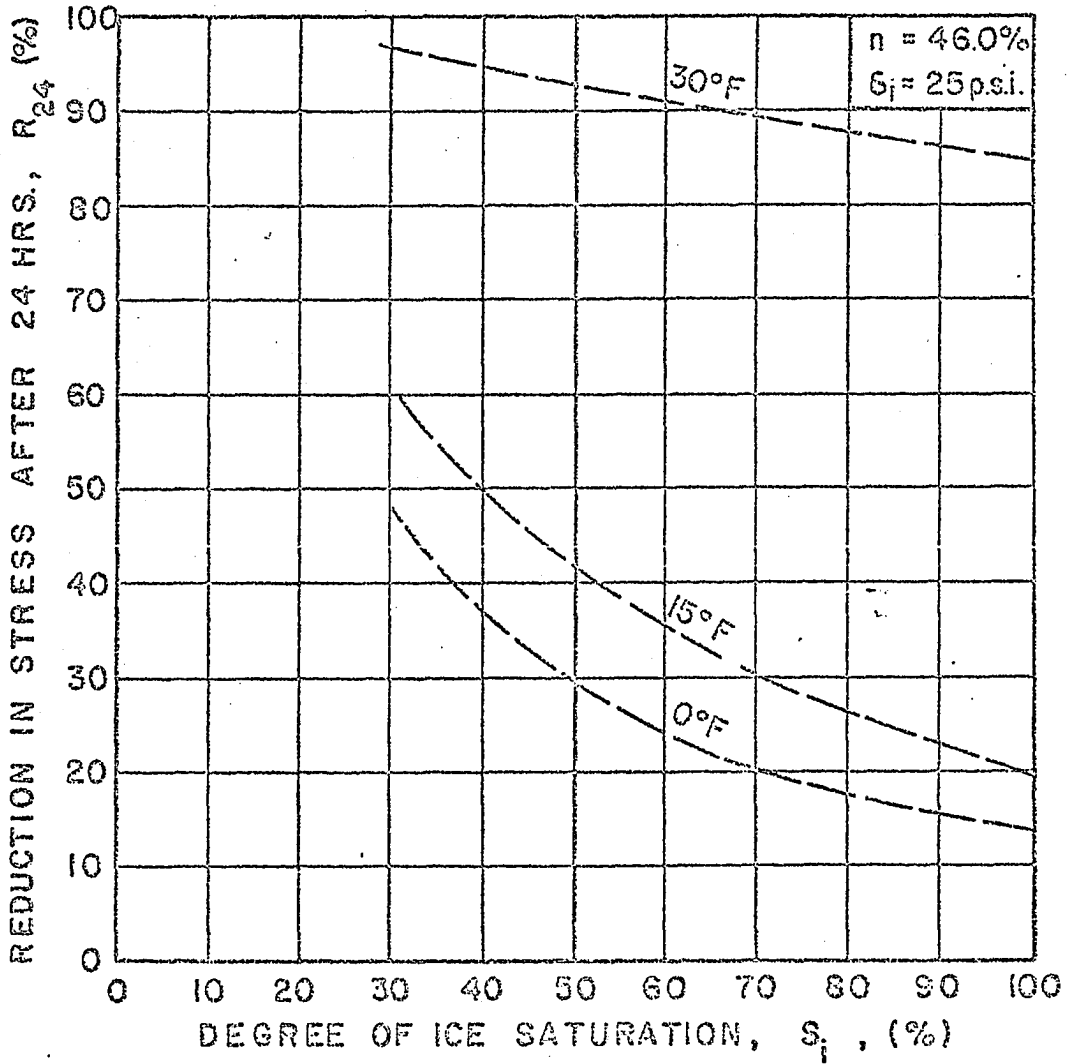
Fig. 50 Theoretical Curves Showing Reduction in
Lateral Stress after 24 Hours vs Degree
of Ice Saturation at Indicated Temperatures.
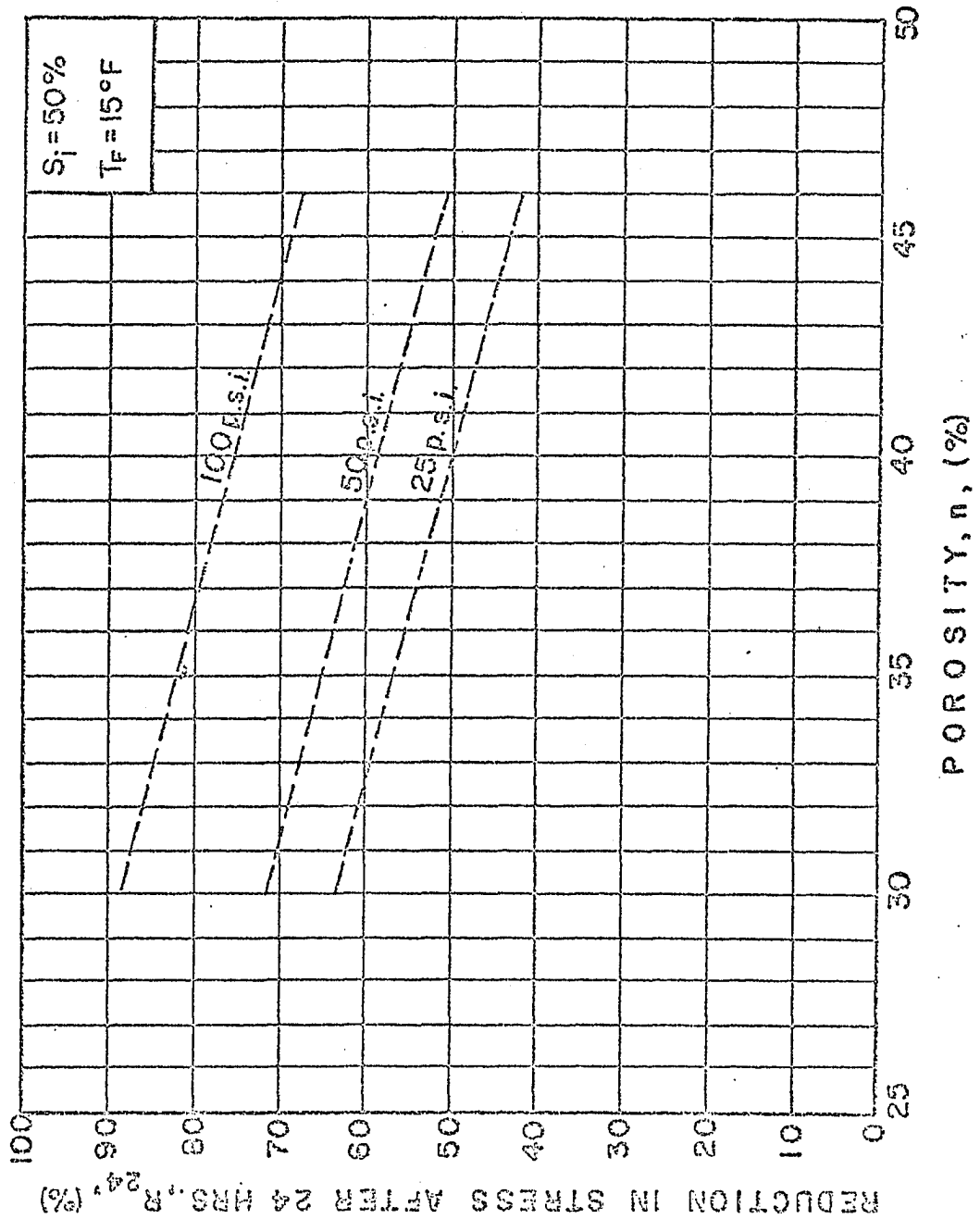
Fig. 51　Theoretical Curves Showing the Reduction in Lateral Stress after 24 Hours vs Initial Porosity at Indicated Initial Pressures.
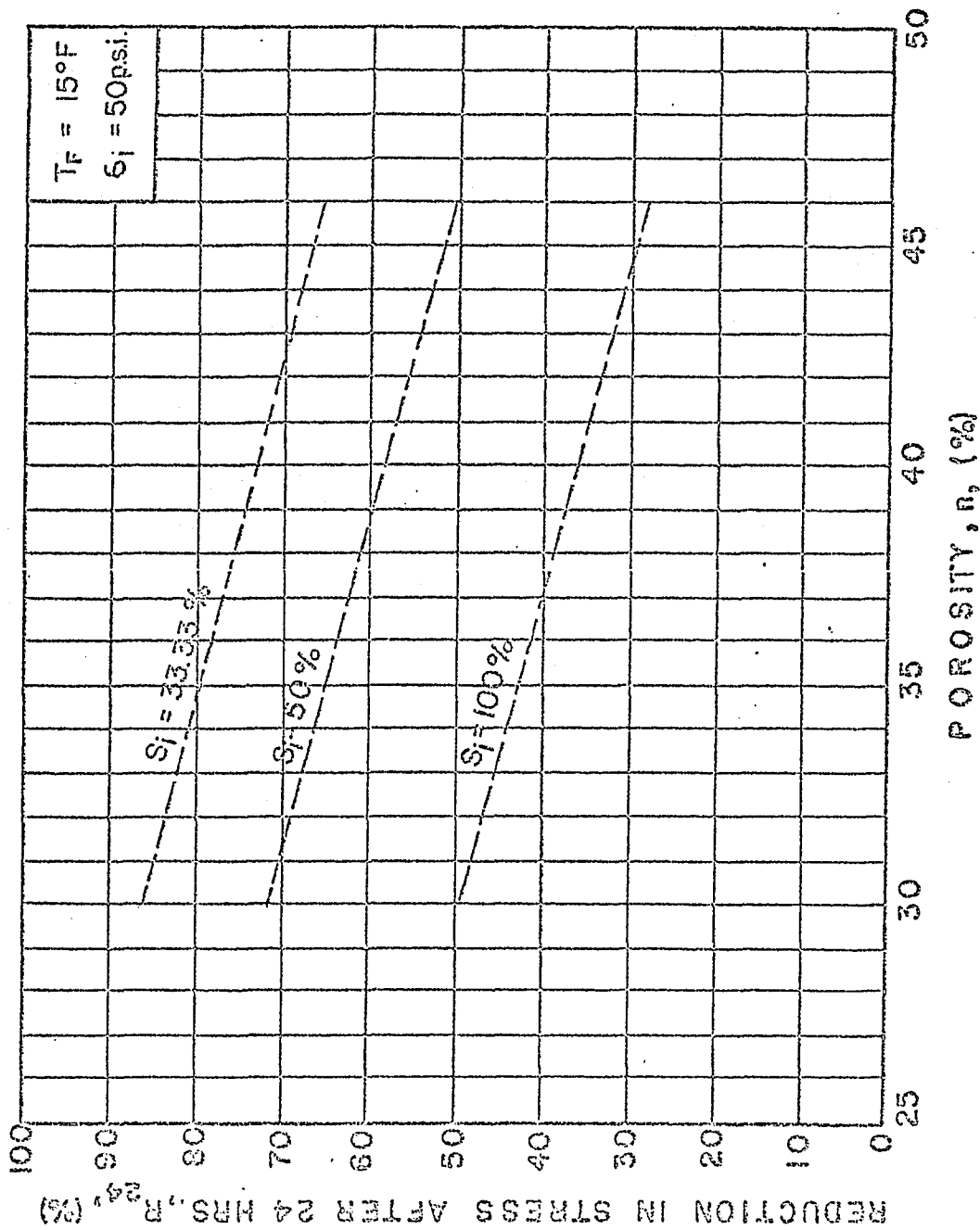
Fig. 52 Theoretical Curves Showing the Reduction in Lateral
Stress after 24 Hours vs Initial Porosity at Indicated
Degrees of Ice Saturation.
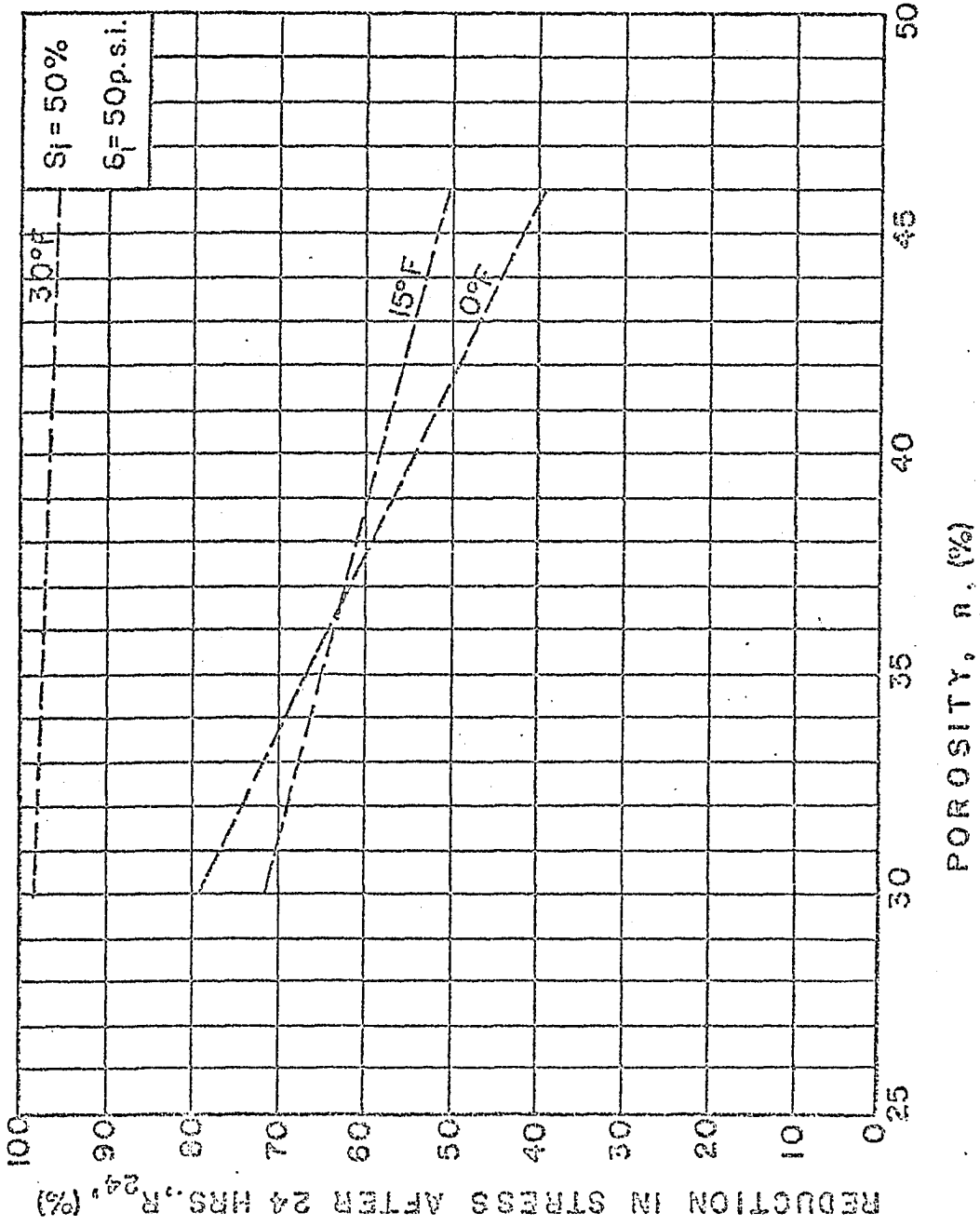
Fig. 53   Theoretical Curves Showing the Reduction in Lateral Stress after 24 Hours vs Initial Porosity at Indicated Temperatures.
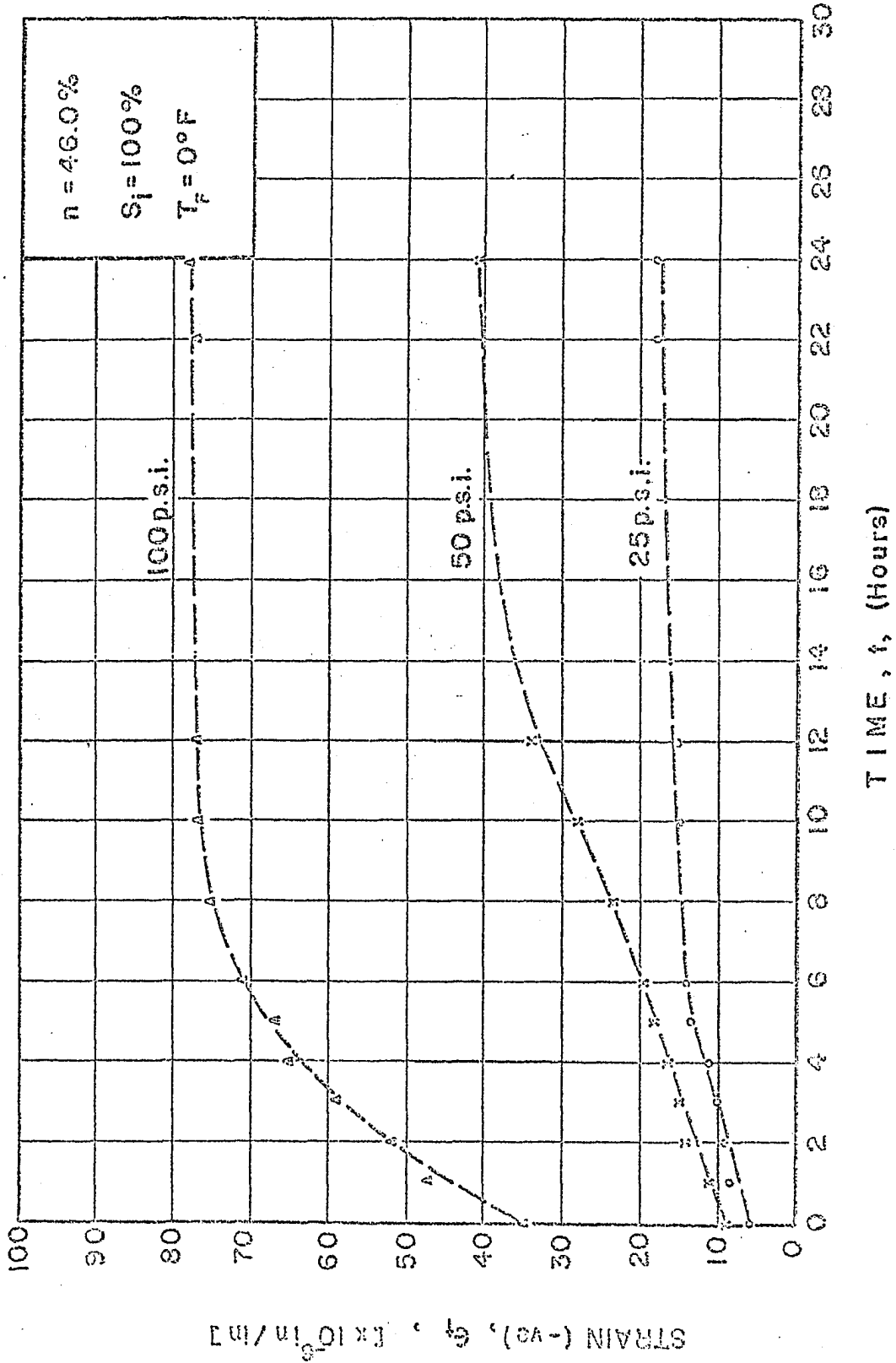
Fig. 54 Experimental Strain-Time Curves for Different Indicated Initial Pressures.
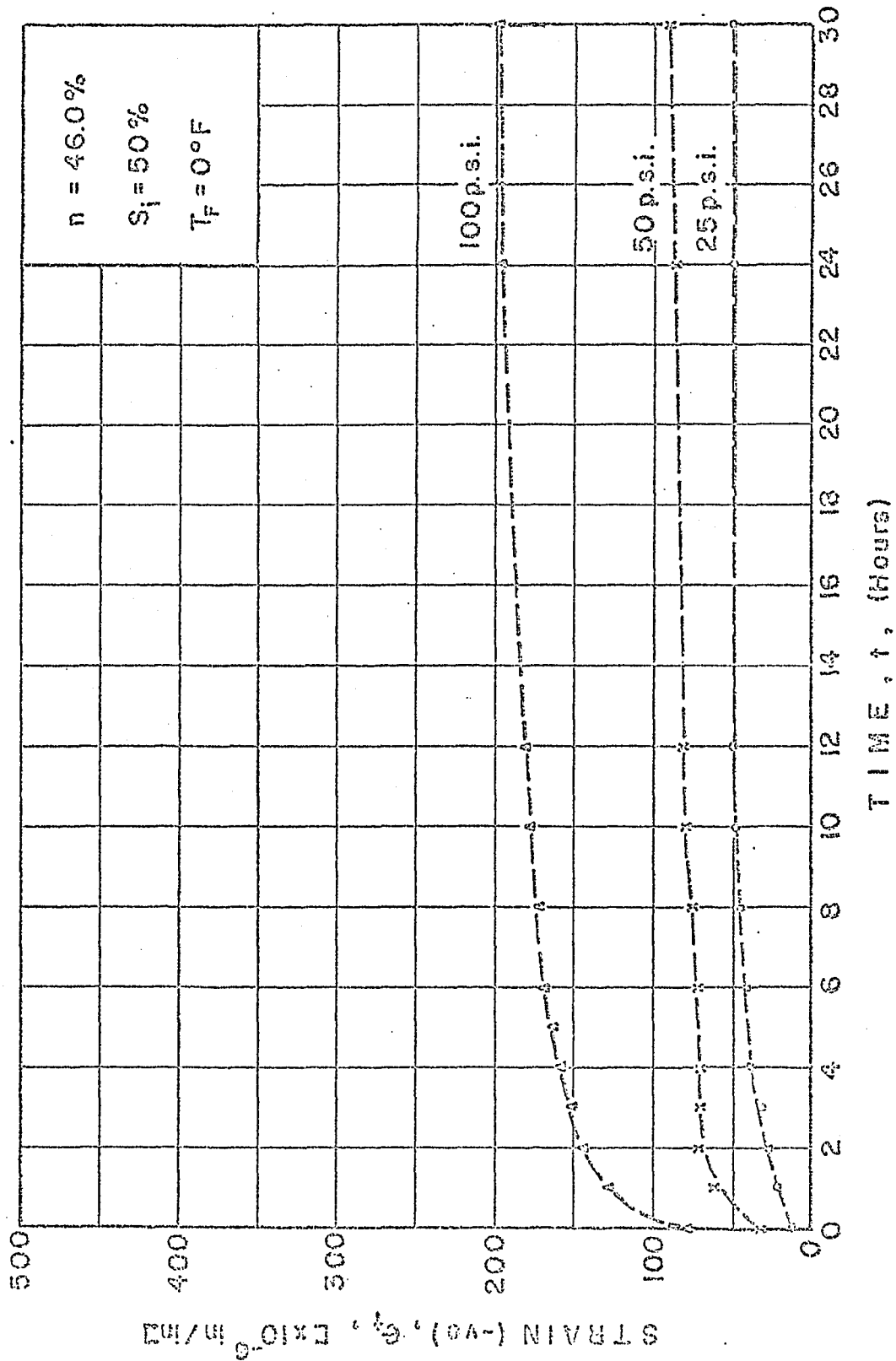
Fig. 55 Experimental Strain-Time Curves for Different Indicated Initial Pressures.
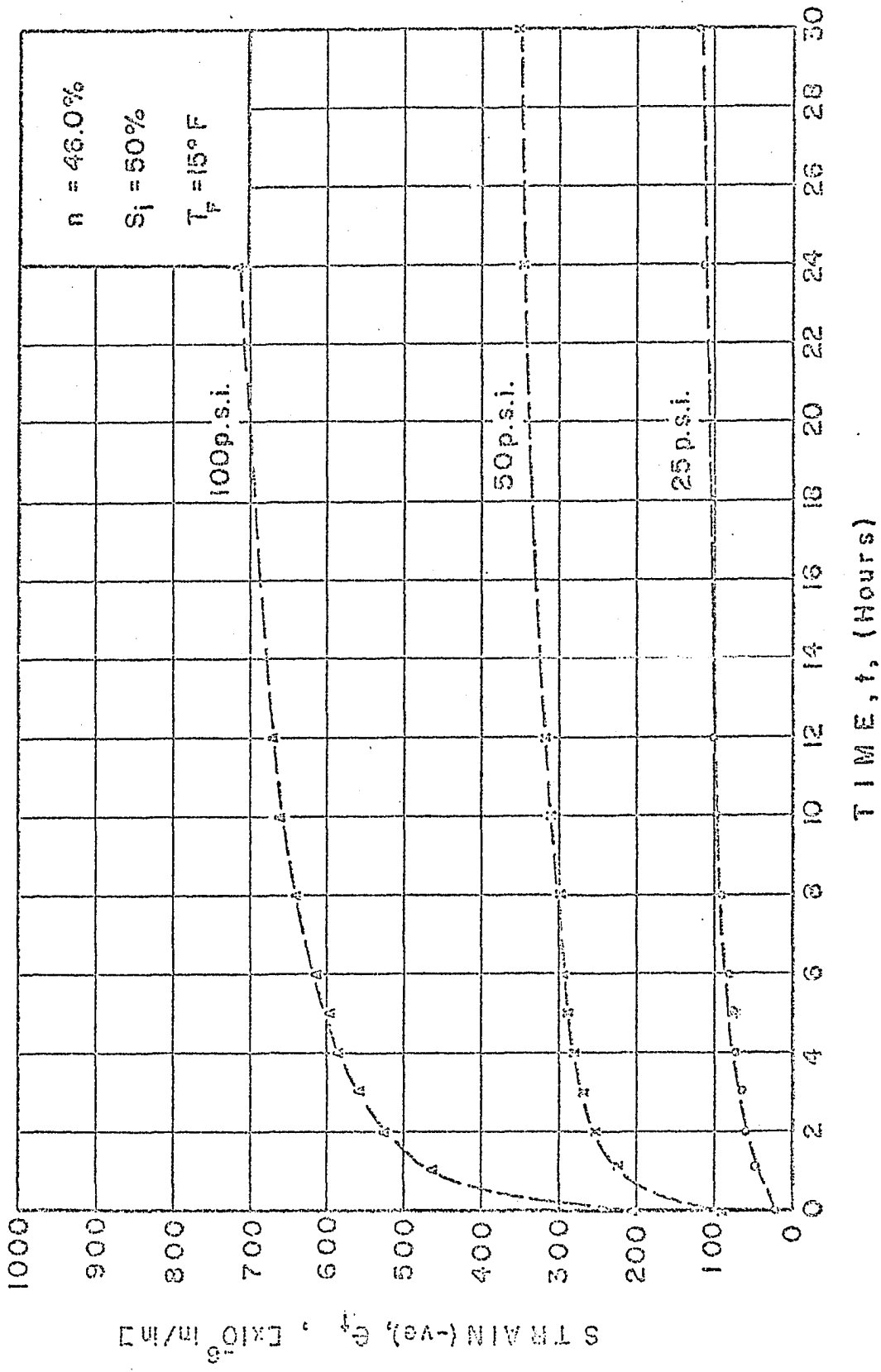
Fig. 56 Experimental Strain-Time Curves for Different Indicated Initial Pressures.
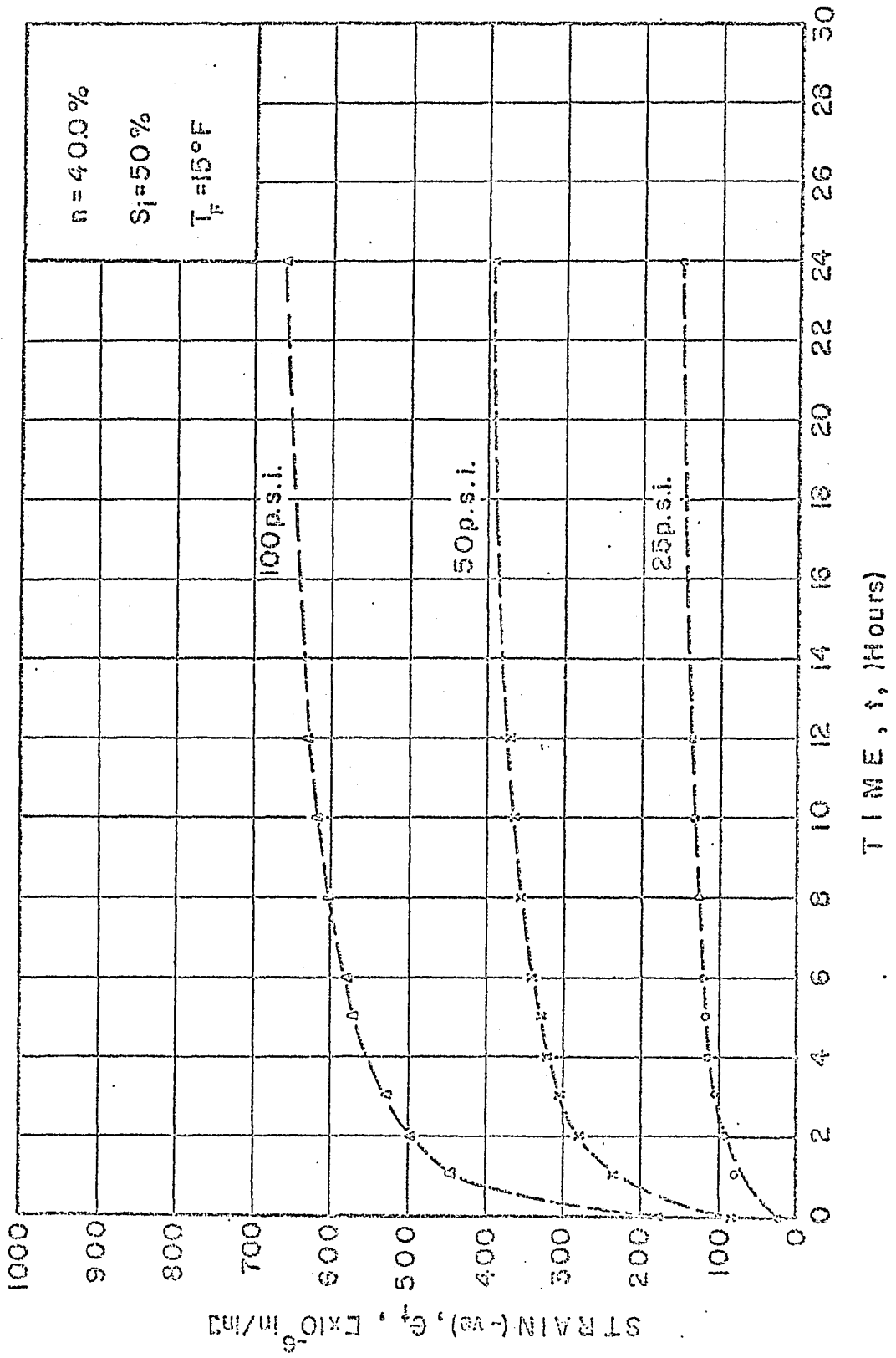
Fig. 57 Experimental Strain-Time Curves for Different Indicated Initial Pressures.
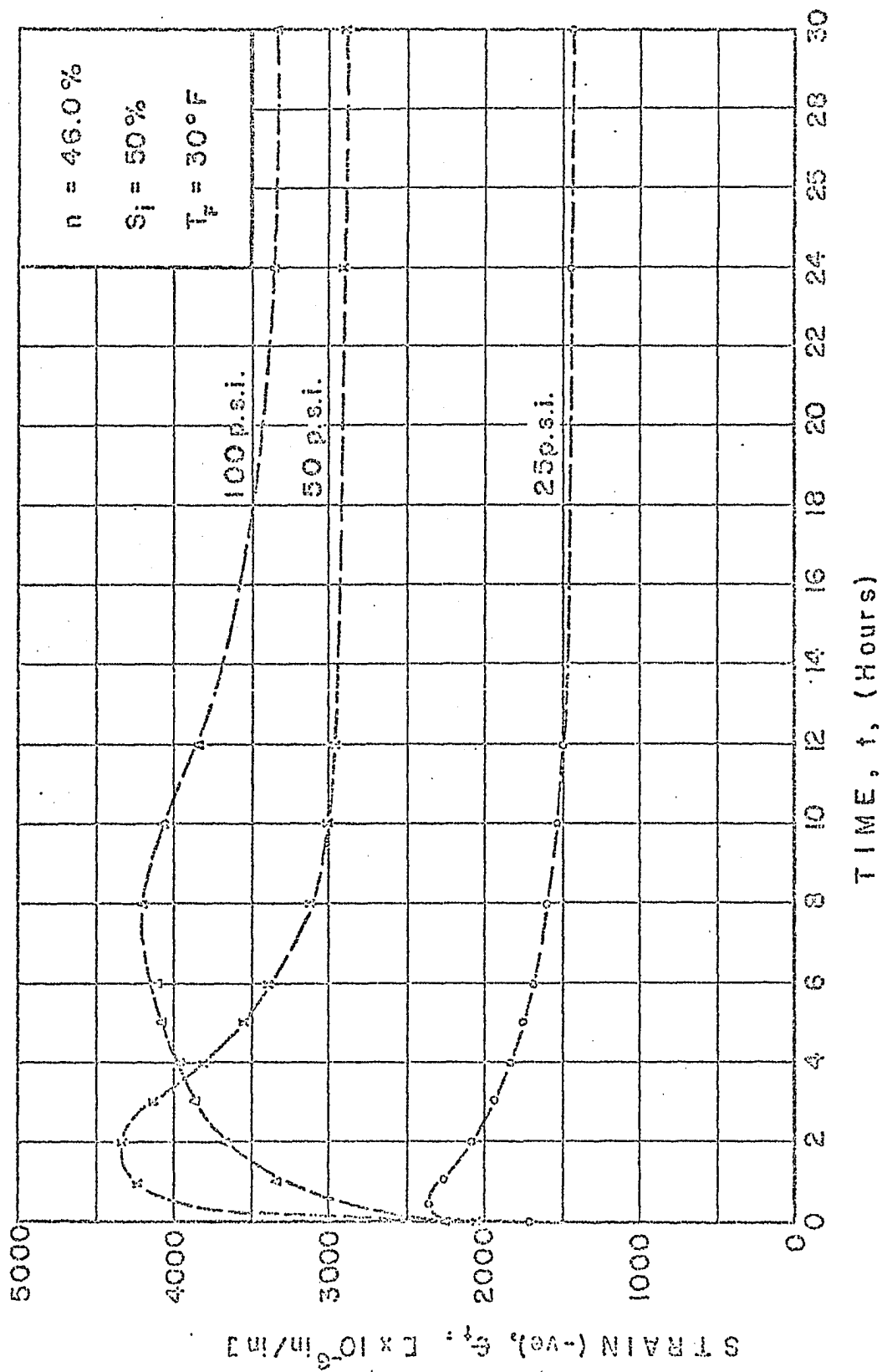
Fig. 58 Experimental Strain–Time Curves for Different Indicated Initial Pressures.

APPENDIX C

TABLES

TABLE 1

Comparison Between Experimentally Obtained And Calculated Values Of σ_{24}

Sand No. 1 $\qquad$ $n = 46.0\%$ $\qquad$ $S_i = 100\%$

T_F (°F)	σ_i (psi)	σ_{24} (psi)	
		Experimental	Theoretical
0	25	22.00	21.58
	50	37.50	38.19
	100	56.00	56.44
15	25	20.10	20.06
	50	35.50	35.96
	100	51.00	55.22
30	25	5.00	3.85
	50	6.00	6.29
	100	10.00	7.03

σ_{24} = value of reduced pressure after 24 hours

TABLE 2

Comparison Between Experimentally Obtained And Calculated Values Of σ_{24}

Sand No. 1   n = 46.0% S_i = 50%

T_F ($^{\circ}F$)	σ_i (psi)	σ_{24} (psi)	
		Experimental	Theoretical
0	25	17.70	17.66
	50	32.00	30.29
	100	46.50	40.47
15	25	14.70	14.50
	50	23.00	24.78
	100	30.00	32.72
30	25	1.50	1.77
	50	1.80	2.11
	100	2.80	0.48

σ_{24} = value of reduced pressure after 24 hours

TABLE 3

Comparison Between Experimentally Obtained

And Calculated Values Of $\acute{6}_{24}$

Sand No. 1 $n = 46.0\%$ $S_i = 33.33\%$

T_F	$\acute{6}_i$	$\acute{6}_{24}$ (psi)	
($^\circ$F)	(psi)	Experimental	Theoretical
	25	13.80	14.15
0	50	22.10	23.23
	100	29.00	26.24
	25	12.00	10.86
15	50	17.00	17.45
	100	22.50	17.97
	25	0.50	1.02
30	50	0.30	0.61
	100	0.20	0.34

$\acute{6}_{24}$ = value of reduced pressure after 24 hours

TABLE 4

Comparison Between Experimentally Obtained And Calculated Values Of δ_{24}

Sand No. 1

n (%)	S_i (%)	T_F (°F)	δ_i (psi)	δ_{24} (psi) Experimental	Theoretical
46	33.33	0	75	28.00	27.26
		25	25	6.50	6.38
	50.00	15	75	28.00	30.85
		25	50	11.80	15.27
	66.67	0	25	19.00	19.70
		15	50	28.50	29.89
40	33.33	15	50	14.50	13.43
	50.00	0	50	24.00	22.73
		15	25	13.50	12.50
			50	19.00	20.76
			75	24.00	24.82
			100	23.10	24.66
		25	50	10.00	13.61
		30	50	1.60	1.63
	66.67	15	50	25.00	25.88
	100.00	15	50	29.00	31.97

δ_{24} = value of reduced pressure after 24 hours

TABLE 5

Comparison Between Experimentally Obtained

And Calculated Values Of σ_{24}

Sand No. 2

n (%)	S_i (%)	T_F (°F)	σ_i (psi)	σ_{24} (psi)	
				Experimental	Theoretical
36	33.33	15	50	11.80	10.75
	50.00	0	50	20.00	17.69
		15	25	11.00	11.17
			50	16.90	18.09
			75	21.00	20.79
			100	22.00	19.29
		25	50	10.00	12.51
		30	50	4.00	1.32
	66.67	15	50	22.00	23.21
	100.00	15	50	31.20	29.30
30	50.00	0	50	12.50	10.13
		15	25	10.80	9.17
			50	12.40	14.07

σ_{24} = value of reduced pressure after 24 hours

TABLE 6

Calculated Values Of A, B and R_{24}

Sand No. 1   n = 46.0% S_i = 100%

T_F (°F)	σ_i (psi)	A From Eqn.(4-5)	B From Eqn.(4-6)	R_{24} From Eqn.(4-2)
0	25	14.04	0.617	13.69
	50	24.14	0.513	23.62
	100	44.33	0.418	43.56
15	25	20.27	0.617	19.76
	50	28.69	0.518	28.07
	100	45.51	0.418	44.72
30	25	85.46	0.247	84.59
	50	88.18	0.207	87.42
	100	93.62	0.167	92.97

TABLE 7

Calculated Values Of A, B and R_{24}

Sand No. 1 $n = 46.0\%$ $S_i = 50\%$

T_F (°F)	δ_i (psi)	A From Eqn.(4-5)	B From Eqn.(4-6)	R_{24} From Eqn.(4-2)
0	25	29.97	0.487	29.37
	50	40.06	0.388	39.42
	100	60.25	0.289	59.53
15	25	42.85	0.487	47.99
	50	51.27	0.388	50.44
	100	68.09	0.289	67.28
30	25	93.68	0.195	92.92
	50	96.40	0.155	95.78
	100	100.00	0.115	99.52

TABLE 8

Calculated Values Of A, B and R_{24}

Sand No. 1   n = 46.0% S_i = 33.33%

T_F (°F)	σ_i (psi)	A From Eqn. (4-5)	B From Eqn. (4-6)	R_{24} From Eqn. (4-2)
0	25	44.15	0.419	43.39
	50	54.25	0.319	53.53
	100	74.44	0.220	73.76
15	25	57.55	0.419	56.56
	50	65.96	0.319	65.09
	100	82.79	0.220	82.03
30	25	96.60	0.168	95.93
	50	99.32	0.128	98.79
	100	100.00	0.088	99.63

TABLE 9

Calculated Values Of A, B and R_{24}

Sand No. 1

n (%)	S_i (%)	T_F (°F)	σ_i (psi)	A From Eqn.(4-5)	B From Eqn.(4-6)	R_{24} From Eqn.(4-2)
46	33.33	0	75	64.34	0.261	63.65
		25	25	76.00	0.419	74.68
	50.00	15	75	59.68	0.380	58.86
		25	50	70.60	0.388	69.47
	66.67	0	25	21.69	0.539	21.21
		15	50	40.97	0.440	40.22
40	33.33	15	50	74.12	0.319	73.14
	50.00	0	50	55.42	0.388	54.53
		15	25	51.01	0.487	49.99
			50	59.43	0.388	58.47
			75	67.84	0.330	66.91
			100	76.25	0.239	75.34
		25	50	73.96	0.388	72.77
		30	50	97.36	0.155	96.73
	66.67	15	50	49.18	0.440	48.23
	100.00	15	50	36.85	0.513	36.06

TABLE 10

Calculated Values Of A, B and R_{24}

Sand No. 2

n (%)	S_i (%)	T_F (°F)	σ_i (psi)	A From Eqn.(4-5)	B From Eqn.(4-6)	R_{24} From Eqn.(4-2)
36	33.33	15	50	79.56	0.319	78.51
	50.00	0	50	65.66	0.388	64.61
		15	25	56.45	0.487	55.32
			50	64.87	0.388	63.83
			75	73.28	0.330	72.28
			100	81.69	0.289	80.71
		25	50	76.20	0.388	74.92
		30	50	98.00	0.155	97.37
	66.67	15	50	54.57	0.440	53.57
	100.00	15	50	42.29	0.518	41.38
30	50.00	0	50	81.02	0.388	79.72
		15	25	64.61	0.487	63.82
			50	73.03	0.388	71.86

TABLE 11

Duplicate Tests Performed On The Same Sand-Ice Samples

Sand No.	n (%)	S_i (%)	T_f (°F)	σ_i (psi)	σ_{12} (psi) Test 1	Test 2	R (psi)	X̄ (psi)	S (psi)	V (psi)
1	46	33.33	15	100	24.00	25.00	1.00	24.50	0.71	2.83
1	46	100.00	0	50	37.70	40.20	2.50	38.95	1.76	4.52
1	46	50.00	0	25	18.00	15.30	2.70	16.65	1.90	11.40
2	36	50.00	15	50	17.50	18.80	1.30	18.15	0.92	5.06
2	36	50.00	30	50	4.60	4.00	0.60	4.30	0.42	9.77

Legend:

σ_{12} = Pressure reading after 12 hours

S = Standard deviation

V = Coefficient of variation

R = Range

X̄ = Mean

DATA SHEET NO.	1		OBSERVATIONS		POROSITY	n	46.0%
SAMPLE NO.	1B				ICE SATURATION	S_i	50 %
EXPERIMENT NO.	1B - 1				TEMPERATURE	T_F	0° F
TESTED BY	K.C Ania				INITIAL PRESSURE	σ_i	25 psi

DATE	LOCAL TIME	TIME ELAPSED $[t]$	STRESS DIAL READING $[\sigma_t]$ (psi)	TOTAL CHANGE IN STRESS $[\sigma_i - \sigma_t]$ (psi)	STRAIN DIAL READING $[\epsilon_t]$ CHANNEL (GAUGE) No. 1	2	REDUCTION IN STRESS $R_t = \frac{\sigma_i - \sigma_t}{\sigma_i} \times 100$ [%]	AVERAGE STRAIN ϵ_t [μ in/in]
	11-30 am	0 min.	25.0	0	10	14	0	12
		0.5 "	24.4	0.6	10	14		
		1 "	24.0	1.0	10	14		
		2 "	23.3	1.7	11	15		
		3 "	23.0	2.0	12	16		
		4 "	22.7	2.3	12	16		
	11-35	5 "	22.5	2.5	12	16		
	11-40	10 "	21.8	3.2	14	18		
	11-50	20 "	21.2	3.8	18	20		
	12-00	30 "	20.9	4.1	20	22	14.4	21
25-4-70	12-10 pm	40 "	20.6	4.4	20	23		
	12-20	50 "	20.5	4.5	20	24		
	12-30	60 "=1 Hr.	20.4	4.6	20	24	18.4	22
	12-50	80 "	20.0	5.0	20	26		
	1-10	100 "	19.8	5.2	20	29		
	1-30	120 " = 2 Hrs.	19.5	5.5	20	29	22.0	24.5
	2-00	150 "	19.2	5.8	21	30		
	2-30	180 " = 3 "	19.0	6.0	26	35	24.0	30.5
	3-30	4 "	18.6	6.4	37	42	25.6	39.5
	4-30	5 "	18.5	6.5	38	44	26.0	41.0
	5-30	6 "	18.5	6.5	38	44	26.0	41.0
	7-30	8 "	18.3	6.7	40	48	26.8	44.0
	9-30	10 "	18.0	7.0	46	50	28.0	48.0
	11-30	12 "	18.0	7.0	47	51	28.0	49.0
26/4/70	7-30 am	20 "	17.8	7.2	47	51	28.8	49.0
	11-30 "	24 "	17.7	7.3	47	51	29.2	49.0
	5-30 pm	36 "	17.7	7.3	47	51	29.2	49.0

TEMP. POTENTIOMETER READINGS [°F]							3.365	3.671	REMARKS
ROTARY SWITCH CHANNEL							BALANCE SETTING		
1	2	3	4	5	6		POLARITY	-ve	
0	0	0	0	0	0		SENSITIVITY	Med.	

WATFOR PROGRAM FOR CALCULATING THE VALUES OF A, B, R_{24} and δ_{24}

```
        SJOB                2050164,RUN=FREE,PAGES=25,TIME=3,KP=29
        SNAME        AZIZ
       .C
        C        WATFOR PROGRAM FOR CALCULATING THE VALUES OF
        C        A,B,RT24,AND PRES24.
        C
1               PRINT 100
2          100 FORMAT (5X,'POR',6X,'SI',6X,'TEMP',5X,'PRES',6X,
               C'A',9X,'B',6X,'RT24',4X,'PRES24',/)
3               E=2.71828
4           10 READ,POR,SI,TEMP,PRES
5               IF (POR.EQ.0.) GO TO 50
6               B=0.46*SI**0.185-0.33*ALOG10(PRES)
7               IF (TEMP.LE.5.) B=B*TEMP/5.
8               D=0.245*ALOG10(TEMP)+0.035
9               G=0.00717*SI*(TEMP**0.5-1.15)
10              F=100./E**G
11              A1=D*PRES+F
12              A=A1+8.*TEMP*(0.46-POR)
13              IF (A.GT.100.) A=100.
14              RT24=A/E**(B/24.)
15              PRES24=PRES-RT24*PRES/100.
16              PRINT 200,POR,SI,TEMP,PRES,A,B,RT24,PRES24
17          200 FORMAT (8F9.3,/)
18              GO TO 10
19           50 STOP
20              END
```

Legend:

POR = Initial Soil Porosity

SI = Degree of Ice Saturation

TEMP = Temperature below freezing point

PRES = Initial Lateral Pressure

RT24 = Reduction in Lateral stress after 24 hours

PRES24 = Pressure retained after 24 hours

SENTRY

POR	SI	TEMP	PRES	A	B	QT24	PRES24
0.460	100.000	32.000	25.000	14.044	0.617	13.688	21.572
0.460	100.000	32.000	50.000	24.138	0.518	23.623	38.128
0.460	100.000	32.000	75.000	34.232	0.460	33.585	49.812
0.460	100.000	32.000	100.000	44.326	0.418	43.560	56.440
0.460	100.000	17.000	25.000	20.275	0.617	19.760	20.060
0.460	100.000	17.000	50.000	28.686	0.518	28.074	35.963
0.460	100.000	17.000	75.000	37.098	0.460	36.394	47.704
0.460	100.000	17.000	100.000	45.509	0.418	44.723	55.277
0.460	100.000	7.000	25.000	40.268	0.617	39.246	15.189
0.460	100.000	7.000	50.000	46.319	0.518	45.331	27.338
0.460	100.000	7.000	75.000	52.370	0.460	51.377	36.467
0.460	100.000	7.000	100.000	58.422	0.418	57.412	42.582
0.460	100.000	2.000	25.000	85.461	0.247	84.587	3.953
0.460	100.000	2.000	50.000	88.180	0.207	87.422	6.289
0.460	100.000	2.000	100.000	93.617	0.167	92.967	7.033
0.460	66.670	32.000	25.000	21.692	0.539	21.210	19.698
0.460	66.670	32.000	50.000	31.786	0.440	31.208	34.398
0.460	66.670	32.000	75.000	41.880	0.382	41.218	44.086
0.460	66.670	32.000	100.000	51.974	0.340	51.242	48.759
0.460	66.670	17.000	50.000	40.965	0.440	40.221	29.869
0.460	50.000	32.000	25.000	29.969	0.487	29.367	17.692
0.460	50.000	32.000	50.000	40.063	0.388	39.421	30.290
0.460	50.000	32.000	100.000	60.251	0.289	59.531	40.480
0.460	50.000	17.000	15.000	38.490	0.560	38.570	9.313
0.460	50.000	17.000	25.000	42.855	0.487	41.993	14.502
0.460	50.000	17.000	50.000	51.266	0.388	50.444	24.771
0.460	50.000	17.000	75.000	59.678	0.330	58.863	30.863
0.460	50.000	17.000	100.000	68.089	0.290	67.275	32.725
0.460	50.000	7.000	50.000	70.598	0.279	69.444	15.252

COR	SI	TEMP	PRES	A	B	PT24	PRESS24
0.460	50.000	2.000	25.000	93.692	0.195	92.934	1.769
0.460	50.000	2.000	50.000	96.400	0.155	95.779	2.110
0.460	50.000	2.000	100.000	100.000	0.115	99.520	0.420
0.460	33.330	32.000	15.000	40.117	0.492	39.303	9.105
0.460	33.330	32.000	25.000	44.155	0.419	43.391	14.152
0.460	33.330	32.000	50.000	54.249	0.319	53.532	23.234
0.460	33.330	32.000	75.000	64.343	0.261	63.646	27.265
0.460	33.330	32.000	100.000	74.437	0.220	73.758	26.243
0.460	33.330	17.000	25.000	57.551	0.419	56.556	10.361
0.460	33.330	17.000	50.000	65.963	0.319	65.091	17.455
0.460	33.330	17.000	100.000	82.786	0.220	82.030	17.970
0.460	33.330	7.000	25.000	75.997	0.419	74.683	6.329
0.460	33.330	7.000	50.000	82.048	0.319	80.964	9.818
0.460	33.330	7.000	75.000	88.100	0.261	87.146	9.641
0.460	33.330	7.000	100.000	94.151	0.220	93.292	6.709
0.460	33.330	2.000	25.000	96.600	0.167	95.928	1.018
0.460	33.330	2.000	50.000	99.319	0.128	98.792	0.604
0.460	33.330	2.000	75.000	100.000	0.104	99.566	0.326
0.460	33.330	2.000	100.000	100.000	0.088	99.634	0.366
0.400	100.000	17.000	50.000	36.846	0.518	36.060	31.970
0.400	66.670	17.000	50.000	49.125	0.440	48.233	25.883
0.400	50.000	32.000	50.000	55.423	0.388	54.535	22.733
0.400	50.000	17.000	5.000	44.286	0.718	42.980	2.851
0.400	50.000	17.000	15.000	47.650	0.560	46.550	8.017
0.400	50.000	17.000	25.000	51.015	0.487	49.989	12.503
0.400	50.000	17.000	50.000	59.426	0.388	58.473	20.763
0.400	50.000	17.000	75.000	67.838	0.330	66.912	24.616
0.400	50.000	17.000	100.000	76.240	0.289	75.338	24.662
0.400	50.000	7.000	50.000	73.958	0.388	72.772	13.614
0.400	50.000	2.000	50.000	93.360	0.155	95.733	1.372

POR	SI	TEMP	PRES	A	B	RT24	PRES24
0.400	33.330	17.000	50.000	74.123	0.319	73.143	13.428
0.360	100.000	17.000	50.000	42.286	0.518	41.384	29.302
0.360	66.670	17.000	50.000	54.565	0.440	53.574	23.213
0.360	50.000	32.000	50.000	65.663	0.388	64.610	17.695
0.360	50.000	17.000	25.000	56.455	0.487	55.320	11.170
0.360	50.000	17.000	50.000	64.866	0.388	63.826	18.087
0.360	50.000	17.000	75.000	73.278	0.330	72.278	20.792
0.360	50.000	17.000	100.000	81.689	0.289	80.713	19.287
0.360	50.000	7.000	50.000	76.198	0.388	74.976	12.512
0.360	50.000	2.000	50.000	98.000	0.155	97.369	1.316
0.300	50.000	32.000	50.000	81.023	0.388	79.724	10.138
0.300	50.000	17.000	25.000	64.615	0.487	63.316	9.171
0.300	50.000	17.000	50.000	73.026	0.388	71.855	14.072
0.300	50.000	7.000	50.000	79.558	0.388	78.282	10.859
0.300	50.000	2.000	50.000	98.960	0.155	98.323	0.839
0.460	100.000	5.000	25.000	51.056	0.617	49.760	12.560
0.460	66.670	17.000	25.000	32.554	0.539	31.830	17.042
0.460	50.000	32.000	75.000	50.157	0.330	49.473	37.896
0.460	50.000	7.000	75.000	76.649	0.330	75.603	18.298
0.460	50.000	7.000	100.000	82.700	0.289	81.712	18.288
0.460	50.000	7.000	25.000	64.546	0.487	63.249	9.168
0.460	50.000	2.000	75.000	99.119	0.132	98.576	1.068
0.460	50.000	1.000	50.000	100.000	0.078	99.677	0.161
0.460	30.000	17.000	50.000	69.578	0.302	63.707	18.647
0.460	20.000	17.000	50.000	82.112	0.240	81.295	9.382
0.460	20.000	17.000	25.000	73.701	0.339	72.666	6.824
0.360	50.000	22.000	50.000	63.899	0.388	62.775	18.533
0.360	33.330	17.000	50.000	78.563	0.319	78.511	16.744
0.300	50.000	17.000	100.000	89.840	0.289	88.775	11.285

VITA AUCTORIS

1946   Khandker Abdul Aziz was born in Khulna, East Pakistan on November 6th, 1946.

1961   He completed his secondary education in Dacca, East Pakistan, obtaining distinction marks and securing tenth position in the first class in Matriculation examination held in March, 1961

1963   He obtained his Higher Secondary Certificate from E. P. Secondary Education Board, Dacca, in May, 1963. He secured the second position in the first class and was awarded a gold medal for distinction marks.

1967   He graduated in November, 1967, from East Pakistan University of Engineering and Technology & obtained the degree of B.Sc. in Civil Engineering. He secured the first position in the first class.

1968   He was working as an Assistant Engineer for Consulting Engineers (Pakistan) Ltd.

1969   He joined the teaching staff of East Pakistan University of Engineering and Technology, Dacca, in the Department of Civil Engineering.

1969   He was awarded Canadian Commonwealth Scholarship and was admitted to the University of Windsor, Windsor, Ontario, for graduate studies in Civil Engineering in September, 1969.